Development of a Continuous Ion Exchange System for Protein Recovery Using Liquid-Solid Circulating Fluidized Bed

By
Qingdao Lan

Graduate program in Engineering Science

Submitted in partial fulfillment for the requirements for the degree of Doctor of Philosophy

Faculty of Graduate Studies
The University of Western Ontario
London, Ontario, Canada
March, 2001

© Qingdao Lan 2001

THE UNIVERSITY OF WESTERN ONTARIO
FACULTY OF ENGINEERING SCIENCES

CERTIFICATE OF EXAMINATION

Chief Advisor

Advisory Committee

Examining Board

The thesis by

Qingdao (Chris) Lan

Entitled:

Development of a Continuous Liquid-Solid Circulating Fluidized Bed Ion Exchange System and its Application in Protein Purification

Is accepted in partial fulfillment of the requirements for the degree of Doctor of Philosophy

Date March 19/01

David Bellhouse
Chair of Examining Board



This is an authorized facsimile, made from the microfilm master copy of the original dissertation or master thesis published by UMI.

The bibliographic information for this thesis is contained in UMI's Dissertation Abstracts database, the only central source for accessing almost every doctoral dissertation accepted in North America since 1861.

UMI® Dissertation Services

From:ProQuest COMPANY

300 North Zeeb Road
P.O. Box 1346
Ann Arbor, Michigan 48106-1346 USA

800.521.0600 734.761.4700
web www.il.proquest.com

Printed in 2002 by digital xerographic process
on acid-free paper

DPPT

INFORMATION TO USERS

This manuscript has been reproduced from the microfilm master. UMI films the text directly from the original or copy submitted. Thus, some thesis and dissertation copies are in typewriter face, while others may be from any type of computer printer.

The quality of this reproduction is dependent upon the quality of the copy submitted. Broken or indistinct print, colored or poor quality illustrations and photographs, print bleedthrough, substandard margins, and improper alignment can adversely affect reproduction.

In the unlikely event that the author did not send UMI a complete manuscript and there are missing pages, these will be noted. Also, if unauthorized copyright material had to be removed, a note will indicate the deletion.

Oversize materials (e.g., maps, drawings, charts) are reproduced by sectioning the original, beginning at the upper left-hand corner and continuing from left to right in equal sections with small overlaps.

Photographs included in the original manuscript have been reproduced xerographically in this copy. Higher quality 6" x 9" black and white photographic prints are available for any photographs or illustrations appearing in this copy for an additional charge. Contact UMI directly to order.

ProQuest Information and Learning
300 North Zeeb Road, Ann Arbor, MI 48106-1346 USA
800-521-0600

UMI®

NOTE TO USERS

Page(s) not included in the original manuscript are unavailable from the author or university. The manuscript was microfilmed as received.

23

This reproduction is the best copy available.

UMI

National Library of Canada
Acquisitions and Bibliographic Services
395 Wellington Street
Ottawa ON K1A 0N4
Canada

Bibliothèque nationale du Canada
Acquisitions et services bibliographiques
395, rue Wellington
Ottawa ON K1A 0N4
Canada

Your file Votre référence

Our file Notre référence

The author has granted a non-exclusive licence allowing the National Library of Canada to reproduce, loan, distribute or sell copies of this thesis in microform, paper or electronic formats.

L'auteur a accordé une licence non exclusive permettant à la Bibliothèque nationale du Canada de reproduire, prêter, distribuer ou vendre des copies de cette thèse sous la forme de microfiche/film, de reproduction sur papier ou sur format électronique.

The author retains ownership of the copyright in this thesis. Neither the thesis nor substantial extracts from it may be printed or otherwise reproduced without the author's permission.

L'auteur conserve la propriété du droit d'auteur qui protège cette thèse. Ni la thèse ni des extraits substantiels de celle-ci ne doivent être imprimés ou autrement reproduits sans son autorisation.

0-612-58401-1

Canada

The UNIVERSITY *of* WESTERN ONTARIO

Faculty of Graduate Studies

In the interests of facilitating research by others at this institution and elsewhere, I hereby grant a licence to:

THE UNIVERSITY OF WESTERN ONTARIO

to make copies of my thesis entitled
Development of a Continuous Ion Exchange System for Protein Recovery Using Liquid-Solid Circulating Fluidized Bed
or substantial parts thereof, the copyright which is invested in me, provided that the licence is subject to the following conditions:

1. Only single copies shall be made or authorized to be made at any one time, and only in response to a written request from the library of any University or similar institution on its own behalf or on behalf of one of its users.

2. This licence shall continue to the full term of the copyright, or for so long as may be legally permitted.

3. The Universal Copyright Notice shall appear on the title page of all copies of my thesis made under the authority of the licence.

4. This licence does not permit the sale of authorized copies at a profit, but does permit the collection by the institution or institutions concerned of charges covering actual costs.

5. All copies made under the authority of this licence shall bear a statement to the effect that the copy in question "is being made available in this form by the authority of the copyright owner solely for the purpose of private study and research and may not be copied or reproduced except as permitted by the copyright laws without written authority from the copyright owner".

6. The foregoing shall in no way preclude my granting to the National Library of Canada a licence to reproduce my thesis and to lend or sell copies of the same.

H.M. Kiabadi
(signature of witness)

(signature of student)

April 23, 2001 — *(date)*

PhD — *(degree)*

Engineering Science — *(graduate program of student)*

ABSTRACT

A liquid-solid circulating fluidized bed continuous ion exchange system (LSCFB) has been constructed and applied for the first time for the continuous recovery of bovine serum albumen (BSA) and whey proteins from unclarified broths using Diaion HPA25 anion exchanger. Under the optimal operating conditions, up to 80% of total protein was removed from the whey feed stream and an overall recovery of approximately 78% was achieved with a throughput of 8.16 g protein/hr·(kg particles). In the case of BSA recovery, up to 98% BSA was adsorbed in the downcomer and an overall protein recovery of up to 84% was obtained in the LSCFB system.

Studies regarding the hydrodynamics in the LSCFB, the kinetics and equilibrium characteristics of protein adsorption onto ion exchangers in finite baths, and continuous protein ion exchange in the LSCFB have been conducted under various operating conditions. A Langmuir-based model has been proposed and established to account for the influence of ionic strength on the capacity and the affinity of the protein adsorption onto ion exchange/affinity adsorbents. Mathematical models for the continuous protein recovery in the LSCFB were also developed and proven to be a useful tool in providing guidelines for the optimization of the system.

KEY WORDS: Ion exchange, Protein Purification, Liquid-Solid Circulating Fluidized Bed, Whey Proteins, Bovine Serum Albumin, Equilibrium, Kinetics, Hydrodynamics, Design

CO-AUTHORSHIP

Title: A Modified Langmuir Model for the Prediction of the Effects of Ionic Strength on the Equilibrium Characteristics of Protein Adsorption onto Ion Exchange/Affinity Adsorbents (Chapter 5)

Authors: Q. Lan, A.S. Bassi, J.X. Zhu, A. Margaritis

All the experiments were conducted by Q. Lan, under the supervision of supervisor Dr. A. Bassi, and co-supervisors Drs. J.-X. Zhu and A. Margaritis. All the drafts were written by Q. Lan. Modifications were carried out under the supervision of the supervisors. This chapter was published in Chem. Eng. J. 81 (1-3): 179-186, 2001

Title: Continuous Protein Recovery Using a Liquid-Solid Circulation Fluidized Bed Ion Exchange System: Modeling and Experimental Studies (Chapter 6)

Authors: Qingdao Lan, Jing-Xu (Jesse) Zhu, Amarjeet S. Bassi, Argyrios Margaritis, Ying Zheng and Gerald E. Rowe

All the experiments were carried out by Qingdao Lan with the assistance from Gerald E. Rowe. Models were developed by Qingdao Lan under the guidance of the supervisors. This chapter was published in Can. J. Chem. Eng. 78: 858-866, 2000

Title: Investigation of a Liquid-Solid Circulating Fluidized Bed Ion Exchange System for Continuous Recovery of Bovine Serum Albumin (Chapter 7)

Authors: Q. Lan, A. Bassi, J.-X. Zhu and A. Margaritis

All the experiments were conducted by Q. Lan. All the drafts were written by Q. Lan. Modifications were accomplished under the guidance of the supervisors. This chapter

has been submitted to AIChE J., 2001

Title: Recovery of Proteins from Cheese Whey Using a Continuous Liquid-Solid Circulating Fluidized Bed Ion-exchange System. (Chapter 8)

Author: Q. Lan, A. Bassi, J.-X. Zhu and A. Margaritis

All the experiments were conducted by Q. Lan. All the drafts were written by Q. Lan. Modifications were carried out under the guidance of the supervisors. This chapter is submitted to Biotech. Bioeng., 2001

To Freeman and

most of all, to Jinlan,

for their Love, Support and Encouragement

ACKNOWLEDGEMENTS

Sincere acknowledgement is dedicated to my chief supervisor Professor Amarjeet Bassi and co-supervisor Professor Jingxu (Jesse) Zhu for their guidance, support and encouragement. Discussion with co-supervisor Professor A. Margaritis is also gratefully acknowledged.

Technical supports from Mr. Jianzhang Wen and Mr. Clayton Cook, and valuable assistance from Mr. Chris Ferris and Mohammad Moghareb are highly appreciated.

Special thanks are given to Dr. Ying Zheng, and to Dr. G. E. Rowe, Dr. Hui Zhang, Shirin Bahrami, Hooshyar Moghim Aliabadi, Sunitha Kandula, Ning Ding, Zouhong Geng, Jingjing Li, Ying Ma, Yaluan Shao, Aijie Yan, Fujing Wan and other friends for their friendship and support.

Financial support from an NSERC strategic grant to the project, the OGSST from the Ontario Ministry of Training, and the SUS and IGSS provided by the University of Western Ontario are gratefully acknowledged.

TABLE OF CONTENT

certificate of examination	ii
Abstract	iii
Co-Authorship	iv
Acknowledgements	vii
Table of Content	viii
List of Figures	x
List of Tables	xv
Structure of the Thesis	xvi
CHAPTER 1. INTRODUCTION	1
CHAPTER 2. LITERATURE REVIEW	4
2.1 Principles of Ion exchange	4
2.2 Ion exchange adsorption Processes	16
Nomenclature	24
References	25
CHAPTER 3. APPARATUS: THE LIQUID-SOLID CIRCULATING FLUIDIZED BED CONTINUOUS ION EXCHANGE SYSTEM	37
3.1 Overall Description of the Liquid-Solid Circulating Fluidized Bed	37
3.2 Design Considerations	38
3.3 Selection of Ion Exchange Particles for the LSCFB ion exchange system	43
References	48
CHAPTER 4. BOVINE SERUM ALBUMIN ADSORPTION ONTO ANION EXCHANGER DIAION HPA25: EQUILIBRIUM AND KINETIC CHARACTERISTICS	57
4.1 Theory	57
4.2 Materials and Methods	60
4.3 Results and Discussion	62
nomenclature	66
References	67
CHAPTER 5. A MODIFIED LANGMUIR MODEL FOR THE PREDICTION OF THE EFFECTS OF IONIC STRENGTH ON THE EQUILIBRIUM CHARACTERISTICS OF PROTEIN ADSORPTION ONTO ION EXCHANGE/AFFINITY ADSORBENTS	74
5.1 Introduction	74
5.2 Theory	75
5.3 Experimental	80
5.4 Results and Discussion	81
5.5 Conclusions	86
Nomenclature	87

References 88

CHAPTER 6. CONTINUOUS PROTEIN RECOVERY USING A LIQUID-SOLID CIRCULATING FLUIDIZED BED ION EXCHANGE SYSTEM: MODELLING AND EXPERIMENTAL STUDIES 100
6.1 Introduction 101
6.2 Experimental 104
6.3 Model Development 106
6.4 Results and discussion 114
6.5 Conclusions 119
Nomenclature 120
References 122

CHAPTER 7. INVESTIGATION OF THE CONTINUOUS RECOVERY OF BSA IN AN LSCFB ION EXCHANGE SYSTEM 138
7.1 Introduction 138
7.2 Materials and Methods 140
7.3 Results and Discussion 145
7.4 Conclusions 157
Nomenclature 158
References 160

CHAPTER 8 RECOVERY OF PROTEINS FROM CHEESE WHEY USING A CONTINUOUS LIQUID-SOLID CIRCULATING FLUIDIZED BED ION-EXCHANGE SYSTEM 177
8.1 Introduction 177
8.2 Material and Methods 179
8.3 Results and Discussion 181
8.4 Conclusions 189
Nomenclature 190
References 192

CHAPTER 9. CONCLUSIONS AND RECOMMENDATIONS 201
9.1 Conclusions 201
9.2 Recommendations 205
Reference 208
Appendix A. Copyright release from the journal "Canadian Journal of Chemical Engineering" 209
Appendix B. Copyright release policy of Elsevier Science: Regarding the inclusion of materials in chapter 5 in this thesis from "Chemical engineering journal" 210
Curriculum Vitae 212

LIST OF FIGURES

Figure 2.1	Schematic illustration of structure of the surface of an anion exchanger	34
Figure 2.2	Diffusion of solute from bulk solution to the ion exchange sites	35
Figure 2.3	Schematic diagram of different fluidized beds (a) packed bed: particles are not fluidized and bed voidage are small; (b) expanded bed: particles suspended but not fully fluidized, bed voidage larger than a packed bed but less than that of a conventional fluidized bed, diverse particle size distribution reduces backmixing; (c) conventional fluidized bed: particles fully fluidized, characterized by large bed voidage and strong backmixing; (d) magnetically stabilized fluidized bed: particles fully fluidized with large bed voidage, backmixing minimized by the orientation of magnetic particles in magnetic field.	36
Figure 3.1	A picture of the pilot liquid-solid circulating fluidized bed ion exchange system in the Department of Chemical and Biochemical Engineering at the University of Western Ontario	50
Figure 3.2	Schematic diagram of the liquid-solid circulating fluidized bed (LSCFB) ion exchange system. (1) Riser; (2) Solids-Liquid separator; (3) Extract Outlet; (4) Raffinate outlet; (5) Washing section of the separator; (6) Top solids return pipe; (7) Solids circulating rate measuring device; (8) Downcomer; (9) Distributor of the downcomer; (10) Washing section of the downcomer; (11) Bottom solids return pipe; (12) The primary stream in the riser distributor; (13) The auxiliary stream in the riser distributor; (14) Liquid distributor of the riser; (15) Butterfly valve	51
Figure 3.3	The riser distributor	53
Figure 3.4	A schematic diagram of the downcomer distributor	54
Figure 3.5	A schematic diagram of the combination of the liquid-solids separator and the top washing section	55
Figure 3.6	Schematic diagram of the base of the LSCFB system: dynamic seal between the riser and the downcomer	56
Figure 4.1	Schematic graph of a batch adsorption/desorption kinetic study system. (1) Bellco reactor; (2) 20 μm porosity filter; (3) Cary 50-Bio UV-visible spectrophotometer; (4) Manostat Cassette pump; (5) Magnetic Stir Rod; (6) Magnetic Stirrer.	68

Figure 4.2 The isotherm of BSA adsorption onto Diaion HPA25 in 10 mM phosphate buffer at pH 7.0 69

Figure 4.3 The pH-dependency of the maximum capacity of BSA adsorption onto Diaion HPA25 in 10 mM buffers (pH 3.0 citric acid/NaOH buffer; pH 4.0 and 5.0 sodium acetate/acetic acid buffer; pH 6.0-8.0 phosphate buffer; and pH 9.0, boric acid, KCl/NaOH buffer). 70

Figure 4.4 The ionic strength dependency of the capacity of BSA adsorption onto Diaion HPA25 in pH 7.0 10 mM phosphate buffer. 71

Figure 4.5 Experimental and predicted kinetics of BSA adsorption onto Diaion HPA25 particles in batch adsorption (C_0 = 2 g/L, V = 100 ml, v = 15 ml, K_d = 0.0103 g/L, q_m = 91.7 mg/g, k_1 = 0.00046 L/g·s). 72

Figure 4.6 Experimental and predicted kinetics of BSA desorption from loaded Diaion HPA25 particles in batch desorption (q_0 = 45.8 mg/g, v = 15 ml, V = 50 ml, k = 0.0107 s^{-1}). 73

Figure 5.1 Comparison between the experimental isotherms (symbol), best-fit Langmuir isoherms for given individual NaCl concentration and the isotherms predicted by the modified Langmuir model. 92

Figure 5.2 Semi-reciprocal plot of BSA adsorption onto Diaion HPA25 at 25 °C, pH 7.0 and different NaCl concentrations. 93

Figure 5.3 Scatchard Plot of BSA adsorption on Diaion HPA25 25 °C, pH 7.0 and different NaCl concentrations. 94

Figure 5.4 Effects of ionic strength on the apparent maximum binding capacity (q_m') of BSA adsorption onto Diaion HPA25 at 25°C and pH7.0. 95

Figure 5.5 Effects of ionic strength on the apparent dissociation coefficient (K_d') of BSA adsorption onto Diaion HPA25 at 25°C and pH7.0. 96

Figure 5.6 Reciprocal of apparent maximum binding capacity ($1/q_m'$) for BSA adsorption as a function of NaCl concentration at 25°C and pH7.0. 97

Figure 5.7 Reciprocal of apparent dissociation coefficient ($1/K_d'$) as a function of NaCl concentration at 25°C and pH7.0. 98

Figure 5.8 Comparison of the predicted and the experimental data for the apparent coefficient (K_d'). 99

Figure 5.9 Comparison of the predicted and the experimental data for the apparent maximum binding capacity (q_m). 100

Figure 6.1 Schematic diagram of the Liquid Solid Circulating Fluidized Bed (LSCFB) ion exchange system 127

Figure 6.2 Flow patterns in the downcomer and the riser: (a) counter-current contact of liquid and solids phases in the dense section of the downcomer; (b) co-current contact of liquid and solids phases in the riser. 129

Figure 6.3 Dependency of solids holdup in the riser on the superficial liquid velocity in the riser (U_{lr}) (Beads: Diaion HPA25®; fluidization fluid: tap water; room temperature). 130

Figure 6.4 Typical experimental BSA adsorption profiles in the downcomer (U_{ld} = 0.0006 m/s, U_{lr} = 0.0113 m/s, G_s = 1.24 kg/m^2·s, H_d = 0.8 m, C_{0d} = 2 mg/mL, pH 7.0 and room temperature). 131

Figure 6.5 Typical experimental BSA desorption profiles in the riser (U_{ld} = 0.0006 m/s, U_{lr} = 0.0113 m/s, G_s = 1.24 kg/m^2·s, H_d = 0.8 m, C_{0d} = 2 mg/mL, pH 7.0 and room temperature) . 132

Figure 6.6 Comparison between the experimental and predicted steady state BSA desorption profiles in the riser at various superficial liquid velocity in the riser (U_{lr}) (U_{ld} = 0.0006 m/s, G_s = 1.24 kg/m^2·s, H_d = 0.8 m, C_{0d} = 2 mg/mL, pH 7.0 and room temperature). 133

Figure 6.7 Comparison between the experimental and predicted steady state BSA adsorption profiles in the downcomer at various solids circulation rates (G_s) (U_{ld} = 0.0006 m/s, U_{lr} = 0.0113 m/s, H_d = 0.8 m, C_{0d} = 2 mg/mL, pH 7.0 and room temperature). 134

Figure 6.8 Simulation of the effects of superficial liquid velocity in the downcomer (U_{ld}) on the BSA adsorption onto and desorption from Diaion HPA25® in the LSCFB: (a) Adsorption in the downcomer; (b) Desorption in the riser. (U_{lr} = 0.0113 m/s, G_s = 1.24 kg/m^2·s, H_d = 0.8 m, C_{0d} = 2 mg/mL, pH 7.0 and room temperature) 135

Figure 6.9 Simulation of the effects of solids circulating rate (G_s) on the BSA adsorption onto and desorption from Diaion HPA25® in the LSCFB system. (a) Adsorption in the downcomer; (b) Desorption in the riser. (U_{ld} = 0.0006 m/s, U_{lr} = 0.0113 m/s, H_d = 0.8 m, C_{0d} = 2 mg/mL, pH 7.0 and room temperature) 136

Figure 6.10 Simulation of the effects of BSA concentration in the feed on the BSA adsorption onto and desorption from Diaion HPA25® in the LSCFB. (a) Adsorption in the downcomer; (b) Desorption in the riser. (U_{ld} = 0.0006 m/s, U_{lr} = 0.0113 m/s, G_s = 1.24 kg/m^2·s, H_d = 0.8 m, pH 7.0 and room temperature). 137

Figure 7.1. Schematic diagram of the liquid-solid circulating fluidized bed (LSCFB) ion exchange system. 164

1. Riser, 2. Liquid-Solids separator, 3. Extract outlet, 4. Raffinate outlet, 5. Top washing section, 6. Top solids return pipe, 7. Solids circulating rate measuring device, 8. Downcomer, 9. Distributor of the downcomer, 10. Bottom washing section, 11. Bottom solids return pipe, 12. The primary stream in the riser distributor, 13. The auxiliary stream in the riser distributor, 14. Liquid distributor of the riser, 15. Butterfly valve, 16. Pressure manometer. 164

Figure 7.2. Schematic illustration of the three sections in the downcomer of an LSCFB system : (a) Freeboard Zone; (b) Dilute section; and (c) Dense Section. 166

Figure 7.3. Dependency of the downcomer dense section height on the liquid velocity (U_{ld}) in the downcomer and the solids circulation rate (G_s), with a total of 3.0 kg Diaion HPA25 anion exchange particles. 167

Figure 7.4 Axial distribution of the solids holdup in the riser (U_{ld} = 0.6 mm/s). 168

Figure 7.5 Influences of the superficial liquid velocity in the riser (U_{lr}) and the solids circulation rate (G_s) on the solids holdup in the riser (ε_{sr}) (U_{ld} = 0.6 mm/s). 169

Figure 7.6 The characteristics of Diaion HPA25 regeneration in the riser (U_{ld} = 0.6 mm/s, U_{lr} = 11.3 mm/s, G_s = 1.24 kg/m^2·s, H_d = 0.8 m, C_{0d} = 2 g/L) 170

Figure 7.7 The effects of solids circulation rate on the characteristics of BSA adsorption in the downcomer (U_{ld} = 0.6 mm/s, U_{lr} = 11.3 mm/s, H_d = 0.8 m C_{0d} = 2 g/L). 171

Figure 7.8 The effects of superficial liquid velocity (U_{ld}) on the characteristics of BSA adsorption onto Diaion HPA25 anion exchange particles in the downcomer (U_{lr} = 11.3 m/s, G_s = 1.24 kg/m^2·s, H_d = 0.8 m, C_{0d} = 2 g/L). (a) BSA concentration profiles. (b) BSA adsorption ratio profiles. 172

Figure 7.9 The effects of superficial liquid velocity (U_{lr}) on the characteristics of BSA desorption from Diaion HPA25 anion

exchange particles in the riser (U_{ld} = 0.6 m/s, G_s = 1.24 kg/m^2-s, H_d = 0.8 m, C_{0d} = 2 g/L). (a) BSA concentration profiles; (b) BSA desorption ratio profiles. 174

Figure 7.10 Hydrodynamic stable operation window of the LSCFB system with 3 kg Diaion HPA25 ion exchange particles. The fluidization liquid in the riser was 0.4 M NaCl buffer and in the downcomer tap water). 176

Figure 8.1 Schematic diagram of the LSCFB system (1. Riser; 2. Liquid-Solids separator; 3. Top washing section; 4. Top solids return pipe; 5. Solids circulating rate measuring device; 6. Downcomer; 7. Distributor of the downcomer; 8. Bottom washing section; 9. Bottom solids return pipe; 10. Liquid distributor of the riser.) 194

Figure 8.2 OD_{600} of the effluent at different bottom wash water flowrate (F_{wb}) (F_{feed} = 5.7 L/hr, F_{buffer} = 30 L/hr, F_{wt} = 1.8 L/hr and G_s = 1.42 kg/m^{2}s. Feed: half diluted whey; Extracting buffer: 0.4 M NaCl). 196

Figure 8.3 Conductance of the raffinate at different top wash water flowrates (F_{wt}) (F_{feed} = 5.7 L/hr, F_{buffer} = 30 L/hr, F_{wb} = 2.1 L/hr and G_s = 1.42 kg/m^{2}s. Feed: half-diluted whey (3.5%); Extracting buffer: 0.4 M NaCl). 197

Figure 8.4 Protein concentration profiles at different locations of the downcomer in a typical continuous whey protein recovery in the LSCFB system. (Experimental conditions: F_{feed} = 5.7 L/hr, F_{buffer} = 30 L/hr, F_{wb} = 2.1 L/hr, F_{wt} = 1.8 L/hr, and G_s = 1.42 kg/m^{2}s.;Extracting buffer: 0.4 M NaCl solution; Feed: quarter diluted whey (1.75% reconstituted whey). 198

Figure 8.5 Protein concentration profiles at different locations of the riser in a typical continuous whey protein recovery in the LSCFB system. (Experimental conditions: F_{feed} = 5.7 L/hr, F_{buffer} = 30 L/hr, F_{wb} = 2.1 L/hr, F_{wt} = 1.8 L/hr, and G_s = 1.42 kg/m^{2}s.;Extracting buffer: 0.4 M NaCl solution; Feed: quarter diluted whey (1.75% reconstituted whey). 199

Figure 8.6 Effects of dilution ratio on the ionic strength of the whey solution and the maximum adsorption capacity of ion-exchange beads. 200

LIST OF TABLES

Table 2.1 Separation techniques used in protein purification 32

Table 2.2 Functional groups found on some typical synthetic ion exchangers 33

Table 3.1 Properties of Diaion HPA25® 49

Table 5.1 Langmuir parameters from literature and experiments 89

Table 5.2 Dissociation coefficient and constant η calculated according to the apparent Langmuir parameters as listed in Table 5.1 90

Table 5.3 Maximum binding capacity and constant ψ calculated according to the apparent Langmuir parameters as listed in Table 5.1 91

Table 6.1 Properties of Diaion HPA25® 125

Table 6.2 Parameters of BSA adsorption/desorption onto/from Diaion HPA25® obtained in our laboratory 126

Table 7.1 Properties of Diaion HPA25® Ion Exchange Particles 162

Table 8.1 Summary of parameters of whey protein recovery under different conditions 193

STRUCTURE OF THE THESIS

- The thesis has been written in the manuscript format, which is an approved format for the Faculty of Engineering. The structure is as follows:
- All tables and figures are at the end of each chapter
- All references are at the end of each chapter
- Chapters are arranged as following:

Chapter 1. Introduction

Chapter 2. Literature Review

Chapter 3. Apparatus: A Liquid-Solid Circulating Fluidized Bed Ion Exchange System

Chapter 4. Bovine Serum Albumin Adsorption onto Anion Exchanger Diaion HPA25: Equilibrium and Kinetic Characteristics

Chapter 5. A Modified Langmuir Model for the Prediction of the Effects of Ionic Strength on the Equilibrium Characteristics of Protein Adsorption onto Ion Exchange/Affinity Adsorbents

Chapter 6. Continuous Protein Recovery Using a Liquid-Solid Circulation Fluidized Bed Ion Exchange System: Modeling and Experimental Studies.

Chapter 7. Investigation of continuous BSA purification using an LSCFB Ion Exchange system.

Chapter 8. Recovery of Proteins from Cheese Whey Using a Continuous Liquid-Solid Circulating Fluidized Bed Ion-exchange System

Chapter 9. Conclusions and recommendations

Chapter 1. Introduction

The interest in recovery of proteins from large volumes of industrial broths and biological wastewater streams has increased in recent years, due to the rapidly growing number of functional proteins made available by genetic engineering and concerns about recycling limited resources and environmental protection. Conventional ion-exchange processes using packed beds have been established for decades as powerful tools for protein recovery due to their high selectivity and ease in operation. However, there are some significant disadvantages associated with this strategy. First, a packed bed column operation requires the cyclic operation of four procedures, namely adsorption, washing, desorption and regeneration in a batch mode. Such an operation is laborious and time-dependent. Secondly, a typical biochemical broth usually contains large amounts of colloidal particulates, which must be removed before being treated by a conventional packed bed ion-exchange system. The removal of small solids using filtration or centrifugation is very difficult. Thirdly, because of the large molecular size of proteins, some internal surface of the ion exchangers are inaccessible to the proteins and intra-pore diffusion of the large proteins in the porous channels of an ion exchange particle is slow due to the steric hinderance effects. This results in relatively low adsorption capacity and low adsorption rate. Therefore, the ion exchangers have to be frequently regenerated. In such a situation, a batchwise strategy is significantly ineffective.

To overcome the above disadvantages, a liquid-solid circulating fluidized bed (LSCFB) ion exchange system has been proposed and constructed in this study and investigated for the continuous recovery of protein from unclarified whole broth. The detailed structure of an LSCFB is discussed in Chapter 3. Conceptually an LSCFB is comprised of a riser, a

downcomer, a liquid-solid separator and other auxiliary components (Figures 3.1 and 3.2). The riser is a "fast column" operating in the circulating fluidization regime and the downcomer a "slow column" operating as a conventional fluidized moving bed. In the two columns of the LSCFB, two different liquid streams can be applied separately with the solid particles circulating between them. In the LSCFB ion exchange system, proteins are adsorbed onto the adsorbents in the downcomer (absorber) and the loaded adsorbents are regenerated simultaneously in the riser (stripper) in a continuous mode thus maintaining the adsorbents in the active form. Therefore, adsorbent of low adsorption capacity and slow kinetics may be used. Another unique feature of the LSCFB system is that the downcomer operates as an expanded bed with adsorbent falling down and liquid phase moving up. The bed voidage can be enlarged to make possible the treatment of feed containing particulates without clogging the bed. The liquid velocity in the downcomer can be controlled in such a range that the particulates are discarded with the deproteinized feed liquor while permitting the ion exchange particles to settle to the bottom and return to the riser. This eliminates the costly solids removal (pre-clarification) operation and significantly simplifies the overall purification scheme.

The design of such an LSCFB ion exchange system requires the understanding of the hydrodynamics of an LSCFB and the investigation of the adsorption and desorption of proteins onto ion exchange particles. Thus in this thesis, the following are considered: (1) investigation of the hydrodynamics of the LSCFB; (2) selection of suitable ion exchange particle; (3) the protein adsorption/desorption kinetics and equilibrium characteristics; (4) continuous protein recovery using the LSCFB ion exchange system using BSA as a model protein; and (5) application of the LSCFB in continuous purification of whey proteins from unclarified cheese whey. The results are presented as follows:

Chapter 2 is a literature review, which provides the necessary background information.

Chapter 3 describes the design of the LSCFB and the selection of ion exchange particles.

Chapter 4 describes the equilibrium and kinetic characteristics of BSA adsorption onto Diaion HPA25 anion exchanger in batch operations.

Chapter 5 reports the results of a study on the equilibrium characteristics of protein adsorption onto ion exchange/affinity adsorbents. A modified Langmuir model is established and validated as a reliable method for the prediction of the effects of ionic strength.

Chapter 6 discusses the modelling of the continuous BSA adsorption and desorption in the LSCFB ion exchange system. Studies show that the models match well with experimental data.

Chapter 7 investigated the influence of different operating conditions on the hydrodynamics and BSA adsorption/desorption in the LSCFB ion exchange system.

Chapter 8 tested the recovery of whey proteins from cheese whey solution using the LSCFB ion exchange system and discussed effects of various operating conditions;

Chapter 9 presents some important conclusions derived from the research and some thoughts regarding the future research in this area.

Appendices include my *Curriculum Vitae* and copyright waiver documents.

Chapter 2. Literature Review

Table 2.1 lists several common separation methods that can be applied to protein purification. Of these, ion exchange adsorption and chromatography are most commonly used for protein purification, for both laboratory purposes and industrial manufacturing, due to the many advantages associated with it. In this chapter, the principles of ion exchange are discussed first, followed by a review of different applications of ion exchange processes, with the emphasis on the application of ion exchange processes in protein purification.

2.1 PRINCIPLES OF ION EXCHANGE

A schematic diagram illustrating the structure of an anion exchanger is shown in Figure 2.1. The ion exchange process can be illustrated by an anion exchanger, for which the counter-ion is E^-. The exchanger can thus be represented as *Resin-*F^+E^-, where *Resin-*F^+ represents the inert matrix containing the positive fixed ion (functional group). When an anion exchange particle is submerged in a solution containing a different anion, A^-, the ion exchange will process as following:

$$\text{Resin}-F^+E^- + A^- \Leftrightarrow \text{Resin}-F^+A^- + E^- \qquad 2.1$$

An ion exchange particle consists of two major components: the matrix and the functional groups. The insoluble matrix provides the support for the functional groups, which are the binding site for the ion exchange. The matrix may be inorganic or may be an organic polymer resin, and is generally porous. The functional groups are ions chemically bound to the matrix and are also called the fixed ions. The ions of opposite

charge to that of the fixed ions are the counter-ions. They are the exchangeable ions. On the other hand, the ions in the aqueous solution of the same charge to the fixed ions are the co-ions and they are un-exchangeable.

When an ion exchange particle placed in an aqueous solution, the pores will fill with water and a sufficient concentration of counter-ions to maintain the overall electric balance in the particle. The counter-ion can move through the matrix by diffusion or under the influence of an electric field. These counter-ions are thus exchanged with ions of the same charge from the bulk solution.

2.1.1 Types of Ion Exchangers

Ion exchangers can be divided into two categories according to their counter-ions: anion exchangers and cation exchangers. Anion exchangers have acidic functional groups, which are positively charged and cation exchangers have negatively charged basic functional groups. Functional groups have significant influence on the properties of ion exchangers. For example, they determine the affinity and selectivity of ion exchange particles to a given solute. They also have a strong influence on the effective pH range and adsorption capacity of an ion exchanger. Some functional groups found in typical ion exchangers are listed in Table 2.2.

2. Ion exchange matrix

Most ion exchangers can be also classified according to their matrices into the following categories: modified-cellulose-based ion exchangers, cross-linked-dextran-based ion exchangers, cross-linked-agarose based ion exchangers, synthetic ion exchangers (e.g. methacrylate polymers based ion exchangers and polysterenic ion exchange resins), and silica-based ion exchange adsorbents. For the adsorption of large biological molecules such as proteins, the problem of enhancing the permeability of ion exchange particles for the purpose of increasing the accessibility of the internal surface has assumed great importance. The accessibility of the functional groups for protein ions is determined largely by the structure of the particle. The most commonly employed ion exchangers in protein recovery include the following categories:

(I) Cellulose based ion exchangers

Cellulose is composed of linear 1,4-β-D cellobiose unit. Commercial cellulose ion exchangers are usually obtained by the oxidization of cellulose. The cellulose molecule has hydroxyl groups at the carbon 2, 3, and 6, to which the active exchange groups are bound. Its loose network is cross-linked by hydrogen bridges and the majority of its active exchange groups are located at distances of about 50 Å, which allows the exchange of large counter-ions. In addition, the cellulose matrix is hydrophilic and thus minimizes the protein-matrix interaction, which is a major cause for the irreversible adsorption.

Cellulose ion exchangers have been widely used in protein recovery (Alam and Qasim, 1998; De-Lange *et al.*, 1979; Foster *et al.*, 1974; Foster *et al.*, 1977; Kurz, 1998; Leaver *et al.*, 1990; Levison *et al.*, 1996; Maggo *et al.*, 1999). However, the poor flow properties associated with the loose structure of cellulose ion exchangers often limit the flowrate achievable with a packed bed and also make them inappropriate for fluidized bed operations.

(2) Dextran-based ion exchangers

Dextran is a linear α-1,6-linked glucose polymer produced by *Leuconostoc mesenteroides*. Sephadex® (cross-linked by glyceryl bridges) and Sephacryl® (allyldextran cross-linked by N,N'-methylenebisacrylamide) are two types of the gels used in ion exchange (and affinity) chromatography of biomolecules.

Since the number of hydroxyl groups is only insignificantly modified by cross-linking, it is possible to prepare esters and ethers by further reactions with suitable reactants and to introduce ionic groups into the dextran molecule, thus obtaining ion exchange materials with polysaccharide as the matrix. For example Sephadex® ion exchangers are obtained when exchanger groups are substituted in neutral Sephadex® types G-25 and G-50. The functional groups are bound to the glucose building blocks of the network by ether bridges. Sephadex® etherified with carboxymethyl or sulfopropyl groups result in weak or strong acid cation exchangers, CM- and SP- Sephadex®, while substitution with diethylaminoethyl or 2-hydroxypropyldiethylaminoethyl groups furnishes weak and strong base anion exchangers, DEAE- or QAE- Sephadex®.

Sephadex® ion exchangers are comparable to corresponding cellulose ion exchangers and in many cases the same method can be used. However, their ultimate capacity is 5-10 times higher than that of cellulose exchangers. The bead-like particles offer favorable flow characteristics in chromatography. Sephadex® ion exchangers are particularly suitable for the separation of sensitive and high molecular weight bio-products such as proteins, nucleic acids and polysaccharides. Their nonspecific adsorption is minimal, and the protein and biologically active materials are generally not denatured. These advantages associated with Sephadex® ion exchangers make them very popular in protein separation (Batista *et al.* 1996; Devi and Rao, 1996; Vujcic *et al.*, 1995). Commercial

Sephadex® ion exchange particles are usually of small diameter (50-100 microns), which is advantageous for packed bed operations due to the relatively large accessible surface, higher capacity and faster kinetics. However, the terminal velocity of such small particles is not sufficient to guarantee functionality in an LSCFB ion exchange system.

(3) Agarose Based Ion Exchange Particles

Agarose is a linear polysaccharide consisting of alternating 1,3-linked β-D-galactopyranose and 2,4-linked-3,6-anhydro-α-galactopyranose. Its macroporous matrix structure, which has 100-300 nm pores, is well suited for the separation of large biological active molecules. The cross-linking of agarose has improved the stability of the beads towards extremes of pH, temperature, and high concentrations of organic solvents. Cross-linking also allows the elevating the flowrate when used in column operation.

Sepharose ion exchangers are the most common agarose-based ion exchangers. They are probably the most widely used ion exchangers for protein recovery (Sunitha *et al.*, 2000; Chan *et al.*, 2000; Patra *et al.*, 2000; Ye *et al.*, 2000). A relatively new Sepharose ion exchanger, Sepharose Fast Flow, has better flow properties and is very popular for application to protein ion exchange chromatography (Gibert, *et al.*, 2000; Levison *et al.*, 1996; Linden *et al.*, 1999; Mccartney J.E., 1991; Nash and Chase, 1998; Oyama and Takahashi, 2000; Ulusu *et al.*, 1999). The same problem of small terminal velocity also exists for commercial agarose-based ion exchangers, which makes them less competitive for use in an LSCFB ion exchange system.

(4) Silica-Based Ion Exchange Particles

Silica-based ion exchange beads are composed of polymer-grafted porous silica beads (Barker and Morr, 1986; Outinen *et al.*, 1996b; Skudder, 1983). The silanols covering the

bead surface are covalently linked to functionalized polymers, which provide ion exchange properties of the material (Ratnayake and Regnier, 1996). The most significant characteristics of silica based ion exchangers is its resistance to swelling and its high density, which make it particularly suitable for fluidized bed ion exchange operations (Finette *et al.*, 1998). The high porosity and large pore size achievable with silica beads, together with its hydrophilic surface which minimizes the interaction between the matrix and the protein structure, make it a good choice for protein recovery (Skudder, 1985; Nichols and Morr, 1985; Finette *et al.*, 1997; Finette *et al.*, 1998). Its high density and rigidity also make it an excellent candidate for operations using an LSCFB ion exchange system. The major disadvantages associated with the silica-based ion exchangers is its high price.

(5) Highly-Porous/Macroporous Synthetic Ion Exchange Particles

Among the commercial ion exchangers, synthetic ion exchangers are the most commonly used type due to the low cost and the diversity of the products in this category. Synthetic ion exchangers were previously deemed unsuitable for protein recovery due to their arguable hydrophobic matrices and their small pore size. However, with the development of highly-porous and macroporous synthetic ion exchangers, this type of ion exchanger was found wide application in the separation of proteins and other types of complex organic molecules (Outinen *et al.*, 1996a; Letourneur *et al.*, 1992; Yu and Sun, 1999).

Highly-porous/macroporous polystyrenic ion exchangers are one example of the synthetic ion exchangers which have been used in protein recovery. They are obtained by copolymerization of styrene and divinylbenzene, where styrene is the building block of the skeleton while divinylbenzene is the cross-linking agent. The polymeric network is further modified to give functional groups influencing the ion exchange properties of the particle.

2.1.2 Properties of Ion Exchangers

1. Capacity

The capacity of an ion exchanger is determined by the number of functional groups per unit weight of the particle accessible for ion exchange. It may be measured in a variety of units, the most common of which are millequivalents of (charge) per gram of dry particle, or millequivalents of (charge) per gram of wet particle. The capacity provided by manufacturers is measured in terms of small exchangeable ions, usually Cl^- or OH^- for anion exchangers and Na^+ or H^+ for cation exchangers. In the case of the adsorption of large bio-molecules such as proteins, the accessibility of the functional groups on the internal surface of the particle is greatly limited and the actual adsorption capacity to such large ions is significantly less than the adsorption capacity measured for small ions. In practical terms, the adsorption capacity for proteins is commonly expressed as g/L or kg/m^3.

2. Selectivity of ion exchange particle

The difference in affinity between the individual ions to certain ion exchange particles is called selectivity. From the perspective of analytical and preparative practice, the control of ion exchanger selectivity is very important. The selectivity of an ion exchanger can be expressed in many ways. For large molecules with multiple surface charges, the convenient way is the equilibrium distribution coefficient, which is given by the ratio of the equilibrium concentrations of the same ions in the exchanger phase and in the bulk solution:

$$D = \frac{q^* m_s}{C^* V} \qquad 2.2$$

where D is the equilibrium distribution coefficient, q^* the equilibrium concentration of the component in the ion exchanger phase (mg/g), m_s the mass of the ion exchangers in the solution (g), C^* the equilibrium concentration of the component in the bulk solution (mg/ml) and V the volume of the bulk solution (ml).

The selectivity of an ion exchanger to individual components depends on the type and concentration of the competing ions as well as on the property of the solvent and the nature of the exchanger. In principle, the selectivity of an ion exchanger depends on the following factors (Korkisch, 1989):

ions with a smaller effective hydrated ionic radius are preferentially adsorbed

if the ionogenic group of the particles forms an ionic pair with the reacting ion, the selectivity of the ion exchanger to this type of ions is increased

if substances in the solution form slightly dissociated compounds, then ions forming a more dissociated compound are preferentially adsorbed

selectivity of the ion exchanger decreases with increasing temperature

3. Ion exchange equilibrium

The adsorption equilibrium of proteins on different ion exchangers has been studied by many authors (Boyer and Hsu, 1990; Finette *et al.*, 1997; Huang *et al.*, 1990; Jenkins, 1989; Whitley *et al.*, 1989; Yoshida *et al.* 1993). Parameters influencing the adsorption equilibrium include the properties of protein such as surface charge (Stahlberg, 1992, Roush, 1994), molecular weight and the configuration of proteins (Sunitha *et al.*, 2000), the properties of ion exchange particles such as the type and intensity of functional groups, the hydrophilicity of the matrix and the accessibility of the binding sites, and the adsorption conditions such as pH, ionic strength and temperature (Finette *et al.*, 1997). Study on the equilibrium behavior of an ion exchange process can provide important information regarding the mechanism of the adsorption and the ability to characterize

equilibrium accurately is important for process modeling. No prediction of column performance could be done without first measuring or estimating the adsorption isotherms of these components under the conditions of interest, and the assurance of the prediction is strongly dependent on the accuracy of these data. Intensive studies have been conducted in the area of ion exchange equilibrium and many different isotherm models, such as the Langmuir (Langmuir, 1916), and the Freundlich's (Freundlich, 1926) models, have been proposed for the adsorption of solutes in a liquid solution onto a solid surface. Due to its simplicity and good fit with experimental data, the Langmuir isothermal model might be the most widely accepted model for the description of ion exchange equilibrium.

4. Ion exchange kinetics

For some small ions, the ion exchange process may be quite rapid and the equilibrium may under certain conditions be reached almost instantaneously. However, for the adsorption of large ions such as proteins, the ion exchange process is much slower because of the limitation of the diffusion of proteins inside and outside the ion exchange particle.

Adsorption of proteins onto the binding sites on the internal surface of a porous ion-exchange adsorbent entails the following macroscopic steps (Figure 2.2): 1) protein movement from the bulk solution phase to the bead surface; 2) protein transfer across a stagnant film layer surrounding the bead; 3) protein diffusion into the pores of the beads; 4) adsorption of protein to the solid phase. Each of these steps contributes to the overall adsorption but the slowest and most significant step will be the rate-governing mechanism. With mixing, bulk diffusion is often considered infinitely fast, therefore, the limiting step is usually anyone of steps 2 to 4.

A number of mathematical models have been developed based on the assumption that one limiting step controls the adsorption rate while the influence of other steps are ignored. Those include the kinetic rate constant model developed by Chase (1987), the pore diffusion model developed by Arnold and his co-workers (1985), the two phase diffusion model suggested by Gramham and Fook (1982), and the novel empirical model proposed by Rowe *et al.* (1999).

(1) The kinetic rate constant model

An empirical model was developed by Chase (1987) describing the adsorption and desorption processes. According to his model, all the mass transfer resistances are lumped into the interaction rate constants, k_1 and k_{-1}, while the two reaction rates are correlated by the dissociation coefficient ($K_d = k_{-1}/k_1$), which can be determined by equilibrium experiments. Those mass transfer resistances include the bulk diffusion resistance, the film diffusion resistance, the pore diffusion resistance and the surface reaction resistance (the resistance on the wall surface of the pore). Hence the k_1 and k_{-1} here are no longer simple rate constants of adsorption and desorption, but lumped constants, which combine all the significant contributions of the mass transfer and adsorbent-adsorbate interaction. The model is based on the same assumption that the ion exchange reaction rate is slow compared with the mass transfer rate so that the protein concentration is the same inside and outside the particle.

The rate equation accounts for the reversible adsorbate-adsorbent interaction is expressed as:

$$C_b = C_0 - \frac{v}{V}\left[\frac{(b+a)(1-\exp\{-2(av/V)k_1 t\})}{\left(\frac{b+a}{b-a}\right)-\exp\{-2(av/V)k_1 t\}}\right] \qquad 2.3$$

where

$$a^2 = b^2 - \left(\frac{C_0 V}{v}\right)q_m \qquad 2.4$$

$$\text{and } b = \frac{1}{2}\left(\frac{C_0 V}{v} + q_m + \frac{K_d V}{v}\right) \qquad 2.5$$

(2) The pore diffusion model

The kinetic constant model developed by Chase is based on the assumption that the mass transfer is much faster than the interaction rate, which is often contradictory to the actual situation. It has been shown that the mass transfer resistance plays an important role in the kinetics of a chromatographic process, especially when the protein/pore size ratio is large or when the particle size is big. Effects that contribute to the slow pore diffusion of protein include (1) the tortuosity of the pore channels; (2) the rotational masking of the protein affected by steric hindrance; (3) non-specific adsorption onto heterogeneous ligands/sites; (4) hydrophobic reaction between the adsorbent matrix and the protein structure.

Arnold *et al.* (1985) developed a pore diffusion model which was based on the assumption that the rate of adsorption was so fast that equilibrium between the internal liquid and the pore surface was achieved and that the film diffusion resistance is also negligible. In other words, the pore diffusion is the rate-limiting step. With the pore diffusion model, the protein concentration in the bulk solution as a function of time is given by the following equations:

$$\frac{D_p(1-\varepsilon)t}{R_0^2\varepsilon} = \frac{1}{3}\ln\left|\frac{a^3+w^3}{a^3+1}\right| + \frac{1}{6a}\ln\frac{(a^2-a+1)(a+w)^2}{(a^2-aw+w^2)(a+1)^2} + \frac{1}{a\sqrt{3}}\{\tan^{-1}\frac{(2-a)}{a\sqrt{3}} - \tan^{-1}\frac{(2w-a)}{a\sqrt{3}}\}$$

2.6

$$\gamma = \frac{\varepsilon C_0}{q_0(1-\varepsilon)\rho_p} \qquad 2.7$$

$$a = \left|(\gamma-1)^{\frac{1}{3}}\right|, \text{ when } \gamma \neq 1 \qquad 2.8$$

$$a = 0, \text{ when } \gamma = 1 \qquad 2.9$$

$$w = \left\{1-\gamma\left(1-\frac{C}{C_0}\right)\right\}^{\frac{1}{3}} \qquad 2.10$$

(3) The tw- phase diffusion model

The two phase diffusion model, which was first used to describe the diffusion of small ions in packed ion exchange columns (Helfferich, 1962), assumes that the ion exchange interaction is fast hence the limit factor is the resistance of diffusion. The overall resistance to diffusion is approximated by two effective films, one in the bulk solution surrounding the particle and the other in the particle itself. Gramham and Fook (1982) applied the two-phase diffusion model to the protein. The two phase diffusion model gives,

$$ln\,[1\text{-}F(t)] = -\frac{3Kt}{R_0}\left(\frac{v}{V}+\frac{1}{m''}\right) \qquad 2.11$$

where t is the time of the adsorption, R_0 the radius of ion exchange particle, v the volume of ion exchange particles in solution, and V the solution volume. $F(t)$ is the fractional conversion, which is given by

$$F(t) = \frac{(q_0 - q)}{(C_0 - C)} \qquad 2.12$$

where q_0 and C_0 are the initial protein concentrations in particle and solution, respectively; and q and C the average protein concentrations in particle and solution at any time t, respectively. K is the overall mass transfer coefficient, and m'' is an equilibrium parameter which is obtainable by the method presented by Graham and Fook (1982).

2.2 ION EXCHANGE ADSORPTION PROCESSES

There are several different column operations being used for ion exchange adsorption processes, including packed beds, conventional fluidized beds, expanded beds, magnetically stabilized fluidized bed (Figure 2.3), and the newly developed liquid-solid circulating fluidized beds. Each process has its advantages and disadvantages and are employed for different purposes.

2.2.1 Packed Bed Processes

Ion exchange adsorption is most commonly conducted in a packed bed column. In a packed bed ion exchange adsorption process, the preclarified broth is introduced from the top or the bottom of a packed bed ion exchange column, effluent is monitored to check the protein concentration in it until most ion exchangers are saturated with proteins, which is indicated by the significant increase of the concentration of the target proteins in the effluent. The column is then washed and stripped with the extracting buffer. The fractions of effluent containing high concentration of target proteins are collected for further purification or/and concentration.

Purification of proteins by adsorption techniques is most commonly carried out using fixed bed techniques. However, although the isolation of proteins from the process liquid is relatively efficient, the liquid has to be free of particulates before being processed by a packed bed. Otherwise, the particulates will be restrained in the bed and will eventually clog the bed. Removal of particles requires an additional separation step upstream of the adsorption column. Unit operations such as filtration, centrifugation and solids settling are commonly used for the removal of particulates from the raw broth. These operations are usually expensive and may result in the loss of considerable amounts of product. This is particularly true in the case for protein recovery since a typical biological broth containing proteins (e.g. fermentation broth) contains a large amount of small solids (e.g. cell debris). Clearly a technique that would enable a protein to be adsorbed from the bulk liquid, without prior removal of particulate matter, is very advantageous.

2.2.2 Fluidized Bed Processes

Conventional fluidized beds have been suggested by Bartels *et al.* (1958) to overcome the limitation of packed bed system. They used fluidized cation exchangers in the purification of streptomycin from whole *Streptomyces* broth. Later, Belter *et al.* (1973) described a whole broth adsorption of novobiocin on fluidized anion exchangers. Sanchez *et al.* (1985) patented a fluidized bed chromatographic process for the protein extraction from unclarified whey.

A conventional fluidized bed consists of a column packed with ion exchange beads where the feeding fluid stream (Figure 2.3) is introduced through a liquid distributor at the bottom of the bed. Above a certain critical fluid velocity, called the minimal fluidization velocity, the ion exchange beads become suspended in the fluid stream. The conventional

fluidized beds have relatively large voidage between the adsorbents, which allows the cell debris and other small particulates to pass through. As long as the terminal velocities of the particulates in the broth are significantly lower than these of the adsorbent beads, the liquid velocity through the bed can be adjusted so that the particulates can be entrained out while the adsorbent beads are retained. This is the rationale of its application in the protein recovery from whole broth.

In the packed bed column, particulates are trapped between the voids between the particles because the voids are fixed and small. However, in a fluidized bed, the velocity of the upward liquid is larger than the minimal fluidization velocity of the particles and the particles are suspended in the column. The voids between the particles can be controlled by the liquid velocity in the column. Therefore, when the liquid velocity in the column is larger than the terminal velocity of the particulates in the feed and less than the terminal velocity of the adsorbents, the particulates will be carried away with the liquid while the adsorbents are restrained in the column. Therefore, an unclarified feed containing small particulates can be treated directly using a fluidized bed adsorption system. However, the conventional fluidized beds have the inherent disadvantage of low dynamic capacity due to the strong backmixing in the bed, which leads to early product leakage.

2.2.4 Expanded Bed Adsorption

A novel technique called expanded bed adsorption has been developed recently to minimize the backmixing problem. The equipment needed for the operation of expanded-bed operation is very similar to that of a conventional fluidized bed. The major differences between a conventional fluidized bed and an expanded bed include: (1) the liquid velocity in an expanded bed is lower than in a conventional fluidized bed thus the

bed is expanded instead of fully fluidized; and (2) the ion exchange particles used for expanded beds usually have high density and large particle size distribution. The density and size distribution of ion exchange particles are critical for the success of an expanded adsorption bed and specially designed ion exchange particles are needed. One strategy for the making of special ion exchange particles for expanded beds has been the development of composite adsorbents, where a core of inert dense component (e.g. quartz) is coated with an ion exchange material (e.g. agarose) to form a new type of ion exchanger with high density (e.g. Streamline^{TM} ion exchangers). Another approach is to use matrices that have an inherent high density (e.g. silica-based Spherosil ion exchange particles).

Streamline^{TM} ion exchangers are a good example of those adsorbents. Because of the inclusion of an inert crystalline-quartz core material provides the required high density for stable bed expansion, the particle size distribution can be controlled to ensure a uniform expanded bed with smaller, lighter particles in equilibrium in the upper part of the column and the larger, heavier particles in the lower part. Backmixing can be minimized under careful control of the fluidization conditions. Expanded bed adsorption for protein recovery has attracted intensive interest due to the advantages associate with it (Beck *et al.*, 1999; Bertrand *et al.*, 1998; Chang and Chase, 1996a and 1996b; Finette *et al.*, 1998; Hansen *et al.*, 1999; Johansson *et al.*, 1996; Karau *et al.*, 1997; Pessoa *et al.*, 1996; Ameskamp *et al.*, 1999).

Draeger and Chase (1990) compared breakthrough curves of fixed and expanded bed adsorption of Bovine Serum Albumin to Q-Sepharose Fast Flow and found that the expanded bed system behaved much the same way as the fixed bed system. This means that good separation performance similar to the fixed bed system can be achieved without the disadvantages of column plugging and high pressure drop. They further studied the adsorption of BSA in the presence of cells of *Alcaligenes eutrophus* in the same system

(Draeger and Chase, 1991). Later, Gilchrist *et al.* (1994) reported several commercial adsorbents (Spherodex DEAE and Spherosil DEAE) and a self-made bead (Ti-Cell-1 DEAE) for the protein adsorption in expanded beds using BSA as a model protein. Hansson *et al.* (1994) recovered a secreted recombinant protein, fusion protein ZZ-M5, to high purity from the culture medium by applying the cell-containing whole broth directly to the expanded bed packed with STREAMLINE^{TM} DEAE. Thommes and his colleagues (1995) discussed the whole broth recovery of monoclonal antibodies by expanded bed adsorption with a commercial adsorbent, STREAMLINE^{TM}-SP, and a self-derived particle, Bioran-SP. The disadvantages of the expanded bed is that it is a batch operation and the adsorbents suitable for expanded bed adsorption are expensive.

The adsorbents for use in expanded beds have been a major obstacle to the implementation of this technology. Attention must be given not only to the adsorption properties of the material, but also to the fluidization properties of the matrix. In addition, the adsorbent beads must have a range of diameters that are suitable for the generation of a stable expanded bed in an appropriate apparatus.

2.2.5 Magnetically Stabilized Fluidized Bed (MSFB)

In late 1970's, Rosensweig and his co-workers (1970) found that fluidization of magnetically susceptible solids can be stabilized in a uniform gradientless magnetic field in which the individual particles experience no net force. Stabilization is observed over a wide range of field strengths and fluidization velocities. The effect of the magnetic field can be viewed roughly as creating a magnetic dipole in each particle, which cause it to become "sticky" in a direction parallel to the field lines.

As is the case in a conventional fluidized bed, the particles in an MSFB behave as a fluid over a wide range of conditions. Unlike the conventional fluidized beds, however, the dispersion and backmixing of particulates in a MSFB are effectively zero. A few authors have reported their effort in using a MSFB for product adsorption. Burns and Graves (1985) described a MSFB system for continuous protein recovery using affinity chromatography. Cocker *et al.* (1997) reported the manufacturing of magnetite adsorbents for the use in a MSFB system. Nixon and his co-workers (1991) studied structure and performance of a MSFB system. Although the MSFB systems have many advantages such as large bed voidage, low pressure drop, good flow quality, and applicability of whole unclarified broth, there are also some significant problems associated those systems. The most significant disadvantages of the MSFB systems include the complexity of the systems and their requirement for specific magnetic adsorbent particles.

2.2.6 Liquid-Solid Circulating Fluidized Bed

The liquid-solid circulating fluidized bed (LSCFB) is a new type of liquid-solids contacting device having great potential in chemical engineering, biochemical engineering, and environmental engineering. Although the concept of a liquid-solid circulating fluidized bed (LSCFB) has been explored for less than a decade, it has attracted much interest due to the many advantages associated with it (Liang *et al.*, 1995; Liang *et al.*, 1997a, 1997b, 1997c; Roy *et al.*, 1997; Zheng *et al.*, 1999; Zhu *et al.*, 2000).

There are two types of LSCFBs: the riser-riser LSCFB and the riser-downcomer. A riser–riser LSCFB is comprised of two risers, which are connected to each other by two solids return pipes (Liang *et al.*, 1995). A riser-downcomer LSCFB system in contract is comprised of a riser and a downcomer with auxiliary parts. Please note, from here on, the

riser-downcomer type LSCFB will be referred to as LSCFB in this thesis. Development of an LSCFB ion exchange system is the topic of this thesis.

An LSCFB ion exchange system is an LSCFB equipped with ion exchange adsorbents of appropriate adsorption and hydrodynamic properties. Generally speaking, an LSCFB is comprised of a riser, a downcomer, a liquid-solid separator and other auxiliary components. The donwcomer is assigned as the absorber for protein adsorption and the riser the stripper for desorption and regeneration. Proteins are thus adsorbed onto the adsorbents in the downcomer and the loaded-adsorbents are regenerated simultaneously in the riser (stripper) in a continuous mode. Upon the achievement of dynamic seal between the two columns, the operating conditions in the two columns of an LSCFB system could be controlled independently with the solids circulating between the two columns (Bassi *et al.*, 2000; Lan *et al.*, 2000, Chapters 5 and 6). This unique feature of an LSCFB system makes it particularly efficient for adsorption processes using adsorbents with high selectivity but low adsorption capacity. For such adsorption, the adsorbents need to be regenerated frequently. In the LSCFB system, adsorption occurs in the downcomer and the loaded-adsorbents are regenerated in the riser. Therefore, the adsorption is carried out continuously with the adsorbents maintained in the active form.

Another unique feature of the LSCFB extractor is that the downcomer operates as an expanded bed with the adsorbent falling down and the liquid phase moving up. The space between particles in the downcomer can be maintained large to allow the passage of the colloids in the feed without clogging the bed. In other words, an unclarified broth containing colloids can be treated directly by an LSCFB extractor without preclarification. This will significantly simplify the overall purification scheme.

NOTE TO USERS

Page(s) not included in the original manuscript are unavailable from the author or university. The manuscript was microfilmed as received.

23

This reproduction is the best copy available.

UMI®

NOMENCLATURE

C protein concentration in bulk solution (mg/ml, g/L)

C_0 initial protein concentration in bulk solution (mg/ml, g/L)

C^* equilibrium solute concentration in bulk solution (mg/ml, g/L)

D distribution coefficient

D_f film diffusivity (cm^2/s)

D_p effective intra-pore diffusivity (cm^2/s)

$F_{(t)}$ Fractional obtainment equilibrium as described by Equation 2.12

k_1 Forward reaction rate constant ($cm^3/mg{\cdot}s$)

k_{-1} reverse reaction rate constant (1/s)

k rate constant of irreversible desorption reaction (1/s)

K overall mass transfer coefficient for film diffusion model (cm/s)

K_d dissociation coefficient (mg/ml, g/L)

m_s mass of ion exchangers (g)

m'' Equilibrium parameter giving the relation between the protein concentration in the solution and the protein concentration in the ion exchanger

q^* equilibrium solute concentration in ion exchanger phase (mg/g)

q_m maximum adsorption capacity (mg/g, mg/ml)

r radius of ion exchange particle (cm)

t time (min)

v volume of ion exchangers in solution (ml)

V volume of bulk solution (ml)

ε voidage in finite bath

ρ_p Density of ion exchange particle ($g\ ml^{-1}$)

REFERENCES

Alam J. M. and Qasim R., "Isolation and biological properties of phospholipases from the venom of sea-snake, Hydrophis spiralis." *Pakistan Journal of Zoology*. 1998; **30** (3): 191-201.

Ameskamp N., Priesner C., Lehmann J. and Luetkemeyer D., "Pilot scale recovery of monoclonal antibodies by expanded bed ion exchange adsorption." *Bioseparation* 1999; 8 (1-5): 169-188.

Anspach, F.B., A. Johnston, H.J. Wirth, K.K. Unger, and M.T.W. Hearn, *J. Chromatogr.*, 476, 205-225, (1989)

Barker C.A. and Moor C.V. Composition and properties of Spherosil-QMA whey protein concentrate. *Journal of Food Science* 51(4), 919-923 (1986)

Bassi, A.; Zhu, J.-X.; Lan, Q.; Zheng, Y. and Margaritis, A., (2000) "A Liquid-Solid Circulating Fluidized Bed Ion Exchange system." *USA and Canadian Patent* (filed October, 2000)

Batista I.F.C.; Oliva M. L.V.; Araujo M.S.; Sampaio M.U.; Richardson M.; Fritz H.; Sampaio C.A.M.; "Primary structure of a Kunitz-type trypsin inhibitor from Enterolobium contortisiliquum seeds." *Phytochemistry*-Oxford. 1996; **41** (4) 1017-1022.

Beck J.T., Williamson B., Tipton B. "Direct coupling of expanded bed adsorption with a downstream purification step." *Bioseparation* 1999; 8 (1-5): 201-207.

Bertrand O., Cochet S., Cartron J. P., "Expanded bed chromatography for one-step purification of mannose binding lectin from tulip bulbs using mannose immobilized on DEAE streamline^{TM}." *J. Chromatogr.* A, 822 (1) 19-28 (1998)

Boyer P. M. and Hsu J. T., "Adsorption equilibrium of proteins on a dye-ligand adsorbent." *Biotechnology Techniques* **4**(1): 61-66 (1990).

Burgess, KJ and Kelly, J. 1979. Selected functional properties of a whey isolate. J. of food technology 14: 325-329.

Burns, M.A. and D.J. Graves, "Continuous Affinity Chromatography Using a Magnetically Stabilized Fluidized Bed." *Biotechnol. Prog.* **1**, 95 – 103 (1989).

Byers, C.H., W.G. Sisson, T.S. Snyder, R.J. Beleski, U.P. Nayak and T.L. Francis, " Zirconium and Hafnium Separation in Sulfate Solutions Using Continuous Ion Exchange Chromatography." *US5618502* (1997).

Chan E.C., Chang C.C., Li Y.S., Chang C.A., Chiou C. C., Wu T.Z., "Purification and characterization of neutral sphingomyelinase from *Helicobacter pylori*." *Biochemistry*, 2000; **39** (16): 4838-4845.

Chang Y. K. and Chase H. A., "Development of operating conditions for protein purification using expanded bed techniques: The effect of the degree of bed expansion on adsorption performance." *Biotech. Bioeng.* 1996a; 49 (5) 512-526.

Chang Y.K. and Chase H.A. "Expanded bed adsorption for the direct extraction of proteins." *Separation for Biotechnology* 3: 106-112 (1993)

Chang Y. K. and Chase H. A., "Ion exchange purification of G6PDH from unclaarified yeast cell homogenate using expanded bed adsorption." *Biotech. Bioeng.* 1996b; 49 (2) 204-216.

Chang Y. K., Chen Y. H., Chien C. H., "Simple two-step procedure for purification of cloned small sialidase from unclarified *E. coli* feedstocks." *Enzyme-and-Microbial-Technology.* 1998; 23(3-4)204-210.

Chase, H.A., "Purification of Proteins by Adsorption Chromatography in Expanded Beds," *TIBTECH* 12, 296-303 (1994).

Cocker, T .M., C.J. Fee and A. Evans, "Preparation of Magnetically Susceptible Polyacrylamide/Magnetite Particles for Use in Magnetically Stabilized Fluidized Bed Chromatography." *Biotech. Bioeng.* **53**, 79-87 (1997).

De-Lamotte F., Klein C., Issaly N., Gautier M. F., Boze H. "Single step purification of a wheat 9 kDa lipid transfer protein secreted by *Pichia pastoris*." Biotechnology Techniques 1999, 13 (5): 351-354.

De-Lange D.J.; Potgieter C.M.; Smit A.J.; Smit L.E., (1979), "The separation and amino acid content of bovine milk whey proteins." South African Journal of Dairy Technology 11(2): 51-55.

Devi N.A. and Rao A.G.A., "Fractionation, purification, and preliminary characterization of polygalacturonases produced by *Aspergillus carbonarius*." *Enzyme and Microbial Technology.* 1996; **18** (1) 59-65.

Draeger N.M and Chase H. A. (1990a), "Protein adsorption in liquid fluidized beds. I". *Chem. E. Symposium Series* No. 118 pp 161-172

Draeger, N.M. and Chase, H.A. (1990b). In *Separations for Biotechnology* (Pyle, D.L., ed.), Elsevier Science Publishers, Barking, England **2**, 325

Draeger, N.M. and Chase, H.A. 1991. "Liquid Fluidized Bed Adsorption of Protein in the Presence of Cells". *Bioseparation* **2**:67-80

Etzel MR. 1995. Whey protein isolation and fractionation using ion-exchangers. In: *Bioseparation processes in food.* R.K. Sight and S.H. Rizvi (eds.). New York : M. Dekker, pp. 390-415.

Finette G.M.S., Baharin B., Mao Q.M. and Hearn M.T.W., "Optimization considerations for the purification of alpha1-antitrypsin using silica-based ion-exchange adsorbents in packed and expanded beds." *Biotechnol. Prog.* 1998; 14 (2) 286-293.

Finette G.M.S., Mao Q.M. and Hearn. M.T.W., "Comparative studies on the isothermal characteristics of proteins adsorbed under batch equilibrium conditions to ion-exchange, immobilised metal ion affinity and dye affinity matrices with different

ionic strength and temperature conditions." *J. Chromatogr.* A. 1997; 763 (1-2) 71-90.

Foster, d.h., Engelbrecht, R.S., and Snoeyink, V.L., "Sorption of proteinaceous materials on weak base ion-excahnge rsins", *American Chemical Society Division of Organic Coatings and Plastics Chemistry* **34**: 48 (1974)

Foster, d.h., Engelbrecht, R.S., and Snoeyink, V.L., "Application of weak base ion-excahnge rsins for removal of proteins", Environmental Science and Technology **11**(1). (1977)

Freundlich H., *Colloid and Capillary Chemistry*. London (1926)

Gailliot, F.P., Gleason, C., Wlson J.J., and Zwarick J., "Fluidized bed adsorption for whole broth extraction." *Biotechnol. Prog.*, **6:** 370-375

Gibert S., Bakalara N., and Santarelli X., "Three-step chromatographic purification procedure for the production of a His-tag recombinant kinesin overexpressed in E. coli." *Journal-of-Chromatography*-B. Jan. 14, 2000; 737 (1-2): 143-150.

Girardet J. M., Paquet D. and Linden G., "Effects of chromatographic parameters on the fractionation of whey proteins by anion exchange FPLC." *MILCHWISSENSCHAFT* 44(11): 692-696 (1989)

Gordon N.F., Tsujimura H., and Cooney C.L. "Optimization and simulation of continuous affinity-recycle extration." *Bioseparation* 1: 9-21, 1990

Haddad P.R.. and Jackson P.E., *Ion Chromatography*, Elsevier Science Publishers B.V., New York, pp. 21 (1990)

Hansen M. B., Lihme A., Spitali M.; King D., "Capture of human Fab fragments by expanded bed adsorption with a mixed mode adsorbent." *Bioseparation* 1999; 8 (1-5): 189-193.

Hajra S. and Chattoraj D. K., "Protein adsorption at solid-liquid interfaces: Part IV. Effects of different solid-liquid systems and various neutral salts." *Indian Journal of Biochemistry and Biophysics* 28(4): 267-279

Harsa, S., Zaror, C. A. and Pyle, D. L, "Adsorption of Kluyveromyces marxianus pectinase on CM- Sephadex® gels", *Enzyme Microb. Technol.* 15 (1993) 906-915.

Hashim, M. A., Chu, K.-H. and Tsan, P.-S., "Effects of ionic strength and pH on the adsorption equilibria of lysozyme on ion exchangers", *J. Chem. Tech. Biotechnol.* 62 (1995) 253-260.

Higgins, I.R., "Continuous Ion Exchange of Process Water." *Chem. Eng. Prog.*, **65**(6), 59-62 (1969).

Himsley, A., "Continuous Countercurrent Ion Exchange Process." *US4279755* (1981).

Hjerten S., Mohammad J. Eriksson K.O., Liao J.L., "General methods to render macroporous stationary phases nonporous and deformable, exemplified with agarose and silica beads and their use in highly-erformance ion-exchange and hydrophobic-interaction chromatography of proteins.", *CHROMATOGRAPHIA* 31(1-2): 85-94 (1991)

Horstmann, B.J., C.N. Kenney, and H.A. Chase, *J. of Chromat.* V361, 179, (1989)

Huang, J-X., Schudel, J. and Guiochon, G., "Adsorption behavior of albumin and conalbumin on TSK-DEAE 5PW anion exchanger", *J. Chromatogr.* 504 (1990) 335-349.

Jenkins W. T., "Thermodynamic bookkeeping: A reinvestigation of proton and dicarboxylic acid binding to aspartate aminotransferase." *BIOCHIMIE* (PARIS) 71(4): 405-410 (1989)

Johnston A. and T.W. Hearn, J. of Chromat., V512, 101, (1990)

Johansson H. J., Jagersten C. and Shiloach J., "Large scale recovery and purification of periplasmic recombinant protein from E. coli using expanded bed absorption chromatography followed by new ion exchange media." *Journal of Biotechnology.* 1996; 48(1-2) 9-14.

Karau A., Benken C., Thoemmes J., Kula M. R., "The influence of particle size distribution and operating conditions on the adsorption performance in fluidized beds." *Biotech. Bioeng.* 55 (1)54-64 (1997)

Korkisch J., Handbook of Ion Exchagne Particles: Their Application to Inorganic Analytical Chemistry, Volume I, pp 30-34, CRC Press, Inc., Florida, US (1989)

Kunin R, "the Theory and Mechanism of ion Exchange", in Ion Exchange Particles, 2nd edition, John Wiley & Ons, Inc. New York, pp5-33 (1963)

Kurz, M.; Guba, W., Vertesy, L.; (1998) "Three-dimensional structure of moenomycin A: A potent inhibitor of penicillin-binding protein 1b." European Journal of Biochemistry. **252** (3): 500-507.

Lan, Q., A. Bassi and A. Margaritis, J.-X. Zhu, and G. Rowe, "Whey Protein Recovery in Liquid Solid Circulating Fluidized Beds". Presentation at 48th Canadian Chemical Engineering Conference. 1998.10, London, Ontario, Canada

Lan Q., A.S. Bassi, J.-X. Zhu and A. Margaritis, "An Investigation on the Protein Adsorption in an LSCFB Ion Exchange System", Presentation at 49th Canadian Chemical Engineering Conference. 1999.10, Saskatchewan, Ontario, Canada

Lan, Q., J.-X. Zhu, A. Bassi, A. Margaritis, Y. Zheng and G. Rowe, "Continuous Protein Recovery Using a Liquid-Solid Circulation Fluidized Bed Ion Exchange System: Modelling and Experimental Studies." *Can. J. Chem. Eng.* **78**: 858-866 (2000)

Lan, Q., A.S. Bassi, J.-X. Zhu and A. Margaritis, "Continuous Protein Recovery Using a Liquid-Solid Circulating Fluidized Bed (LSCFB) Ion Exchange System." *AICHE J.*, submitted (2001a)

Lan, Q., A. Bassi, J.-X. Zhu and A. Margaritis, "Recovery of Proteins from Cheese Whey Using a Continuous Liquid-Solid Circulating Fluidized Bed Ion-exchange System." *Biotech. & Bioeng.*, submitted (2001b)

Leaver, G., Conder, J. R. and Howell, J. A., "Adsorption isotherm of albumin on a cross-linked cellulose chromatographic ion exchanger I." *Chem. E. Symposium Series* 118 (1990) 1-15.

Letourneur D., Migonney V., Muller D., Jozefowicz M., "Phosphorylated polystyrene particles in highly-erformance ion-exchange chromatography." *J. CHROMATOGR.* 589(1-2): 87-92 (1992)

Levison P.R., Jones R.M.H., Toome D.W., Badger S.E., Streater M., Pathirana N.D., "Influence of flow-rate on the chromatographic performance of agarose- and cellulose-based anion-exchange media." *J. Chromatogr.* 1996; **734** (1) 137-143.

Liang, W.G., Z.Q. Yu, Y. Jin, Z.W. Wang, Y. Wang, "Synthesis of Linear Alkylbenzene in a Liuid-Solid Circulating Fluidized Bed Reactor." *J. Chem.Technol. Biotechnol.* **62**: 98 (1995)

Liang, W.-G., J.-X. Zhu, Y. Jin, Z.W. Wang, Z.Q. Yu and J. Zhou, "Radial Nonuniformity of Flow Structure in a Liquid-Solid Circulating Fluidized Bed." *Chem. Eng. Sci.* **51**, 2001-2010 (1996).

Liang, W-G. and J-X. Zhu, "A Core-Annulus Model for the Radial Flow Structure in a Liquid-Solid Circulating Fluidized Bed (LSCFB)." *Chem. Eng. J.* **68**, 51-62 (1997a).

Liang, W-G. and J-X. Zhu, "Effect of Radial Flowrate Nonuniformity on the Alkylation Reaction in a Liquid-Solid Circulating Fluidized Bed (LSCFB) Reactor." *Ind. Eng. Chem. Res.* **36**, 4651-4658 (1997b).

Liang, W-G., S-L. Zhang, J-X. Zhu, Y. Jin, Z-Q. Yu and Z-W. Wang, "Flow Characteristics of the Liquid-Solid Circulating Fluidized Bed." *Powder Technol.* **90**, 95-102 (1997c).

Linden T., Ljunglof A., Kula M.R., Thoemmes J., "Visualizing two-component protein diffusion in porous adsorbents by confocal scanning laser microncopy. *Biotech. Bioeng.*, 1999; **65** (6): 622-630.

Maggo S., Malhotra S.P., Dhawan K., Singh R., "Purification and characterization of protease inhibitor from rice bean (Vigna umbellata T.) seeds." *Journal-of-Plant-Biochemistry-and-Biotechnology.* 1999; **8**(1) 61-64.

Mccartney J.E., "Rapid purification of a recombinant protein using tandem radial flow ion-exchange column chromatography." *BIOTECHNIQUES* **11**(5): 648-649 (1991)

Nash D.C. and Chase H.A."Comparison of diffusion and diffusion-convection matrices for use in ion-exchange separations of proteins." *J. Chromatogr.* 1998; **807**(2)185-207.

Nichols J.A. and Morr C.V., " Spherosil-S ion exchange process for preparing whey protein concentration." *Journal of Food Science* 50(3): 610-614 (1985)

Nixon, L., C.A. Koval, L. Xu, R.D. Noble and G.S. Slaff, "The Effects of Magnetic Stabilization on the Structure and Performance of Liquid Fluidized Beds." *Bioseparation* **2**, 217-230 (1991).

Outinen M., Tossavainen O. and Syvaoja E.L., "Chromatographic fractionation of alpha-lactalbumin and beta-lactoglobulin with polystyrenic strongly basic anion exchange particles." *Lebensmittel-Wissenschaft-and-Technologie.*29 (4) 340-343 (1996a).

Outinen M., Tossavainen O., Tupasela T., Koskela P.,Koskinen H, Rantamaki P., Syvaoja, E.-L., Antila P., and V. Kankare "Fractionation of proteins from whey with different pilot processes". *Lebensmittel-Wissenschaft & Technologie* **5&6**, 411-417 (1996b).

Oyama. E. and Takahashi H., "Purification and characterization of a thrombin-like enzyme, elegaxobin, from the venom of Trimeresurus elegans (Sakishima-habu)." *Toxicon.*, 2000; **38** (8): 1087-1100.

Paterson, R., "Equilibrium Studies". In *An Introduction to Ion Exchange.* Heyden & Son Ltd., London, Great Britain. pp 22-37 (1970)

Patra A.K., Mukhopadhyay R., Mukhija R., Krishnan A., Garg L.C., Panda A.K., "Optimization of inclusion body solubilization and renaturation of recombinant human growth hormone from *Escherichia coli*." *Protein Expression and Purification.* 2000; **18** (2): 182-192.

Pessoa A. Jr, Hartmann R., Vitolo M., Hustedt H., "Recovery of extracellular inulinase by expanded bed adsorption." *J. of Biotechnol.* 1996; 51 (1) 89-95.

Pereira J. A. M., Rosa P. D. T. E., Pastore G. M., Santana C. C. "Expanded-bed adsorption utilizing ion-exchange particle to purify extracellular beta-galactosidase." *Applied Biochemistry and Biotechnology.* Spring, 1998; 70-72 (0) 779-787.

Porter, R.R., "Continuous Ion Exchange Process and Apparatus." US3879287 (1975).

Pungor, E., N.B. Afeyan, N.F. Gordon and C.L. Cooney, "Continuous Affinity-Recycle Extraction: a Novel Protein Separation Technique." *Bio/Technology* **5**, 604-608 (1987).

Ratnayake C.K. and Regnier F.E., "Study of protein binding to a silica support with a polymeric cation-exchange coating." *J. Chromatogr.* 1996; 743 (1) 15-23.

Rodrigues, M.I., C.A. Zaror, F. Maugeri and J.A. Asenjo, "Dynamic Modelling, Simulation and Control of Continuous Adsorption Recycle Extraction." *Chem. Eng. Sci.* **47**, 263-269 (1992).

Roush D. J., Gill D. S., Willson R. C., "Electrostatic potentials and electrostatic interaction energies of rat cytochrome b-5 and a simulated anion-exchange adsorbent surface." *Biophysical Journal.* 1994; 66 (5) 1290-1300.

Rowe, G.E., A. Margaritis, Q. Lan, A. S. Bassi and J.-X. Zhu, "A new kinetic model of protein adsorption on suspended anion-exchange particles", *Biotech. Bioeng.*, 65(6) 613-621 (1999)

Roy, S., J. Chen, S.B. Kumar, M.H. Al-Dahhan and M.P. Dudukovic, "Tomographic and Particle Tracking Studies in a Liquid-Solid Riser." *Ind. Eng. Chem. Res.* **36**:4666-4669 (1997)

Skudder P.J., "Evaluation of a porous silica-based ion-exchange medium for the production of protein fractions from rennet whey and acid-whey." *Journal of Dairy Research* 52(1): 167-182 (1985)

Slater, M.J. and P. Prud'homme, "Continuous Ion Exchange in Fluidized Beds." *Can. Mines Br., Tech. Bull.*, **158**, 1-67 (1972).

Stahlberg, J., "Combined effect of coulombic and van der Waals interactions in the chromatography of proteins", *Anal. Chem.* 64 (1992) 3119-3124.

Sunitha K., Chung B.H., Jang K.H., Song K.B., Kim C.H. and Rhee S.K., "Refolding and purification of Zymomonas mobilis levansucrase produced as inclusion bodies in fed-batch culture of recombinant Escherichia coli." *Protein Expression and Purification* 2000; **18** (3): 388-393.

Turner, J.C.R. and M.R. Church, "A Continuous Ion Exchange Column." *Trans. Instn. Chem. Engrs.* **41**, 283-288 (1963).

Ulusu N.N., Kus M.S., Acan N.L., Tezcan E.F., "A rapid method for the purification of glucose-6-phosphate dehydrogenase from bovine lens." Ulusu N.N., Kus M.S., Acan N.L., Tezcan E.F. *International Journal of Biochemistry and Cell Biology.* 1999; **31** (7):787-796.

Vujcic M.T., Dordevic M. R., Kanazir D. T., Vujcic Z.M., Jankov R.M., "Partial purification of glucocorticosteroid binder IB by cortexolone affinity matrix." *Proceedings of the Indian National Science Academy Part B Biological Sciences.* 1995; 61 (4) 249-258.

Weaver L.E. Jr and Carta G., "Protein adsorption on cation exchangers: Comparison of macroporous and gel-composite media." *Biotechnol. Prog.* 1996; 12 (3) 342-355.

Whitley, R.D., Wachter, R., Liu, F., and N.-H. Wang, (1989) "Ion-Exchange Equilibria of Lysozyme, Myoglobin and Bovine Serum Albumin: Effective Valence and Exchange Capacity." *J. of Chromatogr.* **465,** 137-156

Yamamato, S., Nakanishi, K. and Matsuno R., *Ion-Exchange Chromatography of Proteins*, pp35-106, Marcel Dekker Inc., New York, USA (1988)

Ye X.Y., Wang H.X. and Ng T.B., "Dolichin, a new chitinase-like antifungal protein isolated from field beans(Dolichos lablab)." *Biochemical-and-Biophysical-Research-Communications.* 2000; **269**1): 155-159.

Yoshida H., Nishihara H., Kataoka T., "Adsorption of BSA on QAE-dextran: Equilibria." *Biotech. Bioeng.* 1993; 41 (2) 280-286.

Yu Y. and Sun Y., "Macroporous poly(glycidyl methacrylate-triallyl isocyanurate - divinylbenzene) matrix as an anion-exchange particle for protein adsorption." *J. Chromatogr.* A. **855** (1): 129-136. (1999).

Zheng, Y., J.-X. Zhu, J. Wen, S. Martin, A.S. Bassi, and A. Margaritis, "The Axial Hydrodynamic Behavior in a Liquid-Solid Circulating Fluidized Bed." *Can. J. Chem. Eng.* 77, 284-290 (1999)

Zhu J-X, Zheng Y, Karamanev DG, and Bassi AS, "(Gas-) Liquid-Solid Circulating Fluidized Beds and their Potential Applications to Bioreactor Engineering", *Can. J. Chem. Eng.*, **78**, 82-94 (2000).

Table 2.1 Separation techniques used in protein purification

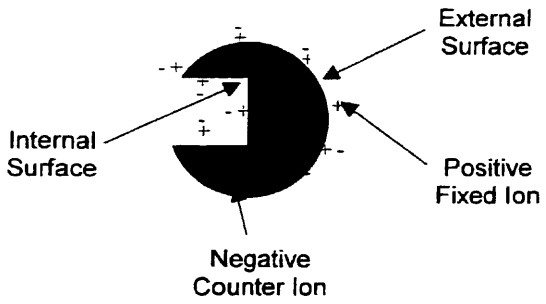
Technique	Examples
Precipitation	Ammonium sulfate precipitation, isoelectric point precipitation, hot-shock precipitation, solvent precipitation etc.
Aqueous two-phase extraction	PEG-Dextran two-phase extraction system, PEG-phosphate two-phase extraction system,
Adsorption	Ion exchange adsorption, affinity adsorption, hydrophobic adsorption
Liquid Chromatography	Ion exchange chromatography, affinity chromatography, hydrophobic chromatography, reverse-phase chromatography, size-exclusion chromatography, gel-filtration, isoelectric point chromatofocusing
Electrophoresis	Isoelectric point focusing electrophoresis, disk electrophoresis, cross-flow continuous electrophoresis
Membrane	dialysis, untralfiltration, cross-flow continuous filtration

Table 2.2 Functional groups found on some typical synthetic ion exchangers (Haddad and Jackson, 1990)

Cation Exchangers		Anion Exchangers	
Type	Functional Group	Type	Functional Group
Sulfonic acid	$-SO_3^- H^+$	Quaternary amine	$-N(CH_3)_3^+ OH^-$
Carboxylic acid	$-COO^- H^+$	Quaternary amine	$-N(CH_3)_2(E_tOH)^+ OH^-$
Phosphonic acid	$-PO_3H^- H^+$	Tertiary amine	$-NH(CH_3)_2^+ OH^-$
Phosphinic acid	$-PO_2H^- H^+$	Secondary amine	$-NH_2CH_3^+ OH^-$
Phenolic	$-O^- H^+$	Primary amine	$-NH_3^+ OH^-$
Arsonic acid	$-AsO_3H^- H^+$		
Selenonic acid	$-SeO_3^- H^+$		

Figure 2.1 Schematic illustration of structure of an anion exchanger

(a)



(b)

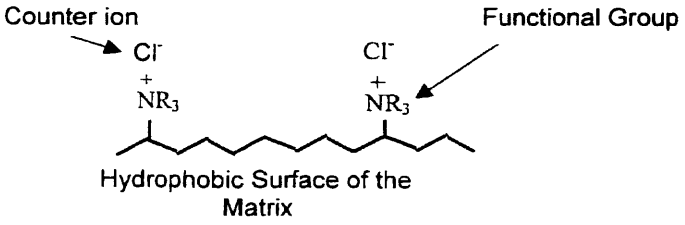


Figure 2.2 Diffusion of solute from bulk solution to the ion exchange sites

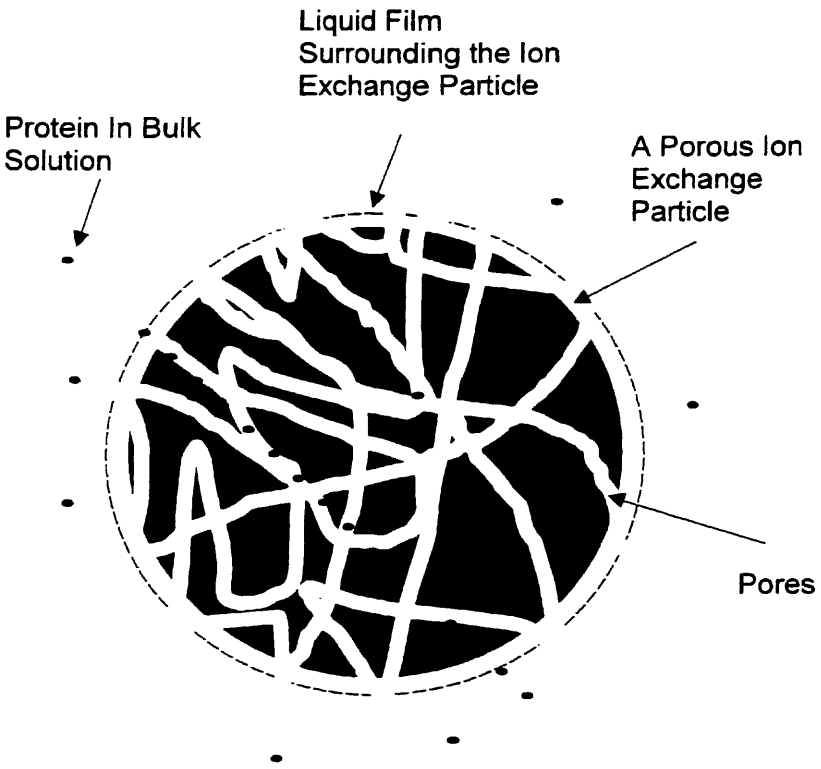
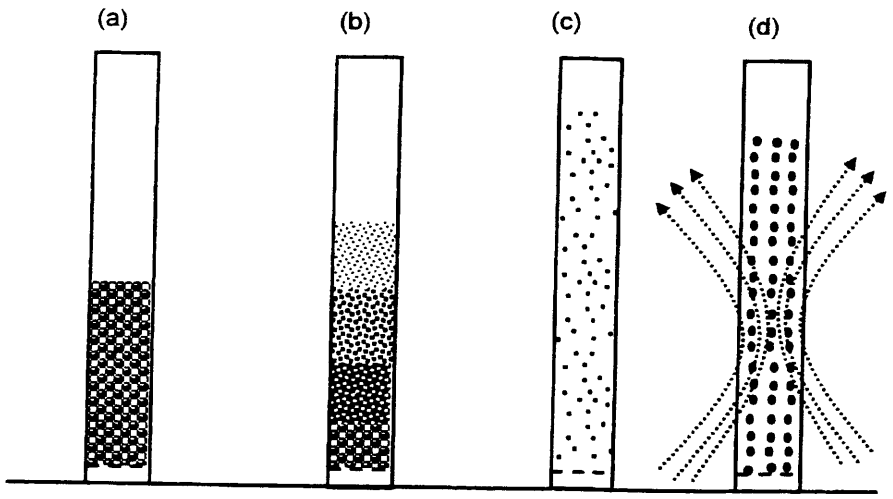


Figure 2.3 Schematic diagram of different fluidized beds (a) Packed Bed: particles are not fluidized and bed voidage is small; (b) Expanded Bed: particles suspended but not fully fluidized, bed voidage larger than a packed bed but less than that of a conventional fluidized bed, diverse particle size distribution reduces backmixing; (c) Conventional Fluidized Bed: particles fully fluidized, characterized by large bed voidage and strong backmixing; (d) Magnetically Stabilized Fluidized Bed: particles fully fluidized with large bed voidage, backmixing minimized by the orientation of magnetic particles in magnetic field.



Chapter 3. Apparatus: the Liquid-Solid Circulating Fluidized Bed Continuous Ion Exchange System

3.1 OVERALL DESCRIPTION OF THE LIQUID-SOLID CIRCULATING FLUIDIZED BED

A picture and a schematic diagram of the liquid-solid circulating fluidized bed (LSCFB) system are shown in Figures 3.1 and 3.2, respectively. The LSCFB system consisted of a Plexiglas riser column (1), a liquid-solid separator (2), a washing section below the separator (5), a top solids return pipe connecting the separator and the downcomer (6), a Plexiglas downcomer column (7), a washing section below the downcomer (9), and a bottom solids return pipe connecting the riser and the downcomer at the base (10). In the LSCFB, the adsorption of the proteins was carried out in the downcomer, and desorption in the riser. This was a continuous process with the ion exchanger particles circulated continuously between the two columns. Two different liquid streams, the feed in the downcomer and the extracting buffer in the riser, were used in this system. The riser was operated in the circulating fluidization regime and the downcomer in the conventional fluidization regime.

In the process of ion exchange, the feed liquor was introduced from the bottom of the downcomer and the regenerated particles from the top of the downcomer. The falling particles and the up-flowing feed liquor contact counter-currently and the proteins in the feed were adsorbed onto the ion exchange particles in the downcomer. The de-ionized

liquor left from the top of the downcomer through the raffinate outlet and the loaded particles fallen to the base of the riser from the bottom solids return pipe, after being rinsed through the washing section. The extracting buffer was applied to the riser at the bottom. The superficial liquid velocity in the riser was maintained in a range higher than the terminal velocity of the ion exchange particles so that the loaded particles were carried upward by the up flowing buffer. The buffer and the loaded ion exchange particles hence contact co-currently while desorption and regeneration of the particles proceeds in the riser. The extract and the regenerated ion exchange particles were separated by a liquid-solids separator on top of the riser. The extract was then collected from the extract outlet and the regenerated ion exchange particles returned to the downcomer through the top solids return pipe, after being rinsed through the washing section.

3.2 DESIGN CONSIDERATIONS

While designing a LSCFB ion exchange system, the following factors must be taken into consideration: 1) the height of downcomer/riser should be able to provide sufficient residency time for adsorption/desorption; 2) smooth solids circulation between the two columns should be easily achieved and maintained; 3) different liquid streams applied to the two different columns should be sealed off from each other; 4) particles must be washed thoroughly before they were transferred from downcomer to riser or from riser to downcomer; 5) the system should be robust. To achieve above requirements, all the components of the LSCFB system must be carefully designed.

3.2.1 Dimensions of the riser and the downcomer

The development of the design equations regarding the bed height of the riser and the downcomer is the major interest of Chapter 5. This chapter deals with only the actual dimensions of the two columns. The riser was an acrylical column of 38.1 mm in I.D. and 3 m in height, and the downcomer of 121 mm in I.D. and 2.5 m in height. The riser was connected to the downcomer on the upper part through the liquid-solids separator, the top washing section and the top solids return pipe. At the bottom, the riser and the downcomer were connected to each other through the bottom washing section and the bottom solids return pipe.

The extract exit on the separator was at the same level as that of the raffinate exit on the downcomer. Under such a design, the only pressure difference between the raffinate exit and the extract exit was caused by the solids holdup in the downcomer, as well as the difference in the riser and the separator. Since the density of the ion exchangers was only slightly higher than that of the water, the pressure difference was minimized and the system was stabilized in a satisfactory range.

The solids entrance on the downcomer was at the point 0.82 m lower from the raffinate exit. This design has two functions: 1) it provided enough vertical distance for the top washing section and the bottom solids return pipe that the regenerated ion exchange particles can be transferred by gravity; and 2) it provided a section of downcomer in which a freeboard free of ion exchange particle can be maintained under the raffinate exit so that the ion exchangers were retained while the raffinate was drained.

3.2.2 Distributors

The distributor of the riser is shown in Figure 3.3. There were two liquid inlets on the distributor, one for the primary stream and the other for the auxiliary stream. The inlet for the primary stream was a stainless steel pipe of 11 mm in I.D. It projected 36 mm into the riser column and thus at the same level as that of the solids entrance at the bottom of the riser. This arrangement increased the pressure drop across the bottom solids return pipe and made the system more stable. The auxiliary stream was introduced into the bottom of the riser through a perforated plate covered by a 100 micron stainless steel mesh. The function of the auxiliary stream was to stir up the particles at the bottom of the riser to be entrained up the riser by the combination of the primary and auxiliary liquid streams.

The distributor for the downcomer, as shown in Figure 3.4, was a cycle of a perforated stainless steel pipe. It allowed the particles to fall through it while introducing liquid into the downcomer.

3.2.3 Liquid-Solids Separator and the Top Washing Section

A schematic graph of the liquid-solids separator and the top washing section is shown in Figure 3.5. The liquid-solids separator was a hydraulic cyclone connected directly to the riser and through a solids return pipe to the downcomer. To prevent the loss of particles through the extract outlet, a 100 microns stainless steel mesh was used to cover the extract outlet. There were three mechanisms contributing to the liquid-solids separation: 1) the diameter of the separator was much larger than that of the riser and thus

the liquid velocity in it much lower than that in the riser. The liquid velocity in the separator was kept less than the terminal velocity of the particles so that the particles were separated from the liquid by gravity; 2) the mesh prevented particles loss in the separator while draining the liquid. It is important to note that if the liquid velocity in the separator is too large, the particles would accumulated in it and eventually block the solids circulation.

The top washing section consists of the funnel bottom of the separator and an acrylic pipe of 40 mm in diameter and 200 mm in height. The wash water was injected into the section through an injector at a level slightly higher than the top solids return pipe. Two features of the washing section help to enhance the washing efficiency: 1) the diameter of the injector was only slightly smaller than that the of the pipe and therefore the chance of particles passing the washing section without contacting fresh wash water was minimized; and 2) since the diameter of the pipe was smaller than the funnel bottom of the separator, the liquid difference in these two parts enhanced the mixing and thus the efficiency of washing. The wash water was combined with the extract and left the system from the extract exit. This arrangement dilutes the extract and was hence a disadvantage. Nevertheless, it dramatically simplified the structure of the system. Besides, the flowrate of the wash water was low compared to that of the extracting buffer, therefore the dilution effect was limited.

3.2.4 Dynamic Seal between the Two Columns

In the LSCFB system, there are two columns in which two distinct unit operations, namely adsorption and desorption, take place simultaneously and they are further linked by the solids flow. In such a system, the dynamic seal between the two columns is of critical importance since two liquid streams of opposite properties (feed of low ionic strength and high concentration of contaminants Vs extract of high ionic strength and low concentration of contaminants) are involved in the two columns and even a partial intermixing of those two streams will result in the failure of the whole operation. The dynamic seal between riser and downcomer is achieved by the maintenance of particle plugs formed in the top and bottom solids return pipes. The formation and maintenance of the ion exchange plugs is depended on the following design features and operation conditions:

Pressure difference across a solids return pipe is readily counter-balanced by the pressure drop across it. This prevents the back flow of liquids.

At the start up stage, initial particle plugs are formed with ion exchange particles fill the solids return pipes.

The operating conditions are kept in the stable operation window so that the particle plugs are maintained at steady state.

Butterfly valves are used to restrain the flow of particles from the solids return pipes and increase the pressure drops across the two solids return pipes.

Washing sections are designed to wash ion exchange particles before being transferred from one column to the other and therefore preventing the residual liquid from one column contaminating the main stream in the other column. Figure 3.5 illustrates the structure of the bottom washing section and the maintenance of dynamic seal at the bottom. Wash water is introduced into the bottom washing section. As far as the ion exchange particles in the bottom solids return pipe is maintained in the packed bed regime, forming a "particle plug", wash water will be forced upward into the washing

cabinets in which complete mixing of solids and liquid is achieved. Because the diameter of the lower part of the washing section is only slightly larger than that of the water injecting pipe, bypassing of ion exchange particles without washing is minimized. Furthermore, because the diameter of the lower part of the washing section is much smaller than that of its upper part, different liquid velocities in those two parts provided stronger mixing and hence more thorough rinsing.

There is no outlet for wash water at the bottom of the downcomer. The wash water hence joins the feed and is discharged from the raffinate outlet. This design has the disadvantage of diluting the feed and increase the liquid velocity in the downcomer (U_{ld}). However, it eliminates the necessity of the dynamic seal between the downcomer and the bottom washing sections, which much simplified the design and control of the whole system.

The dynamic seal between the separator and the downcomer at the top is based on the same principles as discussed above. When the particle plug in the top solids return pipe is properly maintained, the top wash water will rinse the regenerated particles before falling into the solids return pipe and prevent the leakage of proteins and salt in the extract from mixing with the raffinate. Similar to the bottom wash water, the top wash water combines with extract in the separator. Therefore, it will dilute the extract but not affect the liquid velocity in the riser.

3.3 SELECTION OF ION EXCHANGE PARTICLES FOR THE LSCFB ION EXCHANGE SYSTEM

A liquid-solid circulating fluidized bed (LSCFB) ion exchange system is basically a LSCFB equipped with ion exchangers of appropriate hydrodynamics and adsorption properties. Selection of suitable ion exchangers is a complicated process comprising different parameters. Some of the constraints dictating the search for ion exchange particles for an LSCFB ion exchange process are as follows:

1. Density and particle size

The density and particle size of the ion exchange particles will influence the terminal velocity and the mass transfer. The terminal velocity of a spherical particle in a given fluid is determined by the density, diameter and shape of the particle. For the use in an LSCFB system, the density and size of the ion exchangers must be large enough so that their terminal velocity is significantly higher than that of the largest particulates in the feed liquor. Otherwise, the colloids in the feed cannot be separated from the ion exchangers in the downcomer. Large terminal velocity of ion exchange particles also favors a large throughput due to the enlarged liquid velocity in the downcomer. However, when the diameter of the ion exchangers is too large, mass transfer resistance will be remarkably increased and the accessibility of internal surface decreased. Hence the choice of particle size is actually a compromise between different requirements.

2. Porosity

The porosity of ion exchange particles is highly important for an adsorbent for protein processing as it determines the accessibility of the proteins to the ion exchange ligands on the internal surface of an ion exchange particle. Studies demonstrated that the protein adsorption capacity of an ion exchange adsorbent depends remarkably on the pore size of

the adsorbent (Anspach *et al.*, 1989). It is a well-known fact that in protein adsorption, a major part of the internal surface of an adsorbent is not fully used, which is attributed to limited surface access (Unger and Janzen, 1986). The porosity of particles also has strong effects on the kinetics of protein adsorption because of its significant influence on the intra-pore diffusion.

3. Capacity

The adsorption capacity of the particle for the desired product must be of such a magnitude that the required yield, purity, and time cycle can be achieved within the economical constraints of the system (quantity of particles, column size, etc.).

4. Stability

None of the ion exchange particles is totally inert towards the broth and the eluent. Rather, they exhibit a limited lifetime, associated with degradation by dissolution, chemical surface reactions, aging, attrition, and other processes. The knowledge of the stability (chemically and mechanically) of the particles is hence very important for evaluation of the economics and practicality of the particles, especially for a continuous process as an LSCFB ion exchange system. In the case of protein adsorption, since a high porosity and a large pore size is essential for the ion exchange particles, the resistance of the particles to attrition assumes a significant importance.

5. Irreversible protein adsorption and denaturation

A certain degree of irreversible adsorption and protein denaturation is bound to happen in protein separation using ion exchange processes, which causes the loss of both the protein mass and its functionality. Partial unfolding or denaturation of proteins is known to be attributable to eluent-mediated and/or surface-induced dynamic effects (Hearn *et al.*, 1985). Possible hydrophobic interaction between proteins and ion exchanger matrix is hence an important factor to consider in choosing ion exchangers.

6. Fouling

Fouling is a well-known phenomenon in whole broth separation of proteins by adsorption. Colloidal fines or particulates such as cells, cell debris, and hydrolyses might be deposited in the pores of the particles and cause fouling. Fouling might also takes place through irreversible adsorption or protein-protein interaction in the pores.

7. Cost of Ion Exchange Particles

Ion exchange particles for large-scale chromatography should be available at a competitive price.

A number of commercial ion exchangers were considered for the project. Anion exchanger Diaion HPA25®, Sigma Chemical Co. (St Louis, MO), was selected as the most suitable for use in the LSCFB ion exchange extractor. The properties of anion exchanger Diaion HPA25 are shown in Table 3.1 and are discussed as follows:

- The capacity of BSA adsorption onto Diaion HPA25 is 88 mg/g, which is satisfactory for this system;
- The average diameter of Diaion HPA25 particles is 0.32 mm, and the wet density 1.08 kg/m^3, which make a terminal velocity of Diaion HPA25 in water of 0.004 m/s, sufficient for an LSCFB system;
- The exclusive size of Diaion HPA25 particles is larger than 100,000 dalton, which is significantly larger than the molecular weight of bovine serum albumin (BSA, 67,000 dalton) and other whey proteins;
- The pI of BSA and whey proteins are in the range of pH 3.5-5.5, the selection anion exchanger Diaion HPA25 allows the recovery of whey proteins from neutral solution with a pH at around 7.0. Therefore, the potential environmental problem of dealing with large amount of acidic waste stream, which is associated with the use of cation exchangers for those proteins, is avoided;
- The price of the particles is one of the lowest among commercial ion exchange particles. This is a very important factor to be considered for large-scale applications.

REFERENCES

Anspach, F.B., A. Johnston, H.J. Wirth, K.K. Unger, and M.T.W. Hearn, *J. Chromatogr.*, 476, 205-225, (1989)

Hearn M.T.W., A.N. Hodder, and M.I. Aguilar, *J. Chromatogr.*, V327, 47, (1985).

Unger K.K. and R. Janzen, Packing and stationary phase in preparative column liquid chromatography. 225-264,(1986).

Table 3.1 Properties of Diaion HPA25®

Matrix	Polystyrene (highly porous)
Functional Group	Quaternary Alkylamine
Ionic Form	Cl^{-1}
Average Diameter (d_p, mm)	0.32
Wet Density (ρ_s, g/mL)*	1.08
Total Exchange Capacity (Cl^-, meq/mL)	0.6
Protein Adsorption Capacity (BSA, mg/g)	88
Exclusive Size (dalton)	>100,000
Terminal Velocity (U_t, m/s)	0.004
Bed Expansion Index (n)	2.67

* Density of wet Diaion HPA25® particles equilibrated with 10 mM phosphate buffer

Figure 3.1 A of the pilot liquid-solid circulating fluidized bed ion exchange system in the Department of Chemical and Biochemical Engineering at the University of Western Ontario.

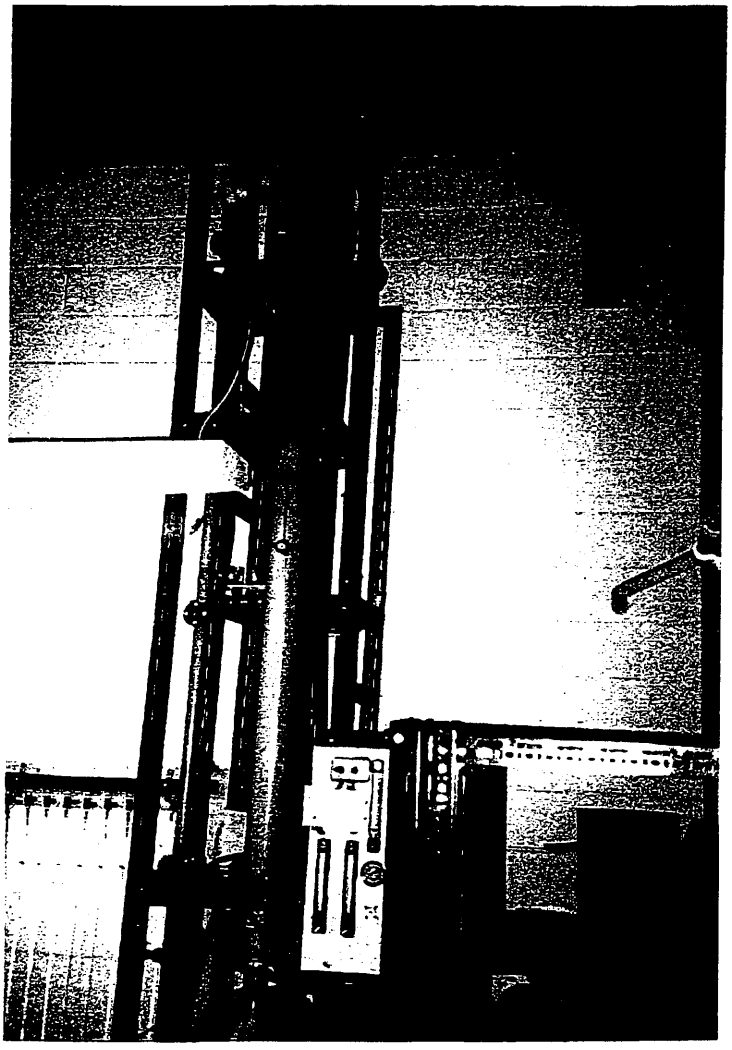


Figure 3.2 Schematic diagram of the liquid-solid circulating fluidized bed (LSCFB) ion exchange system. (1) Riser; (2) Solids-Liquid separator; (3) Extract Outlet; (4) Raffinate outlet; (5) Washing section of the separator; (6) Top solids return pipe; (7) Solids circulating rate measuring device; (8) Downcomer; (9) Distributor of the downcomer; (10) Washing section of the downcomer; (11) Bottom solids return pipe; (12) The primary stream in the riser distributor; (13) The auxiliary stream in the riser distributor; (14) Liquid distributor of the riser; (15) Butterfly valve.

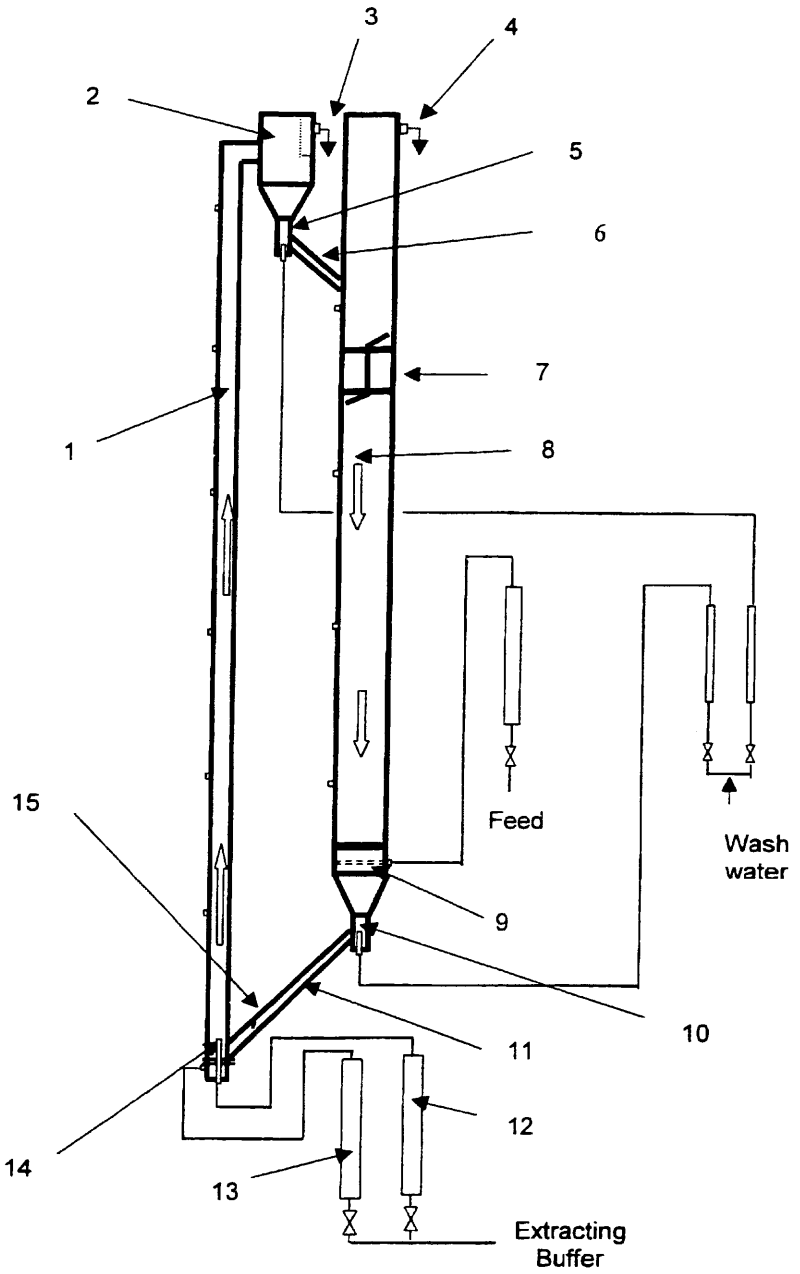

3
4
2
5
6
7
1
8
Feed
Wash
water
15
9
10
11
12
14
13
Extracting
Buffer

Figure 3.3 A schematic diagram of the riser distributor

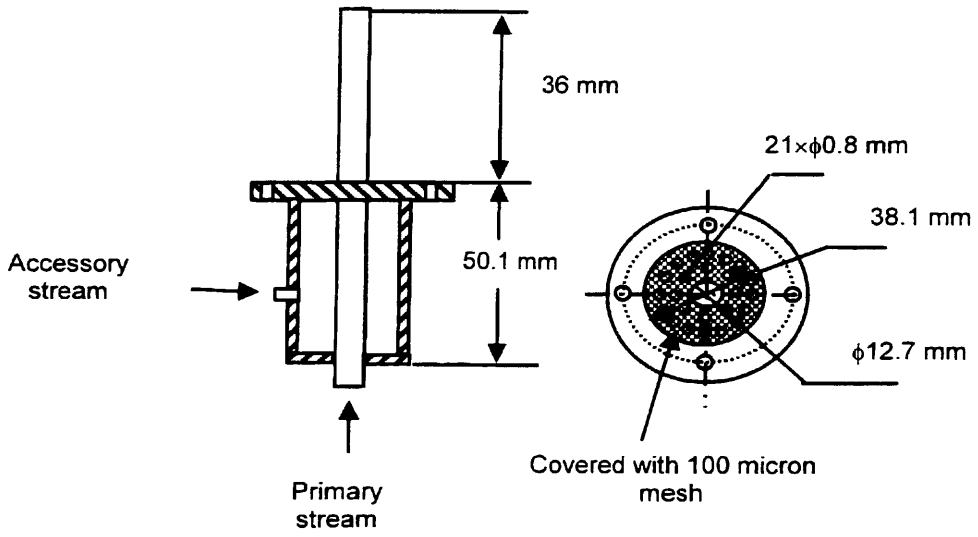


Figure 3.4 A schematic diagram of the downcomer distributor

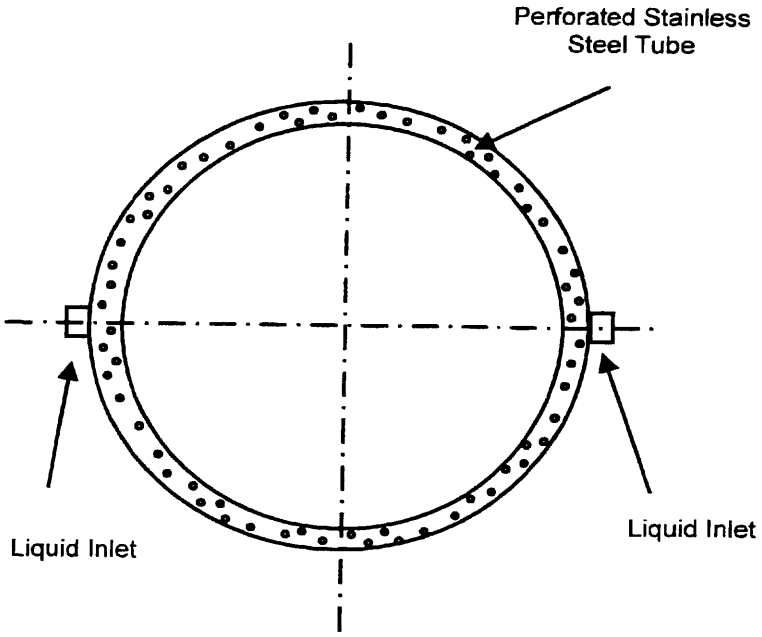


Figure 3.5 A schematic diagram of the combination of the liquid-solids separator and the top washing section

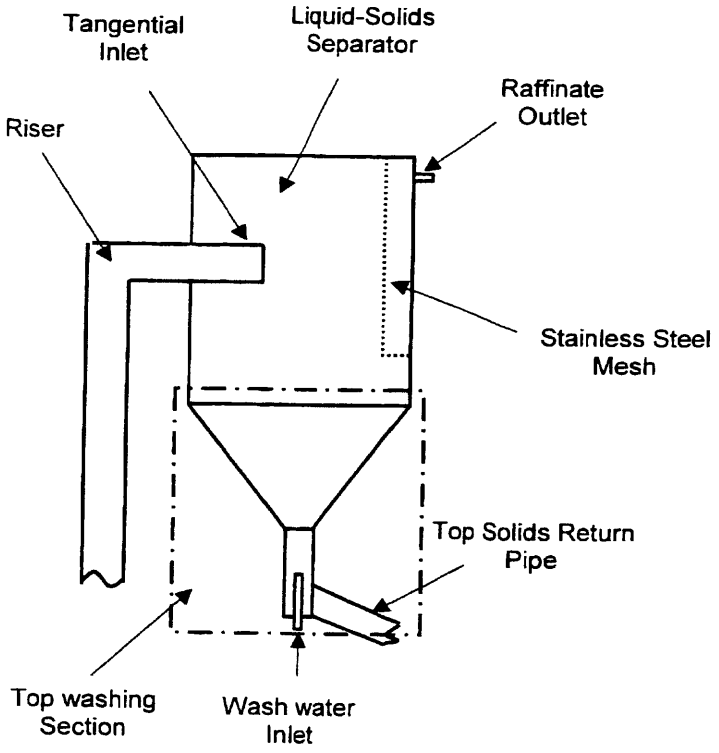
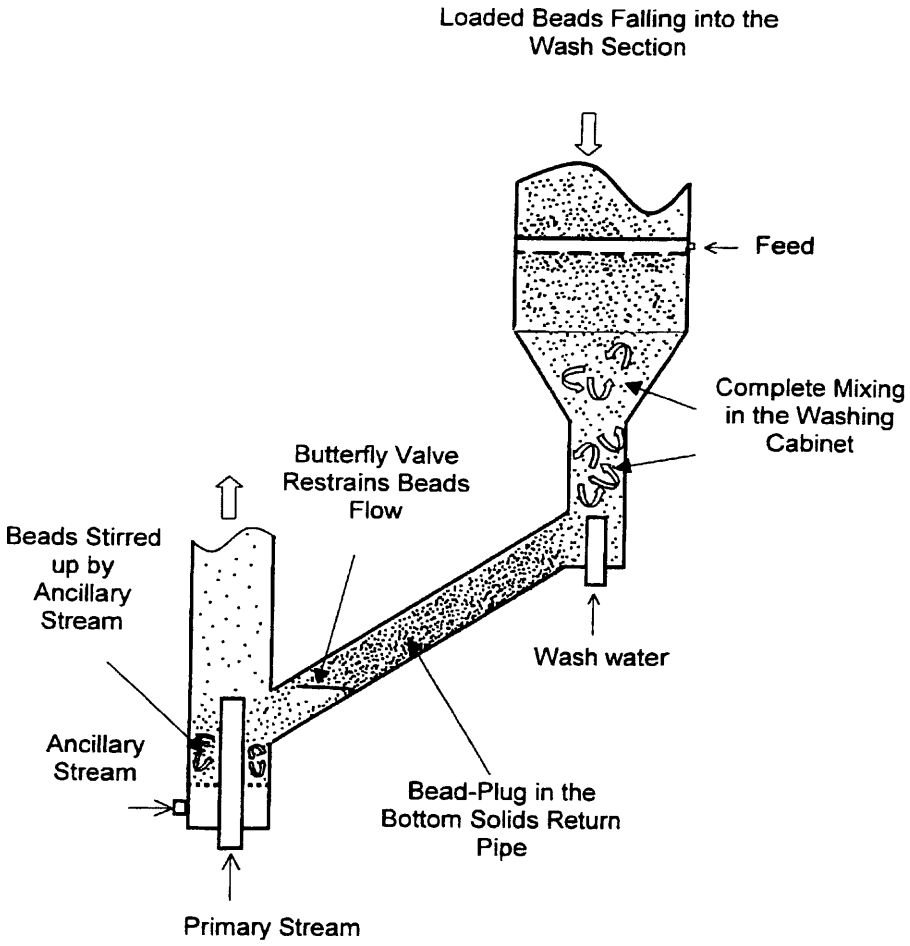


Figure 3.6 Schematic diagram of the base of the LSCFB system: dynamic seal between the riser and the downcomer



Chapter 4. Bovine Serum Albumin Adsorption onto Anion Exchanger Diaion HPA25: Equilibrium and Kinetic Characteristics

4.1 THEORY

4.1.1 Ion Exchange Equilibrium

The adsorption of protein onto an ion exchange adsorbent relies on the ion exchange reaction which can be simply described by equation 4.1, with the assumption that 1) all the adsorption site, S, have the same affinity for the protein, P; 2) one protein binds only to one adsorption sites; 3) protein-protein and protein-matrix interactions are absent and 4) the ionic strength of the bulk solution is low so that the competition from counter-ions are negligible. The ion exchange reaction therefore takes the following form:

$$P + S \underset{k_{-1}}{\overset{k_1}{\rightleftharpoons}} P\text{-}S \qquad 4.1$$

where k_1 and k_{-1} are the lumped forward and reverse reaction rate constants that take into account the mass transfer resistances when protein diffuses from the bulk solution to the adsorption site of the ion exchange reaction, respectively. Therefore, rate of adsorption is given by the following equation with a second order forward and first order reverse kinetics:

$$\frac{dq}{dt} = k_1 C q_f - k_2 q \qquad 4.2$$

where C is the concentration of the protein in the bulk solution, q the protein concentration adsorbed onto the ion exchangers, and q_f the free protein adsorption capacity (free ligands available for further protein adsorption expressed in protein adsorption capacity), which is the difference between the maximum adsorption capacity of the ion exchanger (q_m) and the protein concentration in the ion exchanger (q). Namely,

$$q_f = q_m - q \tag{4.3}$$

In other words, Equation4.2 can be expressed as Equation 4.4:

$$\frac{dq}{dt} = k_1 C(q_m - q) - k_2 q \tag{4.4}$$

At equilibrium conditions, the rate dq/dt is zero and Equation4.4 can be simplified as

$$q^* = \frac{q_m C^*}{K_d + C^*} \tag{4.5}$$

where q^* and C^* are the protein concentrations in the solid phase and the bulk solution at equilibrium, respectively. K_d is the dissociation constant, which is determined by the forward and reverse rate constant of the ion exchange reaction ($K_d = k_{-1}/k_1$).

2. Adsorption Kinetics

Chase (1987) has obtained the analytical solution for Equation 4.4 for the batch adsorption as the following:

$$C = C_0 - \frac{v}{V}\left[\frac{(b+a)(1-\exp\{-2(av/V)k_1 t\})}{\left(\frac{b+a}{b-a}\right) - \exp\{-2(av/V)k_1 t\}}\right] \tag{4.6}$$

where C_0 is the initial protein concentration in the bulk solution, v the volume of ion exchangers, V the volume of the bulk solution, a and b the equation constants determined as follows:

$$a^2 = b^2 - \left(\frac{C_0 V}{v}\right) q_m \qquad 4.7$$

$$\text{and } b = \frac{1}{2}\left(\frac{C_0 V}{v} + q_m + \frac{K_d V}{v}\right) \qquad 4.8$$

3. Kinetics of Protein Desorption in a High Ionic Strength Buffer

When anion exchange particles contact extracting buffer of high ionic strength, the counter-ions in the buffer (e.g. Cl^-) will compete for the functional groups on the ion exchanger and substitute proteins from their binding sites. Because the concentration of counter-ions (in the range of 0.2 - 0.5 M) is overwhelmingly higher than that of protein in both the ion exchanger phase and the external liquid phase (in the range of 1 μM - 0.1 mM), desorption of protein can be considered to be irreversible. The desorption of protein from ion exchangers can thus be represented by the following equation:

$$\text{I} + \text{P-S} \xrightarrow{k} \text{I-S} + \text{P} \qquad 4.9$$

where I is the counter-ion and k is the rate constant of the irreversible desorption.

Based on the same fact of the high concentration of counter-ions, it can be taken as constant throughout the desorption process. Therefore, the kinetics of desorption can be expressed as flowing:

$$\frac{dq}{dt} = -kq \qquad 4.10$$

where q is the concentration of BSA in the ion exchange particles, or in other words, the concentration of P-S.

Integration of Equation 4.7 gives the solid phase protein concentration profile for the desorption in a batch operation:

$$q = q_0 \times \exp(-kt) \qquad 4.11$$

where q_0 is the initial protein concentration in the ion exchangers.

4.2 MATERIALS AND METHODS

1. Equilibrium Studies

Equilibrium studies were conducted by weighing 0.5 g Diaion HPA25 synthetic anion exchanger particles into a 50-ml Erlenmeyer flask containing 25 ml of 10 mM appropriate buffer of specified pH and sodium chloride concentration. Bovine serum albumin (BSA), purchased also from Sigma, was used in adsorption/desorption experiments. Buffers of different pH were prepared as the follows: pH 3.0, citric acid/NaOH buffer; pH 4.0 and 5.0, sodium acetate/acetic acid buffer; pH 6.0-8.0, phosphate buffer; and pH 9.0, glycine NaOH buffer (Perin and Dempsey, 1974). The concentration of buffers was 10 mM and NaCl was used as the neutral salt for adjusting the ionic strength of solutions where necessary. The initial BSA concentration was varied as 0.8, 1.2, 1.6, 2.0, 2.4, 2.8 and 3.2 g/L. The flask was then sealed by parafilm "M" (American Can Company) and put on a shaker controlled at 25 °C and 200 rpm. After adsorption for 36 hours (experiments have shown that this time is enough to achieve

equilibrium under the experimental conditions), the liquid phase was centrifuged at 10,000 rpm for 10 minutes. The protein concentration of the supernatant was analyzed by measuring the absorbance at 280 nm using a Cary 50-Bio UV-visible spectrophotometer. The Langmuir parameters, namely the Maximum Capacity of BSA Adsorption onto Diaion HPA25 and the dissociation constant (K_d), were calculated using the curve fitter provided by the SigmaPlot™ software package according to the Langmuir equation.

2. Adsorption Kinetics

The kinetics of BSA adsorption onto Diaion HPA25 was studied using a Bellco reactor (approximately 200 ml) coupled with a Cary 50-Bio UV-visible Spectrophotometer (Figure 4.1). As shown in Figure 4.1, the setup for the kinetic studies were comprised of a Bellco reactor, a Manostat Cassette pump (VWR) and a Cary Bio-50 UV-visible spectrophotometer with a flowing cell. To study the kinetics of BSA adsorption onto Diaion HPA25, 6 g of Diaion HPA25 particles were pre-equilibrated with pH 7.0 (10 mM) phosphate buffer overnight and BSA solution of 2 g/l was prepared in the same buffer. 100 ml of 2 g/L BSA solution was used in the experiments. The change of the absorbance of the liquid phase was monitored at 280 nm.

3. Kinetics of BSA Desorption

Six grams of Diaion HPA25 was pre-equilibrated in 100 ml 2 g/L BSA solution prepared in 10 mM pH 7.0 phosphate buffer, drained and then washed using cold water three times. The loaded ion exchangers in exactly 100 ml of 10 mM, pH 7.0 phosphate buffer containing 0.4 M NaCl in the stirred Bellco reactor and monitor the absorbence at 280 nm.

4.3 RESULTS AND DISCUSSION

4.3.1 Equilibrium

1. Isotherm of BSA Adsorption onto Diaion HPA25

The isotherm of BSA adsorption on Diaion HPA25 in pH 7.0 phosphate buffer (10 mM) was shown in Figure 4.2. The BSA adsorption onto Diaion HPA25 in the low ionic range matches Langmuir isotherm. The maximum capacity at the above conditions was determined as 88 mg/g.

2. pH Dependence of the Maximum Adsorption Capacity (q_m)

The pH dependency of the maximum capacity of BSA adsorption onto Diaion HPA25 is shown in Figure 4.3. The adsorption capacity was zero when pH was less than pH 4.0. However, q_m increased dramatically to approximately 90 mg/g when the pH increased to 6.0. When the pH was further increased to 7.0, q_m increased slightly to 91.7 mg/g. After that, in the range of pH 7.0-9.0, the q_m decreased slightly with the increase of pH.

The dependency of the maximum capacity of BSA adsorption onto Diaion HPA25 can be explained by the amphoteric property of proteins. The net electric charge on the surface of a protein molecule can be either positive or negative, depending on the solution pH and the isoelectric point of the protein (pI). If the solution has a higher pH than the pI of the protein, the charge on the protein surface will be negative and the protein can be adsorbed onto anion exchanger and vice versa. The value of pH can also affect the conformation of the protein molecule and hence the mass transfer of the protein molecules from the bulk solution to the binding sites, the protein-ligand interaction and the protein-matrix interaction.

The pI of BSA was pH 5.13 (Etzel, 1990). Therefore, when the solution pH was less than 3.0, it was less than the pI of BSA and thus positively charged. Consequently, it could not be adsorbed onto the anion exchanger Diaion HPA25. When pH was above 6.0, the surface of BSA was negatively charged and can be adsorbed onto the anion exchanger Diaion HPA25. The slight change of q_m in the pH range of 6.0-9.0 may be explained by the fact that value of the positive charge on the BSA surface increase with the pH and the configuration also changed with pH. It is worthwhile to note that there was substantial adsorption of BSA onto Diaion HPA25 at pH 5.0, a pH slightly lower than the pI of BSA. This phenomenon may be contributed to the Donna potential existed in the anion exchanger, which created an inside pH approximately one unit high than that in the bulk solution. Therefore, when the bulk solution was at pH 5.0, the solution inside the anion exchanger had a pH of approximately 6.0, remarkably higher than the pI of BSA. From the above results, the optimal pH for BSA adsorption onto Diaion HPA25 under the tested conditions was determined to be pH 7.0.

3. Dependency of the Maximum Adsorption Capacity on Ionic Strength of the Solution

The influence of ionic strength on the capacity of protein adsorption onto ion exchange particles is a well-studied topic (Lan *et al.*, 2000b, see Chapter 6). However, studies are necessary for individual protein/ionic strength pairs to define the suitable ionic strength range for adsorption and desorption. The dependency of maximum adsorption capacity on ionic strength was studied in 10 mM pH 7.0 phosphate buffer using NaCl as the neutral salt for adjusting ionic strength. The maximum adsorption capacity was determined at different NaCl concentrations varied as 0, 0.01, 0.02, 0.03, 0.05, 0.10, 0.015, 0.20, and 0.3 M. As shown in Figure 4.4, q_m decreased significantly with the increase of NaCl concentration and the value of q_m was reduced to zero when NaCl

concentration was increased beyond 0.2 M NaCl. Therefore, a 10 mM pH 7.0 phosphate buffer containing 0.2 M or more NaCl can be used as an extracting buffer for stripping the loaded ion exchange particles. To achieve a thorough desorption and regeneration, a NaCl concentration of 0.4 M was employed for both the batch desorption experiments or a continuous operation in the LSCFB ion exchange system.

4.3.2 Adsorption kinetics

The results of batch adsorption kinetic studies are shown in Figure 4.5. The reaction constant k_1 for equation 3.6 was determined using the non-linear curve fitter provided by the SigmaPlot software package. Under the specified experimental conditions, i.e., BSA concentration 2 g/L, temperature 24 °C, stirring 200 rpm, pH 7.0 and particles/solution ratio 6 g:100 ml, k_1 was calculated as 0.00046 L/g·s.

It is interesting to note that the experimental data in the first stage of the adsorption indicated a remarkably higher rate than the predicted and that in the later stage suggested a significantly lower rate than the predicted. This was reasonable since the proteins must travel longer distance from the bulk solution to the binding sites in the later stage, when most of the sites on the outer layers of the ion exchangers were occupied by proteins.

4.3.3 Desorption Kinetics

A typical graph of desorption kinetics is shown in Figure 4.6. The desorption of BSA from the loaded Diaion HPA25 anion exchangers was very fast in the early stage: in the first 2 minutes, the protein concentration in the particles decreased dramatically from 45.8 mg/g to 9.3 mg/g, indicating approximately 80% of the proteins initially loaded on the ion exchangers were stripped from the particles. The rate constant of desorption under the tested conditions was determined to be 0.0107 s^{-1}.

It is apparent that after 100 seconds, the desorption curve lagged off and the desorption rate significantly decreased. After a period of 120 minutes, the protein concentration in the particles was still about 3.9 g/L, representing a residual ratio of about 8.6%. This may due to the large diameter of the Diaion HPA25 particle (average particle diameter around 300 micron), which made it difficult to diffuse into the bulk solution for a small fraction of proteins originally adsorbed on the binding sites deep inside the particles.

This is very significant in compare the rates of desorption, which approached equilibrium within 2 minutes with a rate constant of 0.0107 s^{-1}, and the adsorption, which took more than 180 minutes to reach equilibrium and with a rate constant of 0.00046 L/g·s. The rapid desorption and slow adsorption kinetics can be partially explained by the different concentration gradients, which are the major driving forces for mass transfer, in desorption and adsorption. In our adsorption experiments, the initial BSA concentration in the bulk solution was 2 g/L. Assuming that the protein concentration in solution in proximity to the adsorption sites was 0 (the equilibrium at the binding sites was established instantly), the concentration difference was only 3×10^{-5} M. However, the initial protein concentration in the ion exchangers in desorption experiments was around 45 mg/g, which is more than 20 times as that of the 2 g/L. Since the concentration of Cl^- was very high (0.4 M) and the diffusion of small Cl^- ions into the ion exchange particles were very fast, the protein molecules would be substituted from the ion exchangers and be released into the solution in proximity of the binding sites. Given the fact that the density of ion exchanger is near 1 g/ml and the voidage of it is much less than unit, it is reasonable to state that the protein concentration inside the ion exchange particles was higher than 45 g/L. At the beginning, the protein concentration in the bulk solution was 0. Therefore, the initial concentration gradient in desorption was more than 20 times as that of adsorption.

NOMENCLATURE

C protein concentration in bulk solution (g/L or M)

C^* protein concentration in bulk solution at equilibrium (g/L or M)

k desorption rate constant (1/s)

k_1 forward adsorption rate constant (g/L·s)

k_{-1} reverse rate constant of the protein adsorption (1/s)

q protein concentration in ion exchangers (the solid phase) (mg/g or g/L)

q^* protein concentration in ion exchangers (the solid phase) at equilibrium (mg/g or g/L)

q_f free protein adsorption capacity (free ligands available for further protein adsorption expressed in protein adsorption capacity) (mg/g or g/L)

q_m maximum protein adsorption capacity of ion exchangers (mg/g or g/L)

t time (min or s)

REFERENCES

Anspach, F.B., A. Johnston, H.J. Wirth, K.K. Unger, and M.T.W. Hearn, *J. Chromatogr.*, 476, 205-225, (1989)

Chang Y.K. and Chase H.A. *Expanded bed adsorption for the direct extraction of proteins.* Separation for Biotechnology 3: 106-112.

Chase, H.A., "Purification of Proteins by Adsorption Chromatography in Expanded Beds," *TIBTECH* **12**, 296-303 (1994).

Chase, H.A., "Prediction of the Performance of Preparative Affinity Chromatography." J. Chromat. **297**, 179-202 (1984).

Etzel MR. 1990 "Whey protein isolation and fractionation using ion-exchangers." In: *Bioseparation Processes in Food.* R.K. Sight and S.H. Rizvi (eds.). New York : M. Dekker, pp. 390-415.

Gregor, H.P., Gutoff, F., and Bregman, J., *J. Colloid Sci.*, V6, 245,(1951)

Hearn M.T.W., A.N. Hodder, and M.I. Aguilar, *J. Chromatogr.*, V327, 47, (1985)

Lan, Q., J.-X. Zhu, A. Bassi, A. Margaritis, Y. Zheng and G. Rowe, "Continuous Protein Recovery Using a Liquid-Solid Circulation Fluidized Bed Ion Exchange System: Modelling and Experimental Studies." *Can. J. Chem. Eng.* **78**: 858-866, 2000 (2000a), in press

Lan, Q., A. Bassi, J.-X. Zhu and A. Margaritis, "A Modified Langmuir Model for the Prediction of the Effects of Ionic Strength on the Equilibrium Characteristics of Protein Adsorption onto Ion Exchange/Affinity Adsorbents". *Chem. Eng. J.* (2000b), in press.

Perin D. D. and Dempsey B., *Buffers for pH and Metal Ion Control.* Chapman and Hall, London, pp.130-148

Unger K.K. and R. Janzen, Packing and stationary phase in preparative column liquid chromatography. 225-264,(1986)

Zheng, Y., J.-X. Zhu, J. Wen, S. Martin, A.S. Bassi, and A. Margaritis, "The Axial Hydrodynamic Behavior in a Liquid-Solid Circulating Fluidized Bed." *Can. J. Chem. Eng.* 77, 284-290 (1999a).

Zheng, Y., J.-X. Zhu, J. Wen, S. Martin, A.S. Bassi, and A. Margaritis, "Hydrodynamic Behavior in a Liquid-Solid Circulating Fluidized Bed." In "Circulating Fluidized Bed Technology - III", J. Werther, Ed., Dechema, Fonkfurt (1999b), pp. 59-64.

Figure 4.1 Schematic graph of a batch adsorption/desorption kinetic study system. (1) Bellco reactor; (2) 20 μm porosity filter; (3) Cary 50-Bio UV-visible spectrophotometer; (4) Manostat Cassette pump; (5) Magnetic Stir Rod; (6) Magnetic Stirrer.

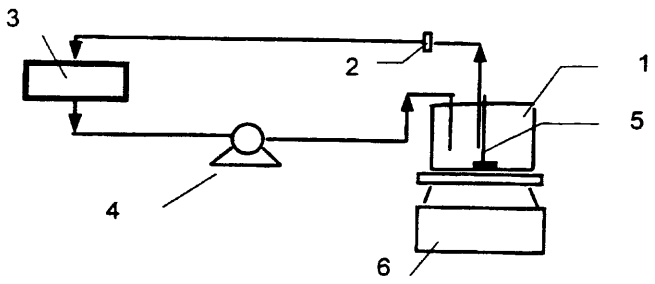


Figure 4.2 The isotherm of BSA adsorption onto Diaion HPA25 in 10 mM phosphate buffer at pH 7.0

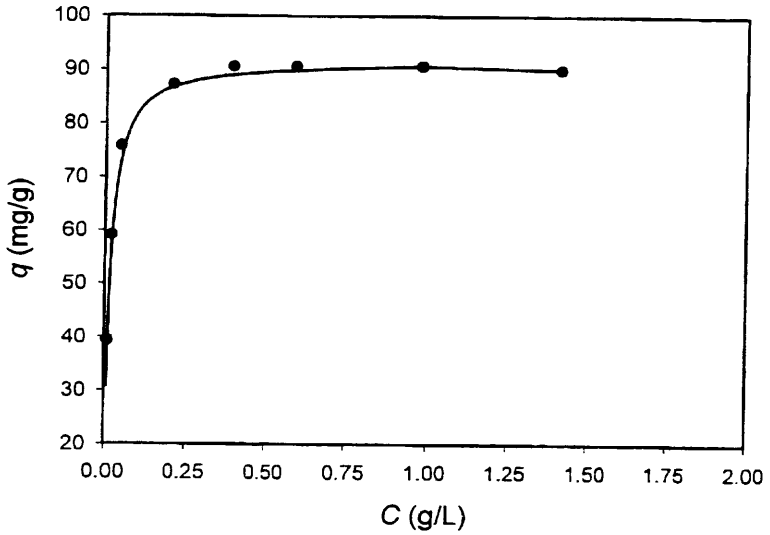


Figure 4.3 The pH-dependency of the maximum capacity of BSA adsorption onto Diaion HPA25 in 10 mM buffers (pH 3.0 citric acid/NaOH buffer; pH 4.0 and 5.0 sodium acetate/acetic acid buffer; pH 6.0-8.0 phosphate buffer; and pH 9.0, boric acid, KCl/NaOH buffer).

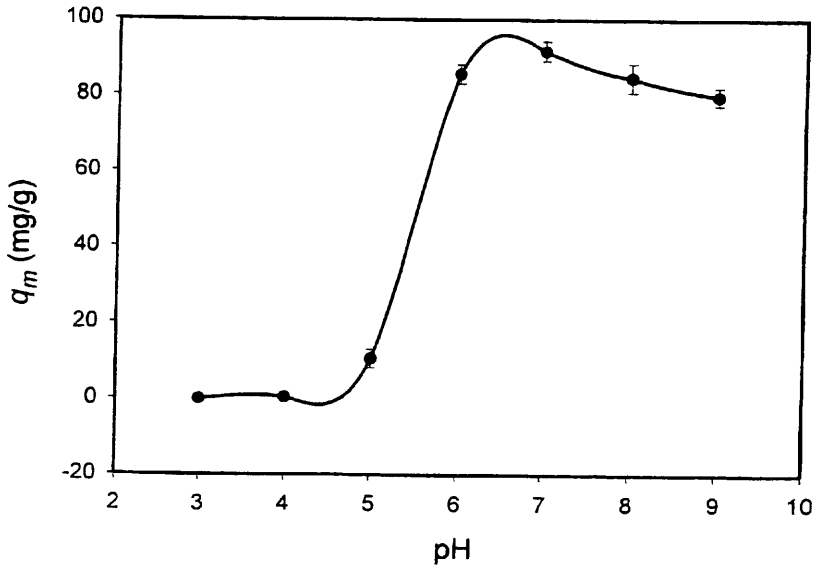


Figure 4.4 The ionic strength dependency of the capacity of BSA adsorption onto Diaion HPA25 in pH 7.0 10 mM phosphate buffer.

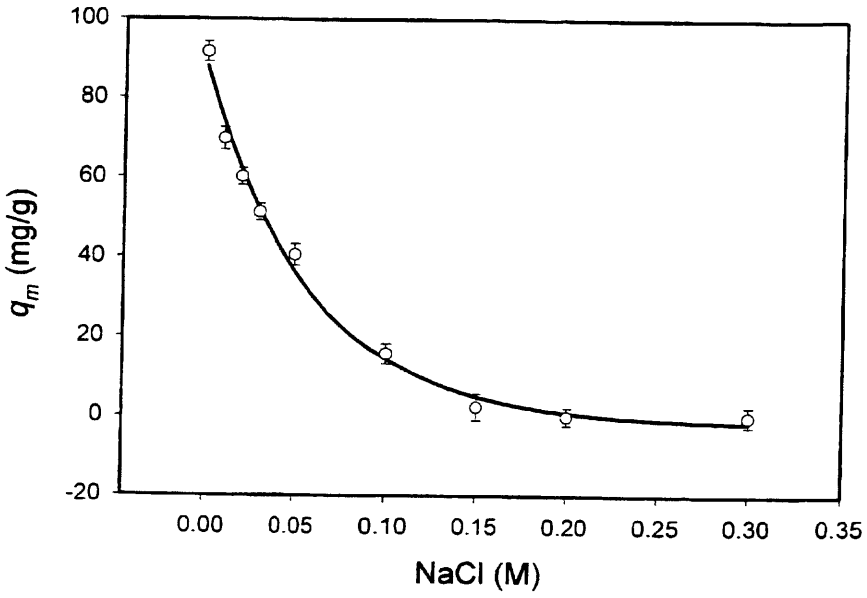


Figure 4.5 Experimental and predicted kinetics of BSA adsorption onto Diaion HPA25 particles in batch adsorption (C_0 = 2 g/L, V = 100 ml, v = 15 ml, K_d = 0.0103 g/L, q_m = 91.7 mg/g, k_1 = 0.00046 L/g·s).

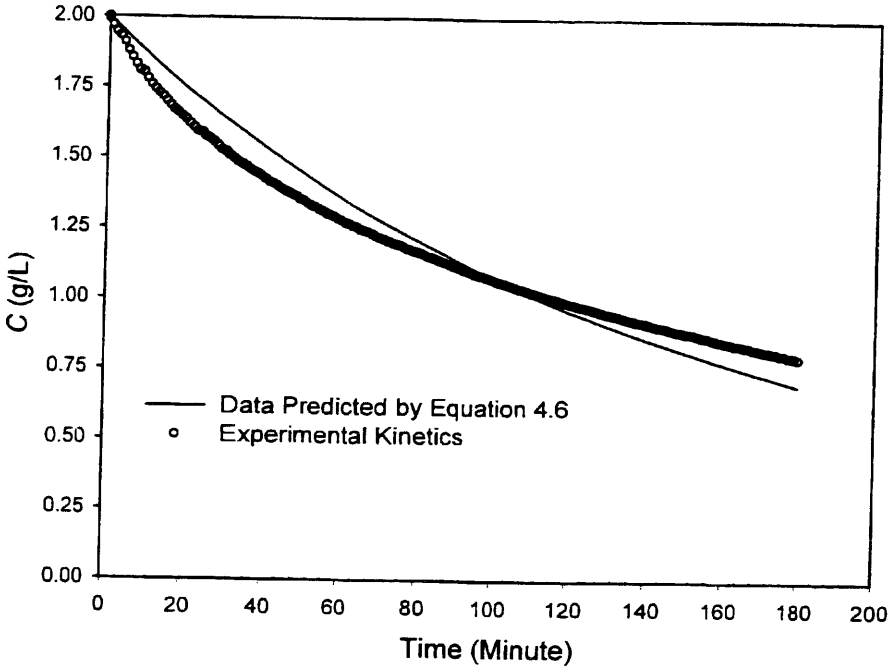
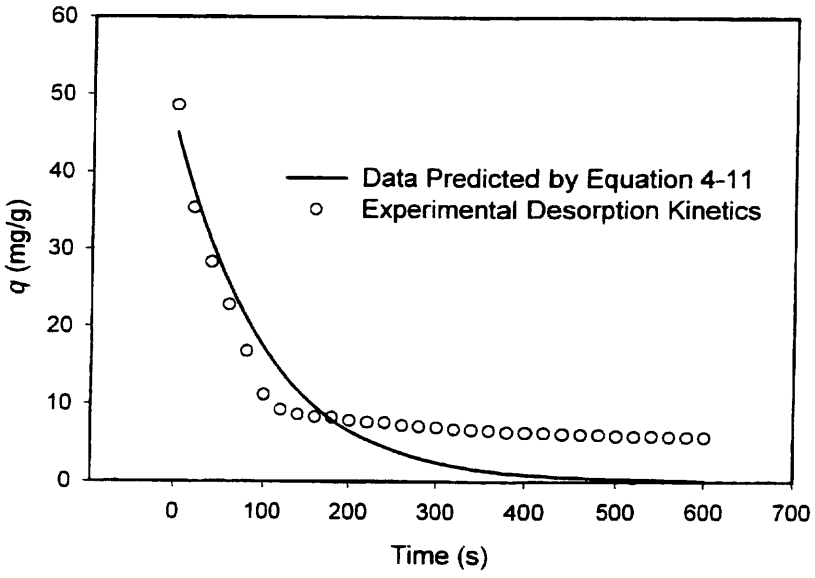


Figure 4.6 Experimental and predicted kinetics of BSA desorption from loaded Diaion HPA25 particles in batch desorption (q_0 = 45.8 mg/g, v = 15 ml, V = 50 ml, k = 0.0107 s^{-1}).



Chapter 5. A Modified Langmuir Model for the Prediction of the Effects of Ionic Strength on the Equilibrium Characteristics of Protein Adsorption onto Ion Exchange/Affinity Adsorbents

5.1 INTRODUCTION

The ability to characterize equilibrium accurately is important in all the chromatography processes including ion exchange chromatography and affinity chromatography. No prediction of column performance could be done without first measuring or estimating the adsorption isotherms of these components under the conditions of interest, and the assurance of the prediction is strongly dependent on the accuracy of these data.

Ionic strength has long been recognized as one of the most important factors affecting the equilibrium characteristics of the adsorption of proteins onto ion exchange/affinity adsorbents. Isotherm data regarding the influence of ionic strength on the protein adsorption have been obtained by studies of various investigators and have been reported in different sources over the years. Finette *et al.* (1997) studied the effects of ionic

---

A version of this chapter has been published.

Q. Lan, A.S. Bassi*, J.X. Zhu and A. Margaritis (2001) "A Modified Langmuir Model for the Prediction of the Effects of Ionic Strength on the Equilibrium Characteristics of Protein Adsorption onto Ion Exchange/Affinity Adsorbents". *Chem. Eng. J.* 81(1-3): 179-186

strength and temperature on the equilibrium characteristics of proteins adsorbed to ion exchangers and affinity adsorbents and noted that ionic strength had much stronger effects than that of temperature. By studying the adsorption of bovine serum albumin (BSA) and other proteins on porous and non-porous anion exchangers, Janzen and Unger (Janzen, 1990) concluded that the increased ionic strengths lead to lower binding strength (higher K_d) and lower binding capacity. Similar phenomena have been reported for various protein/adsorbent pairs by different authors (Harsa *et al.*, 1993; Hashim *et al.*, 1995; Huang *et al.*, 1990; Leaver, *et al.*, 1990). However, to our knowledge, no systematic effort has been made to assemble those data into an informational model for the prediction of ionic strength on protein adsorption.

In this paper we report an empirical model, modified from the Langmuir isotherm model, based on the analysis of literature data for the prediction of the effects of ionic strength on the isotherm of protein adsorption. The model is further tested against the experimental data obtained with BSA adsorption onto a polystyrene-based anion exchanger, Diaion HPA25.

5.2 THEORY

5. 2.1 Langmuir Isotherm

Many different isotherm models, such as the linear, the Langmuir, the bi-Langmuir, the Freundlich and the Freundlich-Langmuir isotherms, have been proposed for the adsorption of solutes in a liquid solution onto a solid surface. Most of those models are essentially empirical although theoretical derivations have been accomplished in some cases. Among all those models, the Langmuir model is probably the most popular one

due to its simplicity and its good agreement with experimental data. It is based on the following equation:

$$q = \frac{q_m C}{(C + K_d)} \qquad 5.1$$

where q and C are the equilibrium concentration of solute in solid and liquid phases, respectively. Constants q_m and K_d are Langmuir parameters. The constant q_m represents the maximum binding capacity and K_d is the dissociation coefficient of the solute-adsorbent complex, which represents the affinity between the solute and the adsorbents.

The Langmuir isotherm for the adsorption of solute from liquid solution was first expanded directly from the corresponding isotherm of gas-solid adsorption and was later on derived thermodynamically (Everett, 1964), kinetically (and stoichiometrically (Finette *et al.*, 1997). All those derivations are based on a few common assumptions. Namely, 1) all binding sites are equivalent, distinguishable and independent; 2) each binding site combines with only one solute molecule; and 3) a molecule adsorbed onto one binding site does not influence the adsorption of another molecule on a neighboring binding site. The Langmuir isotherm has been widely accepted as a practical method for integrating experimental data of protein adsorption onto ion exchange/affinity adsorbents. However, in the case of protein adsorption, some of the above assumptions are not necessarily realistic and the Langmuir model is more an empirical model than a rigorous theoretical one.

5.2.2 Effects of ionic strength on Langmuir parameters

The effect of ionic strength on the protein adsorption onto ion exchange/affinity adsorbents is a very complex phenomenon. It could be considered from the aspects as follows:

the salt counter-ions compete against the protein ions for binding sites;

the salt co-ions shield the protein ions and the charged binding sites from each other;

the change of ionic strength changes the folding and configuration of protein molecules (Stigter and Dill, 1990), resulting in variation of the hydrophobic interaction between the protein and the particle matrix;

the increase of ionic strength may cause the network of the particle to shrink, reducing the porosity of the particles and hence the availability of binding sites (Khare and Peppas, 1995).

There is clearly a need to develop a model to incorporate the effects of ionic strength on the protein adsorption, but it is very difficult to develop a theoretical model for the prediction of such a complex effect. Instead, a semi-empirical model, modified from the Langmuir isotherm model, is proposed here for a bi-component system: one kind of protein under the effect of a sort of small salt:

$$q = \frac{\dfrac{q_m}{(1+\dfrac{I}{\psi})}\,C}{C + \dfrac{\eta}{(\eta - I)}K_d} \qquad 5.2$$

where I is the concentration of the small salt, q and C are the protein concentrations in the bulk solution and the adsorbents, respectively. η and ψ are empirical constants. K_d and q_m are the "true" Langmuir parameters independent of the salt concentration. They are

determined either by experimental data from non-salt protein solution or by the methods described later.

$$\text{Let} \quad K_d' = \frac{\eta}{\eta - I} K_d \qquad 5.3$$

$$\text{And} \quad q_m' = \frac{q_m}{1 + \frac{I}{\psi}} \qquad 5.4$$

Equation 5.2 is therefore:

$$q = \frac{q_m' C}{(C + K_d')} \qquad 5.5$$

Equation 5.5 is an expression of Langmuir model of protein adsorption under the influence of salt ions. Constants K_d' and q_m' are apparent Langmuir parameters. The apparent Langmuir parameters could be obtained by integrating the experimental data at each individual salt concentration with the Langmuir isotherm by the semi-reciprocal plot, the Scatchard plot, or the SigmaPlot® non-linear curve fit program.

5.2.3 Apparent dissociation coefficients K_d', Dissociation Coefficient (K_d) and constant (η)

The dissociation coefficient (K_d) is a measure of the affinity of the protein to the ion exchanger. As pointed out previously, it is independent of ionic strengths. Equation constant η represents the dependence of the apparent dissociation coefficient on the ionic strength. The smaller the value of η, the more significant the dependence of the apparent dissociation coefficient on the change of ionic strength. In the process of determining

model parameters of a specified system, the apparent dissociation coefficient (K_d') are determined directly from the experimental data. On the other hand, in the process of modeling, K_d' at different ionic strength could be calculated according to Equation 5.3 provided that constants η and K_d have been determined before hand. Equation 5.3 describes the relationship between K_d', K_d and I. When salt concentration $I = 0$, Equation 5.3 gives $K_d' = K_d$. Hence K_d could be measured directly in a non-salt system. The dissociation coefficient and the constant η can also be determined by rearranging Equation 5.3. It gives a linear equation as follows:

$$\frac{1}{K_d'} = \frac{1}{K_d} - \frac{\eta}{K_d} I \qquad 5.6$$

Graph of $\frac{1}{K_d'}$ *vs.* I gives a straight line of an intercept of $1/K_d$ and a slope of $-\eta/K_d$.

5.2.4 Apparent maximum capacity, maximum capacity and constant ψ

Equation 5.4 describes the relationship between the apparent maximum capacity, maximum capacity and the salt concentration. The apparent maximum binding capacity, q_m', is a function of salt concentration, I, for a specified protein/adsorbent system. When salt concentration is 0, Equation 5.4 gives $q_m' = q_m$. This confirms the argument that q_m is the maximum capacity at salt concentration 0 and is independent of the concentration and the type of the salt. The value of q_m could be determined from experimental data of non-salt system or by regressing the apparent Langmuir parameters obtained at various individual salt concentrations.

Equation constant ψ is a lumped constant which represents the effects of ionic strength on the binding capacity of the ion exchanger to the protein. It is an indication of the interaction between the protein and the salt ions. The smaller the value of ψ, the more dependent the apparent capacity is on the ionic strength. The values of q_m and ψ can also be determined by rearranging Equation 5.4:

$$\frac{1}{q_m'} = \frac{1}{q_m} + \frac{1}{q_m \psi} I \qquad 5.7$$

Plotting $1/q_m'$ *vs.* I gives a straight line with an intercept of $1/q_m$ and a slope of $\frac{1}{q_m \psi}$. In the process of modeling, the apparent maximum binding capacity at different ionic strength could be calculated according to Equation 5.4 with given constants q_m and ψ.

5.3 EXPERIMENTAL

Bovine serum albumin (BSA) Fraction V, Anion exchange particle Diaion and other chemicals were bought from Sigma Co. Equilibrium studies were conducted by weighing exactly 0.5 g wet ion exchange beads Diaion HPA25 into a 50-ml flask containing 25 ml of 2 mM phosphate buffer (pH 7.0) of appropriate concentrations of BSA and sodium chloride. The flask was then sealed by Parafilm "M" (American Can Company) and put on a shaker controlled at 25 °C and 200 rpm. After adsorption for 36 hours (previous experiments had shown that equilibrium was reached under this condition), the liquid phase was centrifuged at 10,000 rpm for 10 minutes. The protein concentration of the supernatant was analyzed by Lowry's method. Samples of high protein concentration were diluted to ensure that the protein concentration did not exceed the upper limitation of the Lowry's method.

5.4 RESULTS AND DISCUSSION

5.4.1 Isotherms of BSA adsorption onto Diaion HPA25

From the experimental data obtained from the batch adsorption experiments under different ionic strength at 25°C and pH 7.0, the adsorption isotherms were constructed and are shown in Figure 1. The apparent maximum capacity (q_m') and the apparent dissociation constant (K_d') at each salt concentration were determined using non-linear curve fitting. Data were also analyzed using the semi-reciprocal plots (*C/q vs. C*) and the Scatchard plots *(q/C vs. q).*

The semi-reciprocal plots (Figure 5.2) and the Scatchard plots (Figure 5.3) of equilibrium data indicate that the adsorption of BSA onto Diaion HPA25 obeys the Langmuir isotherm in the tested ionic strength range of 0.0 M to 0.05 M NaCl. The dependency of apparent Langmuir parameters on the ionic strength is shown in Figure 5.4 and 5.5. As shown in Figure 5.4, when the NaCl concentration of the solution increases from 0.0 M to 0.05 M, the apparent maximum capacity decreases from 91.69 mg/g to 35.6 mg/g, a loss of about 61.2% of the capacity of Diaion HPA25. It is also evident from Figure 5.5 that the increase of ionic strength causes dramatic increase of the apparent dissociation coefficient. When the sodium chloride concentration was zero, the apparent dissociation coefficient was 0.00907 mg/ml. However, the apparent dissociation coefficient is enhanced to 0.0373 mg/ml when the NaCl concentration of the solution is 0.05 M (more than 3.5 times of that at 0.0 M NaCl).

The significant decrease of the binding capacity and affinity (increase of apparent dissociation coefficient, K_d') resulted from the increase of ionic strength can be attributed to the interactions between salt ions and protein molecules and between salt ions and adsorbents. Those effects influence the electrostatic interactions and the van der Waals interactions between the protein molecules and the ion exchanger particles (Stahlberg, 1992).

It is to be noted that the maximum binding capacity of BSA to Diaion HPA25 is 1.368×10^{-6} moles/g, which is only a very small fraction of the total capacity of the ion exchanger for small salt ions (2.4 meq/g). At least three factors as follows contribute to the failure of the stoichiometric match of the total capacity of the ion exchanger to the small counterions and the available capacity of it to the BSA molecules: 1) the molecular screening effects make a fraction of the binding sites located on the internal surface of the particles, which are readily available to small counterions, not accessible to the BSA molecules (Todd *et al.*, 1994); 2) the bulk BSA molecules, when bound to the binding sites, shield some neighboring sites and make them inaccessible to other protein molecules; 3) BSA is a multi-valence protein, and each protein ion is capable of occupying more than one binding sites.

5.4.2 Verification of the proposed model against experimental and literature data

Apparent Langmuir parameters of the adsorption of various proteins onto different ion exchanger/dye affinity adsorbents reported by different authors have been collected and listed in Table 5.1. Those adsorbents include three cation exchangers, Sp Sepharose, Fractogel EMD and Fractogel TSK; two anion exchangers, Diaion HPA25 and TSK-DEAE 5PW (5PW); and one dye-affinity adsorbent, Cibacron Blue F3G-A immobilized onto LiChroprep DIOL (F3G). Five different proteins, BSA, human serum albumin (HSA), hen egg white lysozyme (HEWL), lysozyme and conalbumin, are involved in the studies. Those adsorbents and proteins have been studied as seven different adsorbent/protein pairs chosen by the authors. Except the Diaion HPA25/BSA pair, which is the system reported in this paper, the other six adsorbent/protein pairs are taken from three papers from different sources. Necessary transformations have been applied to some data as noted in the following text.

Huang and his coworkers (Huang *et al.*, 1990) reported adsorption isotherms of albumin and conalbumin on anion exchanger TSK-DEAE 5PW in Tris-acetate/sodium acetate buffers (pH 8.6) of salt concentration 0, 0.025 and 0.05 M, respectively. The Langmuir isotherm was found to be appropriate for integrating the conalbumin adsorption data and the Binary Langmuir isotherm for the albumin adsorption. Hence only the conalbumin adsorption data are included in our analysis. It is to be noted that $\Sigma A/B$ is equivalent to q_{m} and $1/B$ to K_d in that paper. Hashim *et al.* (1995) studied the effects of ionic strength on the the equilibrium behaviors of the adsorption of lysozyme on three strong cation exchangers, Sp Sepharose, Fractogel EMD and Fractogel TSK, in acetate/sodium acetate

buffers (pH 5.0) of salt concentrations of 0.07, 0.10 and 0.13 M. Langmuir model was used for the integration of all the experimental data and the apparent Langmuir parameters of all the three adsorbent/protein pairs are used in our analysis. Data from the work reported by Finette *et al.* (1997) were regarding the effects of ionic strength on the isotherm of the adsorption of HAS and HWEL on a dye-affinity adsorbent, Cibacron Blue F3G-A immobilized onto LiChroprep DIOL. Experiments were conducted in 50 mM Tris-HCl buffer (pH 7.0). The ionic strength of the buffers were adjusted with NaCl of four different concentrations: 0, 0.05, 0.10 and 0.20 M. Those seven adsorbent/protein pairs represent a wide range of adsorbents, proteins and buffers. The validity of the model is tested against those data, as follows.

The linear dependence of $1/q_m'$ and $1/K_d'$ on the NaCl concentration of our experimental data, as a characteristic of the model, is shown in Figures 6 and 7, respectively. The r^2 values of the $1/K_d'$ *vs.* I plot and the $1/q_m'$ *vs.* I plot are about 0.997 and 0.990, respectively (Tables 5.2 and 5.3). Those high r^2 values are a clear indication of the validity of the model under the tested conditions.

Tables 5.2 and 5.3 show the r^2 values of the $1/K_d$ *vs.* I correlation and the $1/q_m$ *vs.* I correlation of all the seven adsorbent/protein pairs, respectively. As shown in Tables 2 and 3, the r^2 values for most cases are above 0.920. In the best cases, the r^2 values are 0.997 and 0.950 for Sp Sepharose/lysozyme pair and o.997 and 0.990 for Diaion HPA25/BSA pair, respectively. Those results indicate that the model is applicable to a

wide range of different ion exchangers and affinity adsorbents. However, keeping in mind the complexity of the protein adsorption process, it is not surprising to find that in some cases, the r^2 values are relatively low (0.839 in the lowest case of the $1/K_d$ *vs.* I correlation for the lysozyme adsorption onto Fractogel EMD). In the cases of low linear correlation, nevertheless, the experimental data still follow the general tendency as predicted by the model. Namely, the apparent maximum binding capacity decrease with the increase of ionic strength, while the apparent dissociation coefficient increase with the increase of ionic strength.

Figures 5.8 and 5.9 compare the experimentally obtained apparent Langmuir parameters of those seven adsorbent/protein pairs as listed in Table 5.1 against the corresponding predicted data calculated according to the proposed model. To facilitate a more clear comparison, appropriate multiplication factors have been applied to some of the data as indicated in those two figures. As shown in the figures, the model predictions agree well with the experimental results, except for a few cases where some deviations were found. Most of the deviations were found in the predication of K_d' values. As shown in Figure 5.8, four cases out of the 25 points have an error larger than 10%. The other 21 points are either within or very close to the ±10% error lines. For the prediction of q_m' values, it is interesting to note that the only substantial deviation is in the case of conalbumin adsorption onto 5PW at salt concentration 0.0 M, as shown in Figure 5.9. The errors between the experimental and the predicted q_m' values of all the other 24 points are either within or very close to the ±10% error lines. This result shows that the proposed model could be used satisfactorily for correlating the apparent Langmuir

parameters and the effects of ionic strength for a wide range of ion exchange/affinity adsorbents.

Figure 5.1 also compares the experimental isotherms of the BSA adsorption onto Diaion HPA25-BSA (symbols), the best-fit Langmuir isotherms under each individual NaCl concentration (solid lines) and the isotherms predicted by the new model (dashed lines) under NaCl concentrations of 0.0 M, 0.01 M, 0.02 M, 0.03 M and 0.05 M, respectively. Both the Langmuir and the modified Langmuir isotherms match well with the experimental data. It is to be noted that in comparison with the best-fit Langmuir isotherms for each individual salt concentration, the new model does generate a somewhat larger deviation. However, this is reasonable considering that the new model has incorporated the salt concentration as an additional parameter. This allows the direct prediction of the effects of ionic strength on the adsorption behavior an important feature that the original Langmuir model does not possess.

5.5 CONCLUSIONS

As a conclusion, the proposed model has been established as a good approach for predicting the effects of ionic strength on the equilibrium characteristics of protein adsorption onto ion exchange/affinity adsorbents. It is shown that the proposed model is applicable to various proteins/adsorbent systems. The accuracy of the predicted data generated by the model is satisfactory in terms of q_m', K_d' and the isotherms.

NOMENCLATURE

C	equilibrium concentration of protein in the bulk solutions (mg/ml or M)
I	concentration of the small salt in the bulk solution (M)
K_d	dissociation coefficient of the protein-ligand complex (mg/ml or M)
K_d'	apparent dissociation coefficient of the protein-ligand complex (mg/ml or M)
q	equilibrium protein concentration in solid phase (mg/g or moles/g)
q_m	maximum protein binding capacity (mg/g, mg/ml, moles/g or M)
q_m'	apparent maximum protein binding capacity (mg/g, mg/ml, moles/g or M)

Greek Symbols

η	empirical equation constant (M)
ψ	empirical equation constant (M)

REFERENCES

Everett, D. H., "Thermodynamics of adsorption from solution: Part 1. – perfect systems", *Trans. Faraday Soc.* 60 (1964)1803-1813.

Finette, G. M. S., Mao, Q.-M. and Hearn, M. T. W., "Comparative studies on the isothermal characteristics of proteins adsorbed under batch equilibrium conditions to ion-exchange, immobilized metal ion affinity and Ion exchange matrices with different ionic strength and temperature conditions", *J. Chromatogr. A* 763 (1997) 71-90.

Harsa, S., Zaror, C. A. and Pyle, D. L, "Adsorption *of Kluyveromyces marxianus* pectinase on CM- Sephadex® gels", *Enzyme Microb. Technol.* 15 (1993) 906-915.

Hashim, M. A., Chu, K.-H. and Tsan, P.-S., "Effects of ionic strength and pH on the adsorption equilibria of lysozyme on ion exchangers", *J. Chem. Tech. Biotechnol.* 62 (1995) 253-260.

Huang, J-X., Schudel, J. and Guiochon, G., "Adsorption behavior of albumin and conalbumin on TSK-DEAE 5PW anion exchanger", *J. Chromatogr.* 504 (1990) 335-349.

Janzen, R. and Unger, K. K., "Adsorption of proteins on porous and non-porous poly(ethylenemine) and tantacle-type anion exchangers", *Chromsymp.* 2009 (1990) 77-93.

Khare, A.R. and Peppas, N.A., "Swelling/deswelling of anionic copolymer gels", Biomaterials 16 (1995) 559-567.

Leaver, G., Conder, J. R. and Howell, J. A., "Adsorption isotherm of albumin on a cross-linked cellulose chromatographic ion exchanger", *I. Chem. E. Symposium Series* 118 (1990) 1-15.

Stahlberg, J., "Combined effect of coulombic and van der Waals interactions in the chromatography of proteins", *Anal. Chem.* 64 (1992) 3119-3124.

Stigter, D. and Dill, A., "Charge effects on folded and unfolded proteins", *Biochemistry* 29 (1990) 1262-1271.

Todd, R., R. Johnson and F. Arnold, "Multiple-site binding interactions in metal-affinity chromatography: I. Equilibrium binding of egineered histidine-containing cytochrome C", *J. Chromatogr.* 662 (1994) 13-26

Table 5.1 Langmuir parameters from literature and experiments

Adsorbent	Protein	Buffer	Salt concentration (M)	q_m' (mg/g)	K_d' (mg/ml)
Sp Sepharose [1]	Lysozyme	Sodium acetate + Acetate (pH 5.0)	0.07	111.6	0.009
			0.10	71.97	0.014
			0.13	62.22	0.026
Fractogel EMD [1]	Lysozyme	Sodium acetate + Acetate (pH 5.0)	0.07	103.73	0.011
			0.10	67.29	0.014
			0.13	63.82	0.028
Fractogel TSK [1]	Lysozyme	Sodium acetate + Acetate (pH 5.0)	0.07	38.38	0.012
			0.10	28.39	0.015
			0.13	25.38	0.030
Diaion HPA25 (This study)	BSA	2 mM phosphate + NaCl (pH 7.0)	0.00	91.69	0.010
			0.01	68.94	0.013
			0.02	60.23	0.015
			0.03	51.72	0.020
			0.05	42.59	0.037
TSK-DEAE 5PW [2] (5PW)*	Conalbumin	Tris acetate + Acetate + Sodium acetate (pH 8.6)	0	30.8 mg/ml	0.247
			0.025	13.2 mg/ml	0.361
			0.050	4.8 mg/ml	2.381
Cibacron Blue F3G-A Immobilized onto LiChroprep DIOL [3] (F3G)*	HEWL	50 mM Tris-HCl + NaCl (pH 7.0)	0	16.16	0.46
			0.05	13.70	0.82
			0.10	11.51	0.94
			0.20	10.90	1.65
	HSA	50 mM Tris-HCl + NaCl (pH 7.0)	0	5.09	0.31
			0.05	4.10	0.43
			0.10	3.75	0.72
			0.20	2.08	0.91

* Abbreviation used in the text and figures

[1] Hashim *et al.*, 1995

[2] Huang *et al.*, 1990

[3] Finette *et al.*, 1997

Table 5.2 Dissociation coefficient and constant η calculated according to the apparent Langmuir parameters as listed in Table 5.1

Ion Exchanger	Protein	Salt	K_d		η	r^2
			(mg/ml)	($M\times10^7$)	(M)	
DiaionHPA25	BSA	NaCl	0.00907	1.35	0.07194	0.997
5PW	Conalbumin	SA*	0.237	35.37	0.0582	0.972
Sp Sepharose	Lysozyme	SA	0.0052	3.63	0.161	0.997
Fractogel EMD	Lysozyme	SA	0.00648	4.63	0.1766	0.978
Fractogel TSK	Lysozyme	SA	0.00694	4.85	0.173	0.971
F3G	HSA	NaCl	0.34	50.74	0.2789	0.855
F3G	HWEL	NaCl	0.53	370.62	0.267	0.839

* SA: sodium acetate

Table 5.3 Maximum binding capacity and constant ψ calculated according to the apparent Langmuir parameters as listed in Table 5.1

Ion Exchanger	Protein	Salt	q_m		ψ	r^2
			(mg/g)	(moles/g $\times 10^6$)	(M)	
Diaion HPA25	BSA	NaCl	87.9	1.31	0.0466	0.990
5PW	Conalbumin	SA	56.82	0.848	0.0050	0.920
Sp Sepharose	Lysozyme	SA	909.1	63.57	0.00928	0.997
Fractogel EMD	Lysozyme	SA	303.0	21.19	0.0328	0.970
Fractogel TSK	Lysozyme	SA	88.49	6.19	0.0508	0.960
F3G	HSA	NaCl	5.79	0.086	0.1215	0.878
F3G	HWEL	NaCl	15.29	1.69	0.4395	0.928

Figure 5.1 Comparison between the experimental isotherms (symbol), best-fit Langmuir isoherms for given individual NaCl concentration (——) and the isotherms predicted by the modified Langmuir model (----).

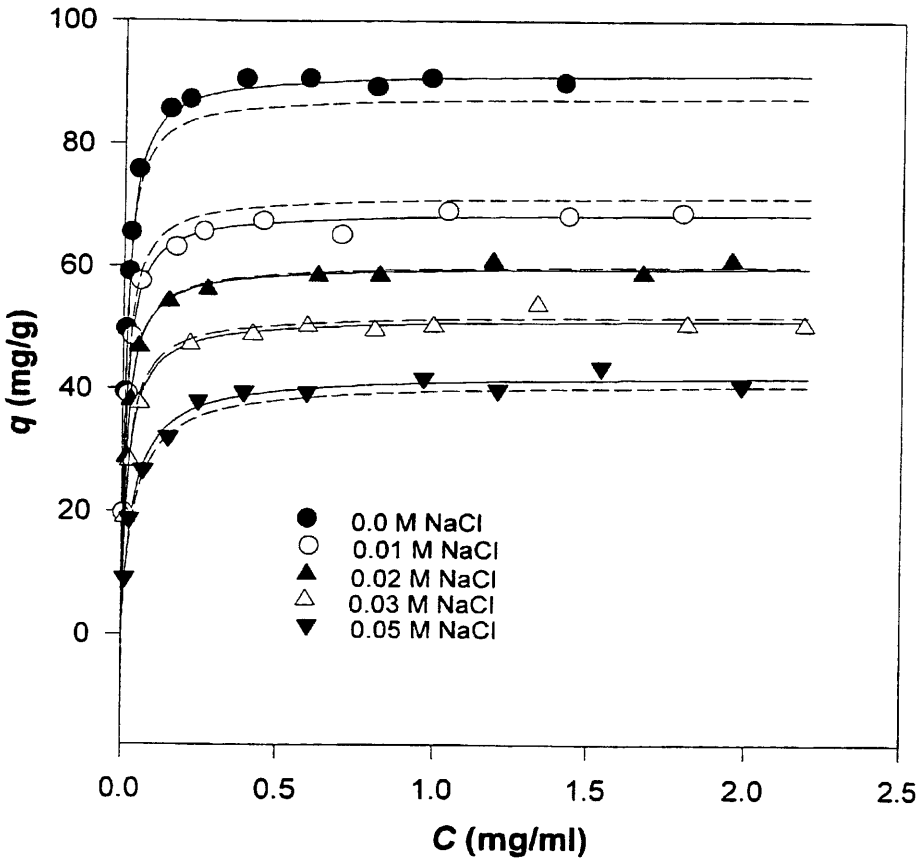


Figure 5.2 Semi-reciprocal plot of BSA adsorption onto Diaion HPA25 at 25 °C, pH 7.0 and different NaCl concentrations.

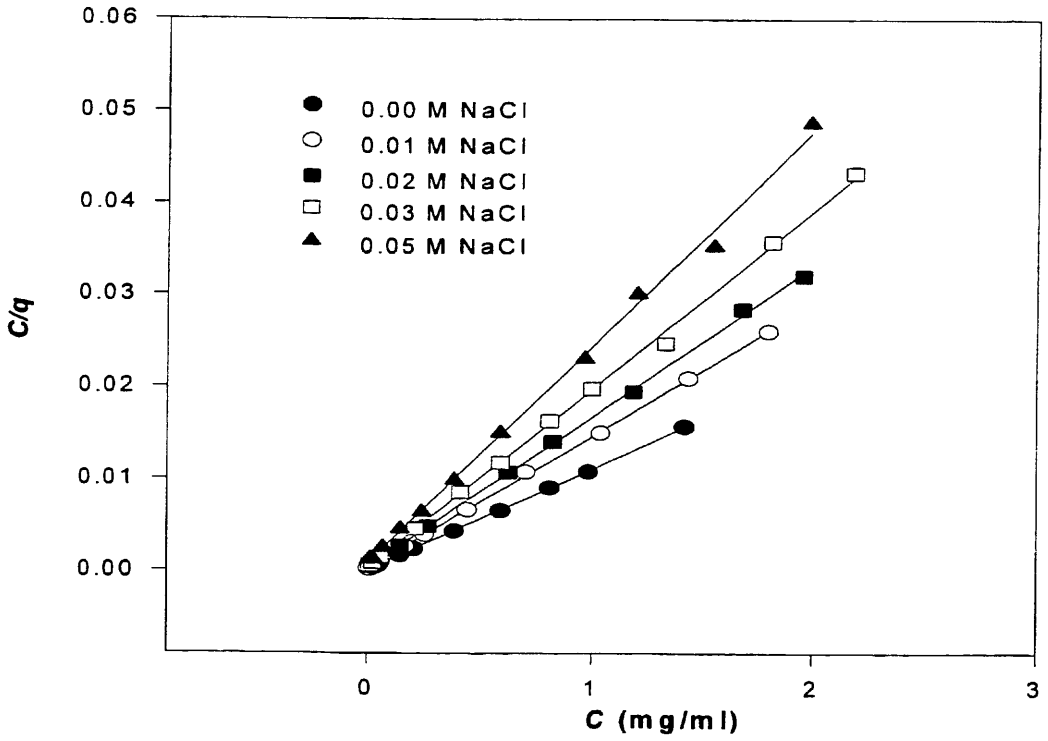


Figure 5.3 Scatchard Plot of BSA adsorption on Diaion HPA25 25 °C, pH 7.0 and different NaCl concentrations.

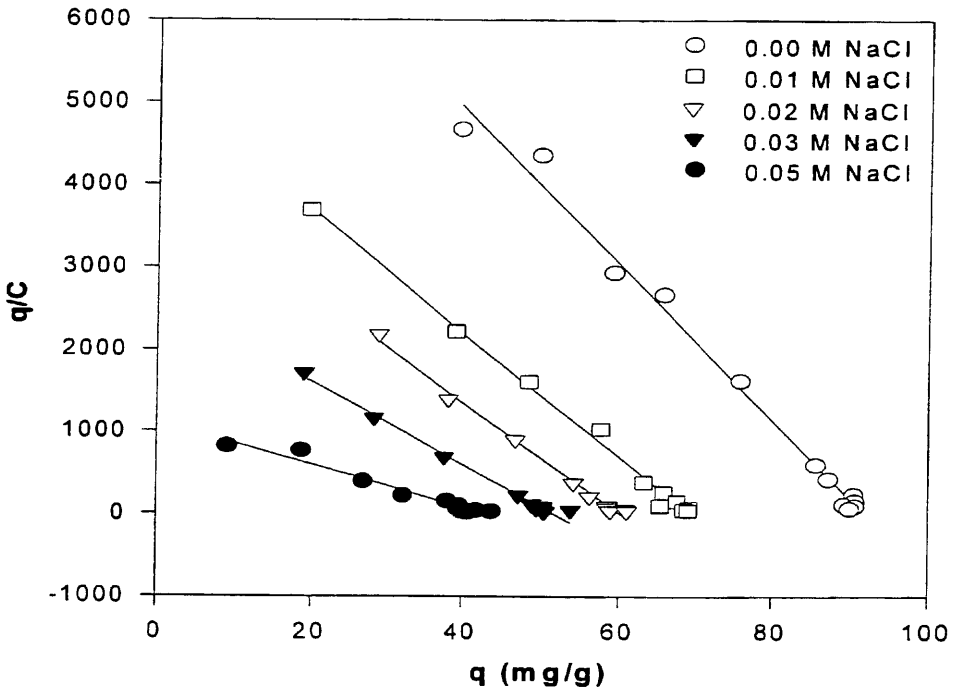


Figure 5.4 Effects of ionic strength on the apparent maximum binding capacity (q_m') of BSA adsorption onto Diaion HPA25 at 25°C and pH7.0.

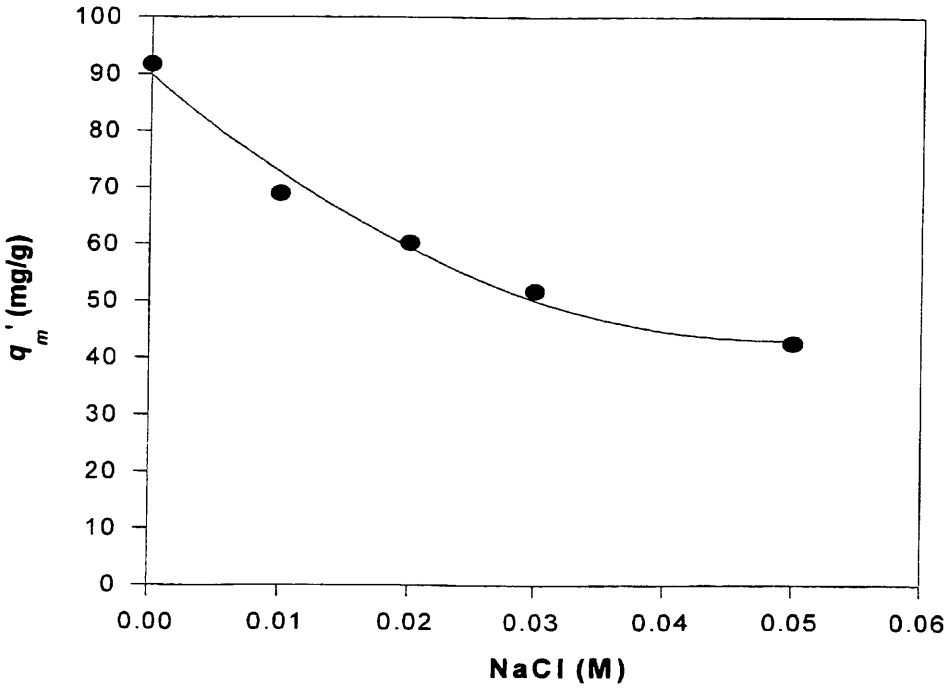


Figure 5.5 Effects of ionic strength on the apparent dissociation coefficient (K_d') of BSA adsorption onto Diaion HPA25 at 25°C and pH7.0.

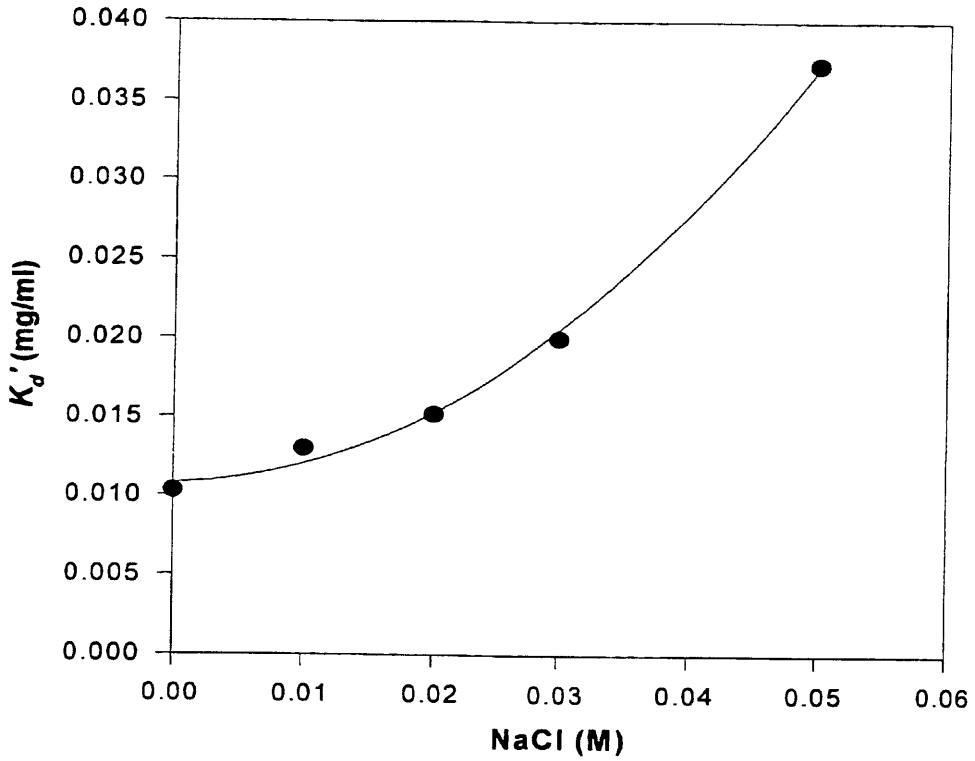


Figure 5.6 Reciprocal of apparent maximum binding capacity ($1/ q_m'$) for BSA adsorption as a function of NaCl concentration at 25°C and pH7.0.

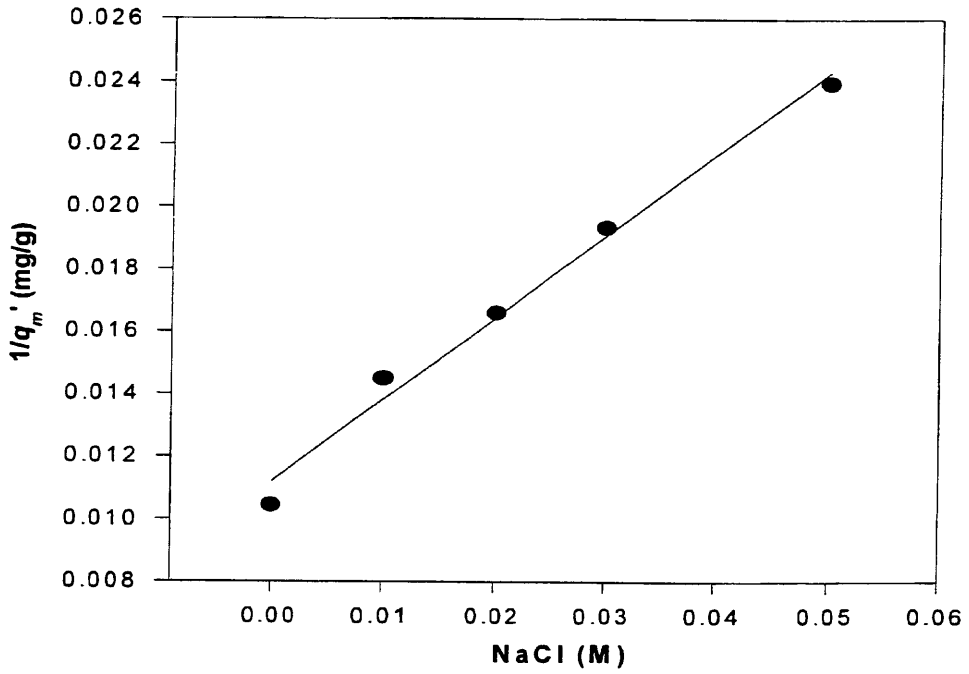


Figure 5.7 Reciprocal of apparent dissociation coefficient ($1/K_d'$)as a function of NaCl concentration at 25°C and pH7.0.

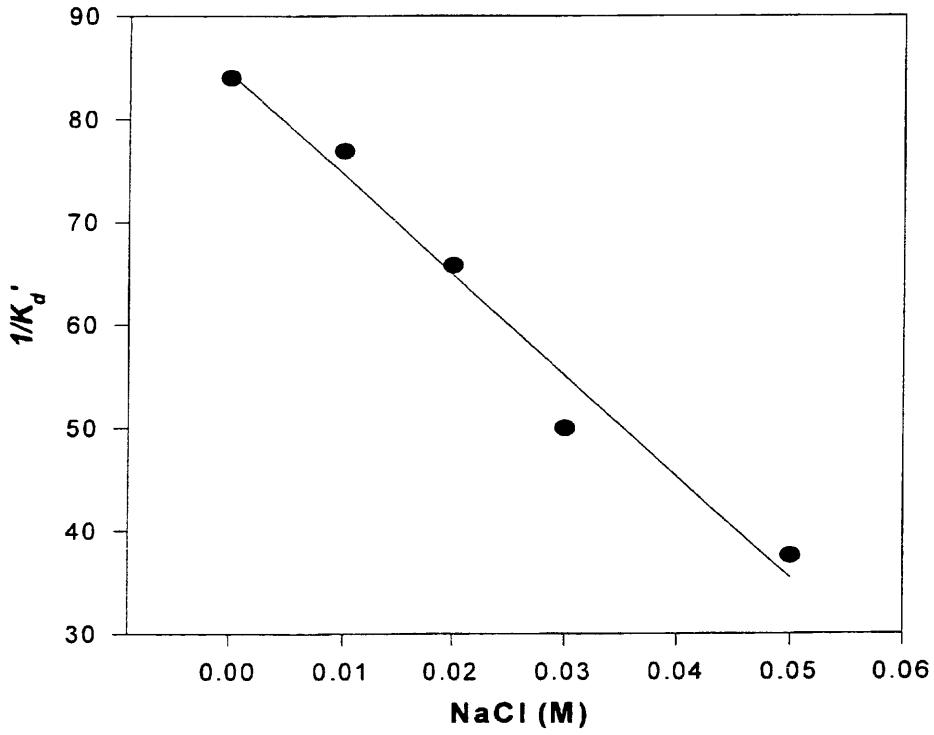


Figure 5.8 Comparison of the predicted and the experimental data for the apparent coefficient (K_d').

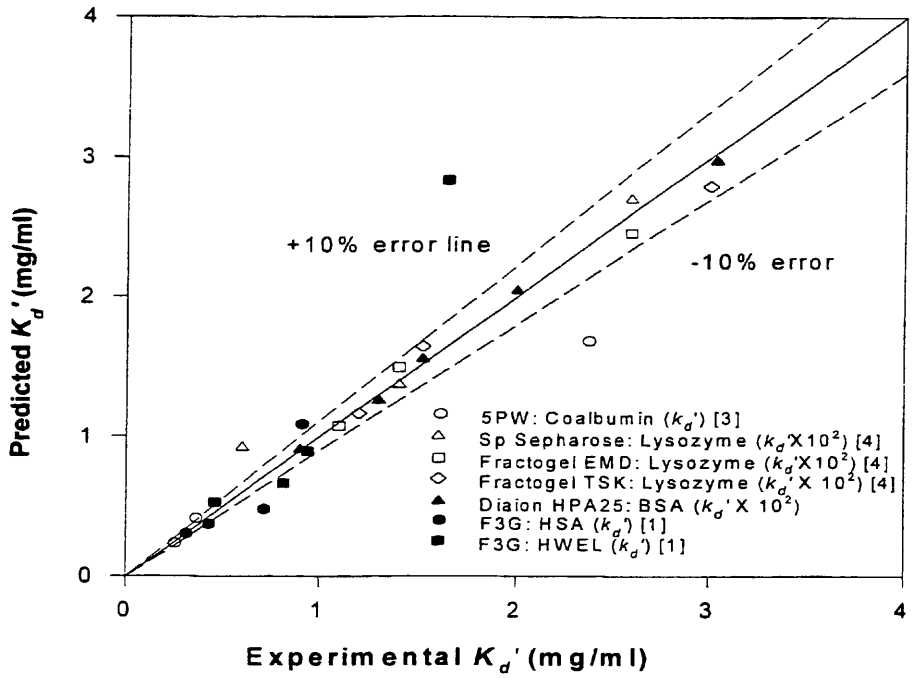
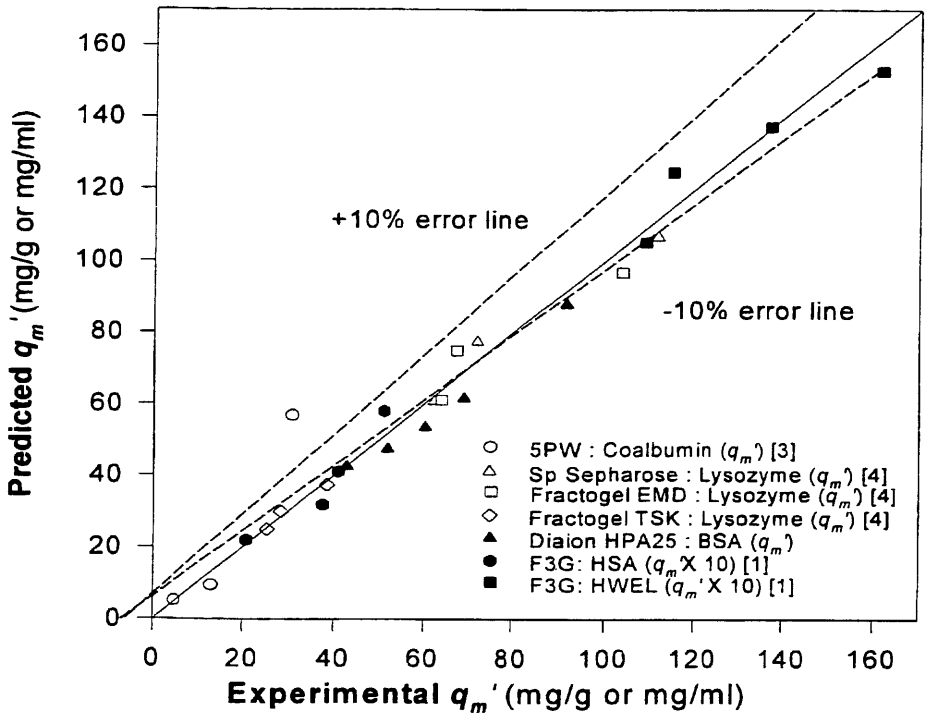


Figure 5.9 Comparison of the predicted and the experimental data for the apparent maximum binding capacity (q_m').



Chapter 6. Continuous Protein Recovery Using a Liquid-Solid Circulating Fluidized Bed Ion Exchange System: Modelling and Experimental Studies

6.1 INTRODUCTION

Ion exchange has long been established as a useful method for protein separation. It is an essential component in many protein purification processes. In the fields of pharmaceutical and food industries, many valuable proteins are produced in large-scale with low initial protein concentrations. In such cases, large amounts of fermentation broth must be dealt with in the early stages of downstream processing. Therefore, the efficiency and economics of the purification of protein have received much attention.

The development of continuous ion exchange systems has been of intensive interest since 1960s (Turner and Church, 1963; Higgins, 1969; Slater and Prud'homme, 1972; Porter, 1975; Himsley, 1981; Pungor *et al.*, 1987; Burns and Graves, 1989; Gordon *et al.*, 1990; Rodrigues *et al.*, 1991; Byers *et al.*, 1997).

A version of this chapter has been published.

Qingdao Lan, Jing-Xu (Jesse) Zhu, Amarjeet S. Bassi*, Argyrios Margaritis, Ying Zheng and Gerald E. Rowe, (2001) "Continuous Protein Recovery Using a Liquid-Solid Circulating Fluidized Bed Ion Exchange System: Modelling and Experimental Studies". *Can. J. Chem. Eng.* 78: 858-866

Burns and Graves (1989) suggested a two-column magnetically stabilized fluidized bed system for the continuous chromatography of biochemical products. Those authors, however, treated the system as comprised of two identical columns and no discussion was provided about the solids transportation between those two columns. In addition, the magnetically stabilized fluidized bed system is complicated and costly. Gordon *et al.* (1990) reported the continuous affinity recycle extraction of proteins using well-mixed reactors. This system, although simple and easy to control, has the disadvantage of a stirred tank system – the ion exchange efficiency is low and large processing volumes are essential for even a moderate throughput requirement.

The LSCFB ion exchange system is a very attractive strategy for the continuous recovery of protein from unclarified whole broth. The essential concept is that the adsorption and desorption (regeneration) of proteins are carried out separately in the downcomer and the riser of the LSCFB, respectively, in a continuous mode. Since adsorption of protein onto ion exchange particles is much slower than the desorption process, the downcomer, which provides longer residence time due to its lower operating liquid velocity, is used for the adsorption process. The riser, with its high liquid velocity and good plug flow characteristics, is suitable for the fast desorption process.

The advantages of the LSCFB ion exchange system are obvious. In addition to all the advantages of a conventional fluidized bed, e.g., the direct application of unclarified whole broth feed and the low and stable bed pressure drops (Chase, 1994), the LSCFB system has some special features:

- It operates continuously with simultaneous adsorption and desorption;
- Higher throughput is achievable due to the high liquid velocity in the riser;
- Mass transfer is more efficient as a result of the higher liquid velocity;

- Independent control of solids hold-up is possible in the riser from the liquid flowrate by changing other operating conditions;
- Near plug flow conditions can be maintained in the riser.

The design, optimization, and scale up of an LSCFB ion exchange system requires that the hydrodynamics of the LSCFB system and the equilibrium and kinetics of the adsorption and desorption of the ion exchanger-protein pair are fully understood. Equilibrium and kinetics of protein ion exchange have been under intensive study for the last thirty years. Many equilibrium and kinetic models have been published for different protein-ion exchanger pairs (Chase, 1984; Skidmore *et al.*, 1990; Mao *et al.*, 1993; Habbaba and Ulgen, 1997). Hydrodynamic studies of the LSCFB are also of major interest in the recent years (Liang *et al.*, 1996; 1997; Zheng *et al.*, 1999a; 1999b) and some models have been published (Liang and Zhu, 1997a; 1997b). However, to our knowledge, no work has been published in terms of integrating ion exchange and LSCFB to develop a continuous protein recovery process.

The purpose of this study was to introduce the concepts of using an LSCFB ion exchange system for the continuous recovery of protein and to develop mathematical models based on known kinetics and ideal hydrodynamic assumptions so as to provide guidelines for the scale-up and optimization of the system.

6.2 EXPERIMENTAL

6.2.1 Setup of the LSCFB system

As shown in Figure 6.1, the major components of the LSCFB system included a riser, a downcomer, a liquid-solid separator and two particle returning pipes, one connecting the base of the separator and the upper part of the downcomer and the other connecting the base of the downcomer and the riser. The riser was 3.0 m tall and 38 mm in diameter and the downcomer was 2.5 m tall and 120 mm in diameter. Two separate liquid streams were used to fluidize the particles in the riser and the downcomer while the particles circulated between the two units. The riser was operated in the high-velocity circulating fluidization regime and the downcomer in the low-velocity conventional fluidization regime. To secure the pressure balance between the riser and the downcomer, the liquid outlets on the top of the downcomer and the separator were located at the same level. The distributor for the downcomer was a tubular ring which was carefully designed in order to have a uniform liquid distribution while allowing the solids to follow through.

The distributor for the riser was designed to divide the incoming stream into two sub-streams: the primary and the auxiliary streams. The primary stream entered through a tubing of 1.1 cm in I.D. extending 5.1cm into the riser. The outlet of the primary distributor was located right above the solids entrance at the bottom of the riser. This design helped to increase the pressure drop across the particle returning pipe at the bottom, which was very important for the dynamic seal between the riser and the downcomer and the stabilization of the whole system. The inlet of the auxiliary stream was at the bottom of the riser. The purpose of the auxiliary stream was to mobilize the particles at the bottom, which were then carried up the riser by the combination of the primary and the auxiliary streams.

6.2.2 Continuous BSA ion exchange in the LSCFB system

Continuous BSA ion exchange in the LSCFB ion exchange system was conducted with 2 g/L BSA solution as feed and 0.4M NaCl solution as extracting buffer unless otherwise indicated in the text. Anion exchange particles Diaion HPA25®, purchased from Sigma (St Louis, MO), were used for all hydrodynamic and kinetic studies. The properties of Diaion HPA25® are listed in Table 6.1. Bovine serum albumin (BSA) purchased also from Sigma was used as model protein in the experiments. Both BSA and NaCl solutions were prepared in 10 mM, pH 7.0 phosphate buffer. Other conditions are indicated in the text.

In the continuous BSA ion exchange studies in the LSCFB, the feed BSA solution was introduced from the tubular distributor into the base of the downcomer. The regenerated Diaion HPA25® ion exchange particles were returned to the top of the downcomer via the return pipe. The liquid velocity was maintained such that the downcomer operated in the conventional fluidized regime, whereas the ion exchange particles moved downwards countercurrent to the rising feed liquid. The liquid velocity in the downcomer was maintained lower than the terminal velocity of the ion exchange particles to allow them to fall down. As the particles and feed broth contacted counter-currently in the downcomer, the BSA in the broth was adsorbed onto the ion exchange particles. The de-proteinized solution was discarded from the top of the downcomer. The loaded particles were transferred to the base of the riser from the downcomer through the particle return pipe. The extracting buffer, which was 0.4M NaCl solution in 10 mM pH 7.0 phosphate buffer, was introduced from the riser base. The superficial velocity in the riser (U_{lr}) was the combination of the primary and the auxiliary stream velocity, and it was kept higher than the terminal velocity of the Diaion HPA25® particles. The loaded particles were carried

upward by this NaCl stream while desorption proceeded. In the liquid-solid separator, the regenerated particles and the effluent were separated and the regenerated particles were continuously returned to the downcomer.

In the continuous ion exchange LSCFB system, two different liquid streams of opposite properties, i.e., protein solution of low ionic strength and extract buffer of high ionic strength, were involved in the two columns separately. In this process, maintenance of a dynamic seal between the two columns to prevent the mixing of the two liquid streams was of crucial importance. This dynamic seal was achieved by keeping the solids in the returning pipes in the packed bed regime, which is discussed in detail in elsewhere (Lan *et al.*, 2000b). In addition, wash water streams were introduced between the riser and downcomer at the base and top of the LSCFB. Thus the operation in the riser and the downcomer was maintained independent of each other except for continuous circulation of solids between the two columns. The two wash water streams displaced and diluted the feed and the extraction buffer streams before the particles entered the return pipes.

6.3 MODEL DEVELOPMENT

6.3.1 Ion exchange kinetics

The ion exchange reaction can be represented as:

$$AB + RE \rightleftharpoons AE + RB \qquad 6.1$$

where A and R represent the co-ions in the liquid phase and the fixed ions of the ion exchange particles, respectively; B and E represent the exchangeable ions of the liquid and the particles phase, respectively; k_1 and k_{-1} are reaction constants.

Assuming that the surface reaction is slow compared to the mass transfer and internal diffusion rates so that the protein concentration is the same inside and outside the particle, i.e., if the process is reaction rate controlling, the kinetic rate equation is given as (Yang and Tsao, 1982; Chase, 1984):

$$R_{ld} = -\frac{dC_d}{dt} = k_1 C_d (q_m - q_d) - k_1 q_d \qquad 6.2$$

where R_{ld} is the protein adsorption rate (the "reaction rate"), which takes place in the downcomer, C_d is the protein concentration in liquid phase of downcomer, q_m is the maximum capacity of the ion exchange particles, q_d is the protein concentration of the solids phase in the downcomer, k_1 is the forward reaction rate constant, and k_{-1} is the backward reaction rate constant. Under the equilibrium assumption, k_{-1} could be related to the dissociation coefficient of the protein-ion exchanger complex as

$$k_{-1} = k_1 K_d \qquad 6.3$$

where K_d is the dissociation coefficient which could be determined by equilibrium studies or calculated according to isothermal models (Lan *et al.*, 2000a).

It should be mentioned that the reaction rate controlling assumption is often an approximation as in most cases of ion exchange, the rate of surface reaction is very fast compared with that of mass transfer. Under this assumption, the reaction constants, k_1 and k_{-1}, are lumped constants which represent the overall influence of ion exchange reaction as well as mass transfer. Nevertheless, Equation 6.2 has been used successfully by many authors for the modelling of adsorption behavior in packed beds and finite baths, among which are the Thomas solution (Thomas, 1944) and the more recent model developed by Chase (1984).

The desorption of protein from ion exchange particles is often a very fast process in comparison with the adsorption of protein onto ion exchange particles. For simplification, the kinetics of protein desorption in the riser can be represented by (Yang and Tsao, 1982):

$$R_{sr} = \frac{dq}{dt} = -kq_r \qquad 6.4$$

where k is the reaction constant and q_r is the protein concentration in the solids phase in the riser. Equation 6.4 represents the first order kinetics of protein desorption from ion exchangers.

6.3.2 Design Equation of the Downcomer

The downcomer is operated as a conventional fluidized moving bed (Kwauk, 1992) in which the solids and liquid contact counter-currently: the liquid moves upward and the solids downward. The downcomer is divided into three sections according to the different solids holdups: the freeboard, the dilute section and the dense section (Lan *et al.*, 2000b). The freeboard is the section from the column top to the solids entrance of the top solids return pipe. There is a small amount of ion exchange particle in the freeboard. The function of the freeboard is to prevent the ion exchange particle from being lost into the effluent stream at the top of the downcomer. The dilute section extends from the solids outlet of the top solids return pipe to the upper boundary of the dense section. Ion exchange particles fed from the top solids returning pipe falling through the dilute section to the surface of the dense section. The solids holdup of the dilute section is very low in comparison with that of the dense section. The bed voidage of the dense section could be calculated by the modified Richardson and Zaki equation (Richardson and Zaki, 1954; Kwauk, 1992). That is

$$\frac{V_{ld}+V_{sd}}{U_t}=\varepsilon_d^{n-1} \qquad 6.5$$

where n could be determined experimentally or from the correlation:

$$n=\left(4.4+18\frac{d_p}{D}\right)\mathrm{Re}_t^{-0.1} \qquad 6.6$$

Re_t is the Reynolds number with respect to the particle terminal velocity, which is given as:

$$\mathrm{Re}_t=\frac{U_t d_p \rho_l}{\mu} \qquad 6.7$$

and U_i is the superficial liquid velocity at $\varepsilon = 1$, which could be determined by the following correlation (Richardson, 1971):

$$logU_i = logU_t - \frac{d_p}{D} \qquad 6.8$$

The protein concentration in the liquid stream of the dilute section, after being adsorbed by the dense section, is also very low. It is hence assumed that there is no adsorption in the dilute section. That is, to understand the adsorption in the downcomer, we need only to consider the dense section height as the effective bed height. Figure 6.2a shows the counter-current contact between the liquid and solids phases in the dense section in the downcomer. Protein in the bulk liquid is adsorbed onto the ion exchanger particles. For a finite element in the liquid phase, the conservation of mass gives

$$U_{ld}\frac{\partial C_d}{\partial z_d}-D\frac{\partial^2 C_d}{\partial z_d^{\,2}}-R_{ld}=\frac{\partial C_d}{\partial t} \qquad 6.9$$

At steady state, the protein concentration at a particular point along the bed height will not change with time, i.e., $\partial C/\partial t = 0$. For simplicity, it is further assumed that the downcomer operates in plug flow so that the axial dispersion is zero. This is reasonable

since the downcomer is in the uniformly suspended particulate fluidisation regime and the liquid velocity is very low (<0.01m/s). Equation 6.9 is thus reduced to:

$$U_{ld}\frac{\partial C_d}{\partial z_d} - R_{ld} = 0 \qquad 6.10$$

In the downcomer, the boundary conditions are:

$$z_d = 0, \quad C_d = C_{0d}, \quad q_d = q_{ed}$$

$$z_d = H_d, \; C_d = C_{ed}, \; q_d = q_{0d} = q_{er} \qquad 6.11$$

As the density of the ion exchange particles is very small (1.05 - 1.10 g/mL) and the liquid velocity in downcomer is very low (less than 0.01 m/s), it is reasonable to assume that the axial particle distribution is uniform (Zheng *et al.*, 1999a). Under this assumption, the mass balance of protein in the downcomer gives:

$$q_d = \frac{U_{ld}}{U_{sd}}(C_d - C_{ed}) + q_{0d} \qquad 6.12$$

Substituting Equation 6.12 into Equation 6.2 gives

$$R_{ld} = \alpha_{ld}C_d^{\,2} + \beta_{ld}C_d + \gamma_{ld} \qquad 6.13$$

where

$$\alpha_{ld} = -k_1\delta_{ld} \qquad 6.14$$

$$\beta_{ld} = k_1 q_m + k_1\delta_{ld}C_{ed} - k_1 q_0 - k_1 K\delta_{ld} \qquad 6.15$$

$$\gamma_{ld} = k_1 K\delta_{ld}C_{ed} - k_1 K q_0 \qquad 6.16$$

$$\delta_{ld} = \frac{U_l}{U_s} \qquad 6.17$$

Substituting Equation 6.13 into Equation 6.10 and integrating, we have:

$$\frac{z_d}{U_{ld}} = \int_{C_{0d}}^{C_d} \frac{dC_d}{\alpha_{ld} C_d^{\,2} + \beta_{ld} C_d + \gamma_{ld}} \qquad 6.18$$

The analytical solution for Equation 6.18 is therefore

$$\frac{z_d}{U_{ld}} = B_{ld} - \frac{1}{\phi_{ld}} \ln\left(\frac{2\gamma_{ld} C_d + \beta_{ld} - \phi_{ld}}{2\gamma_{ld} C_d + \beta_{ld} + \phi_{ld}}\right) \qquad 6.19$$

where

$$\phi_{ld} = \sqrt{\beta_{ld}^{\,2} - 4\alpha_{ld}\gamma_{ld}} \qquad 6.20$$

$$B_{ld} = \frac{1}{\phi_{ld}} \ln\left(\frac{2\gamma_{ld} C_{0d} + \beta_{ld} - \phi_{ld}}{2\gamma_{ld} C_{0d} + \beta_{ld} + \phi_{ld}}\right) \qquad 6.21$$

Considering the boundary conditions, i.e., when $z_d = H_d$, $C_d = C_{ed}$, the parameter C_{ed} is given by the following formula:

$$\frac{H_d}{U_{ld}} = B_{ld} - \frac{1}{\phi_{ld}} \ln\left(\frac{2\gamma_{ld} C_{ed} + \beta_{ld} - \phi_{ld}}{2\gamma_{ld} C_{ed} + \beta_{ld} + \phi_{ld}}\right) \qquad 6.22$$

The bed height of the downcomer for the required protein adsorption, i.e., for a given value of C_{ed}, is therefore:

$$H_d = U_{ld}\left[B_{ld} - \frac{1}{\phi_{ld}} \ln\left(\frac{2\gamma_{ld} C_{ed} + \beta_{ld} - \phi_{ld}}{2\gamma_{ld} C_{ed} + \beta_{ld} + \phi_{ld}}\right)\right] \qquad 6.23$$

Equation 6.23, in conjunction with Equations 6.15–6.17, and Equations 6.21 and 6.22, can be employed to calculate the required bed height for a given protein adsorption ratio (X_d) under certain operating conditions. In such cases, the protein concentration at the outlet of the downcomer is given by

$$C_{ed} = C_{0d}(1 - X_d) \qquad 6.24$$

Rearranging Equation 6.19 and dividing by C_{0d} gives:

$$C_{d} = \frac{\beta_{ld} - \phi_{id} - (\beta_{ld} + \phi_{ld}) \exp[(B_{ld} - \frac{z_{d}}{U_{ld}})\phi_{ld}]}{2\gamma \exp[(B_{ld} - \frac{z_{d}}{U_{ld}})\phi_{ld}] - 2\gamma} \qquad 6.25$$

Combining Equation 6.12 and Equation 6.25 gives

$$q_{d} = \delta_{ld}\{\frac{\beta_{ld} - \phi_{ld} - (\beta_{ld} + \phi_{ld}) \exp[(B_{ld} - \frac{z_{d}}{U_{ld}})\phi_{ld}]}{2\gamma C_{0d} \exp[(B_{ld} - \frac{z_{d}}{U_{ld}})\phi_{ld}] - 2\gamma C_{0d}} - C_{ed}\} + q_{0d} \qquad 6.26$$

Equations (25) and (26) give the axial protein concentration profiles in the liquid and solids phases, respectively.

The solids phase protein concentration at the solids exit at the bottom of the downcomer is a very important parameter, which is given from Equation 6.13 as follows:

$$q_{ed} = \delta_{ld}(C_{0d} - C_{ed}) + q_{0d} \qquad 6.27$$

6.3.1 Design equation of the riser

Figure 6.2b shows the co-current flow of liquid and solids in the riser. Similarly, by assuming plug flow of both the liquid and solids phases in the riser, we can obtain the integration equation for the axial profile of the protein concentration in the solids phase in the riser following the procedure below.

The conservation of mass in a finite element of the solids phase in the riser gives:

$$U_{sr}\frac{\partial q_r}{\partial z_r} - R_{sr} = 0 \qquad 6.28$$

In most cases, the desorption of protein from ion exchangers is very fast and can be described by a first order equation in terms of the depletion of protein from the solids phase as Equation 6.8 (Yang and Tsao, 1982).

Substituting Equation 6.8 to Equation 6.28 and integrating gives:

$$\frac{z_r}{U_{sr}} = -\int_{q_{0r}}^{q_r}\frac{dq_r}{kq_r} \qquad 6.29$$

The analytical solution of Equation 6.29 is given as:

$$\frac{z_r}{U_{sr}} = \frac{1}{k}\ln(q_{0r}/q_r) \qquad 6.30$$

The boundary conditions in the riser are:

$$z_r = 0, \quad C_r = C_{0r} = 0, \; q_r = q_{0r} = q_{ed}$$
$$z_r = H_r, \; C_r = C_{er}, \qquad q_r = q_{er} \qquad 6.31$$

The equation to calculate the height of the riser required for a given protein desorption is:

$$H_r = \frac{U_{sr}}{k}\ln\left(\frac{1}{1-X_r}\right) \qquad 6.32$$

where X_r is the protein recovery of the desorption process (desorption ratio) in the riser and is given by:

$$X_r = \frac{q_{0r} - q_{er}}{q_{0r}} \qquad 6.33$$

Rearranging Equation 6.32 gives axial profile of the protein concentration the solids phase in the riser:

$$q_r = \exp(-\frac{kz_r}{U_{sr}})q_{0r} \qquad 6.34$$

Mass balance of protein in the riser gives

$$q_r = q_{0r} - C_r \frac{U_l}{U_s} \qquad 6.35$$

Substituting Equation 6.35 into Equation 6.34 and rearranging gives the axial protein concentration profile in the liquid phase in terms of the protein concentration in the riser:

$$C_r = \frac{U_{lr}}{U_{sr}} q_{0r}[1 - \exp(-\frac{kz_r}{U_{sr}})] \qquad 6.36$$

6.4 RESULTS AND DISCUSSION

6.4.1 The Bed Expansion Index

The bed expansion characteristics of Diaion HPA25® were investigated in the riser but without solids circulation. The ion exchange beads were placed in the bed and the height of the packed bed was 0.25 m. Tap water was introduced at the bottom of the bed. Liquid velocity was varied in the range of the minimal fluidization velocity (U_{mf}) and the terminal velocity (U_t) of the particles. The bed height corresponding to different liquid velocities were recorded after the change of the flowrate, when the bed height stabilized. The bed expansion index (n), which is the slope of the linear curve of the logarithm plot of reduced liquid velocity versus bed voidage, i.e., $\ln(U_l/U_t)$ versus $\ln(\varepsilon)$, was determined to be 2.67. This value is very close to that calculated from Equation 6.6.

6.4.2 Relationship Between Solids Holdup and Superficial Liquid Velocity in the Riser

When other operating conditions such as the solids circulation rate are constant, increase of superficial liquid velocity in the riser results in the decrease of solids holdup in the column. In other words, the same solids flux is mixed with and carried up by a larger liquid flux and hence the bed is more "diluted". Figure 6.3 shows the relationship between the solids holdup and superficial velocity in the riser under condition of U_a = 6 mm/s, G_s = 1.24 kg/m^2·s, H_d = 0.8 m and U_{ld} = 0.6 mm/s in the LSCFB with 3 kg Diaion HPA25® as solids and tap water as fluidization liquid. The turning point as reported by Zheng *et al.* (1999a) is not detected in the experiments, possibly due to the limited liquid velocity range involved in the experiments.

6.4.3 Continuous BSA Ion Exchange in the LSCFB System

Figures 6.4 and 6.5 show typical experimental concentration profiles during BSA adsorption in the downcomer and the desorption in the riser, respectively. The BSA adsorption/desorption experiments were conducted in conditions as follows: U_{lr} = 0.0113 m/s, U_{ld} = 0.6 m/s, G_s = 0.124 kg/m^2·s and C_{0d} = 2 g/L. During those experiments, the expanded dense section height in the downcomer was kept at 0.8 m, i.e., H_d = 0.8 m. Figure 6.4 shows the two stages of the BSA adsorption in the downcomer. In the developing stage, the BSA concentration in the liquid phase increases rapidly after the introduction of the BSA solution into the downcomer. As the process goes on, the steady state was established and the BSA concentration at each location along the bed remains constant with time. In the steady state stage, the BSA concentration in the loaded particles was also constant. This was very important for the establishment of steady state

in the riser. Figure 6.5 shows that the desorption of BSA from loaded Diaion HPA25® in the riser could be divided into three stages: the initial stage, the developing stage and the steady state stage. At the initial stage, only fresh ion exchange particles in the bottom solids returning pipe were introduced into the riser. Therefore, the BSA concentration in the liquid phase of the riser at any bed height was zero. As partially protein loaded particles started to be introduced into the riser, the BSA concentration in the riser increased rapidly with time. After this initial or developing stage, the steady state was established in which the BSA concentration in the riser did not change with time. The time required to reach steady state in the riser was much longer than that in the downcomer. This phenomenon could be explained as follows: (i) the steady state in the riser could be established only after the downcomer reached steady state and (ii) it was further delayed by the necessity of transporting the particles in the lower solids return pipe.

6.4.4 Validation of the Model

With the model proposed above, the efficiency of ion exchange in an LSCFB system could be calculated for a given set of operating conditions. On the other hand, the required bed dimensions could also be calculated for a required recovery rate of BSA. To validate the model, the predicted BSA concentration profiles in the riser under C_{0d} = 2 g/L, U_{ld} = 0.6 mm/s, G_s = 1.24 kg/m^2·s and various U_{lr} and corresponding solids holdup (ε_s) are shown in Figure 6.6. The hydrodynamic, kinetic and equilibrium parameters used for the simulations are presented in Tables 6.1 and 6.2. The bed height of riser is 3 m and the height of dense section in the downcomer is taken as 0.8 m in the simulations. Experimental data obtained under the same operating conditions are also shown in Figure

6.6. It can be seen that the predicted results have good agreement with the experimental data. With the increase of the superficial velocity in the riser, when other conditions such as the solids circulation rate and protein concentration in the entering beads were kept constant, the protein concentration in the extract decreased significantly. Given the large overall reaction constant of desorption, it was reasonable to find both experimentally and theoretically that the equilibrium was established early in the column. Only 0.5 m of the 3 m riser seemed essential for desorption. However, the remaining bed height was necessary for solids transportation and regeneration.

The simulated and experimental results of BSA adsorption in the downcomer under conditions of C_{0d} = 2 g/L, U_{ld} = 0.6 mm/s, U_{tr} = 0.0113 m/s and various G_s are shown in Figure 6.7. The experimental results agreed well the simulated data. Both the experimental and predicted data showed the significant influence of the solids circulation rate (G_s) on the BSA adsorption in the riser: At a high G_s of 1.42 kg/m^2·s, almost all the BSA in the feed had been removed. However, when G_s was reduced to 1.06 kg/m^2·s, only about 70% of the BSA in the feed was loaded onto the particles. When the flow-rate and the concentration of the feed were kept constant the removing ratio of BSA is determined by the total capacity of the regenerated ion exchange particle flux. The deviation of the experimental data from the simulated data at the lower portion of the downcomer (z_d/H_d<0.3) was possibly caused by the back mixing of ion exchange particles in the distributor zone of the downcomer.

6.4.5 Effects of Liquid Velocity in the Downcomer

With the model validated, simulations were used to carry out a parametric study on the protein recovery in the LSCFB. The parameters used in the simulations were the same as discussed in the validation of the model.

The significant effects of liquid velocity in the downcomer (U_{ld}) are shown in Figure 6.8. The influences of U_{ld} on the performance of an LSCFB system could be identified in many aspects. First of all, U_{ld} directly affected the residence time of the liquid phase in the downcomer. Secondly, it influenced the bed voidage in the downcomer as described by Equation 6.5. Thirdly, when the solids circulation rate was constant, change of U_{ld} changed the feed rate of BSA into the system and therefore changed the mass balance of BSA in the downcomer. As shown in Figure 6.8, the BSA concentration at the outlet of the riser, C_{er}, increases with U_{ld}. However, the adsorption ratio decreases with U_{ld} as the BSA concentration in the raffinate at the outlet of the downcomer, C_{ed}, increases with U_{ld}. The value of C_{ed} is an indication of BSA lost into the effluent stream from the downcomer (the raffinate stream). It should be noted that when the liquid velocity is too high, the liquid/solids ratio will become so large that the total protein in the liquid phase will exceed the capacity of the ion exchange particles. This situation should be avoided because it will cause the loss of protein and result in a dramatic decrease of the protein adsorption ratio.

6.4.6 Effects of Solids Circulation Rate

The solids circulation rate is a parameter which indicates how fast the solids circulate between the riser and the downcomer. The higher the G_s, the higher the efficiency of the LSCFB system. This is clearly shown in Figure 6.9, where the simulation results on the effects of G_s on the performance of the system confirmed that a higher G_s was beneficial to the performance of an LSCFB ion exchange system.

6.4.7 Effects of Protein Concentration in the Feed

As shown in Figure 6.10, the model simulation results showed that the protein concentration in the solids phase at the bottom of the downcomer (q_{ed}) and the liquid phase protein concentration at the top of the riser (C_{er}) increased with C_{0d}. However, an increase of the C_{0d}, without being balanced by the decrease of U_{ld}, will increase the loading rate of BSA to the system. If the loading rate goes up above the BSA adsorption capacity of the system, significant amount of BSA will be lost.

6.5 CONCLUSIONS

A continuous ion exchange process using a liquid-solid circulation fluidized bed has been developed for the continuous protein recovery using a commercially available polystyrene anion exchange, Diaion HPA25, as the adsorbent. The dynamic seal between the riser and the downcomer was achieved by maintaining the solids in the solids return pipes in the packed moving bed regime. This system was proven to be stable and its application to the continuous ion exchange of BSA was successful. A model has been developed for the LSCFB ion exchange system based on established ion exchange kinetics and the plug flow assumption for the downcomer and the riser of the LSCFB. Experiments and simulations have been conducted to investigate the effects of various operating conditions. Comparison between the experimental and simulated results showed good agreement, indicating that the model provides useful guidelines for the practical design of such a system.

NOMENCLATURE

B_{ld} constant, as defined by Equation 6.21, s

C concentration of protein in the liquid phase, mg/mL

d_p particle mean diameter, m

D column diameter, m

H_r riser height, m

H_d dense section height in the downcomer, m

k_1 lumped reaction rate constant of ion exchange adsorption, mL/mg·s

k_2 backward reaction rate constant of ion exchange adsorption, 1/s

k irreversible desorption reaction constant, 1/s

K_d dissociation coefficient of ion exchanger protein complex ($K_d = k_{-1}/k_1$), mg/mL

n coefficient as defined in Equation 6.3

q concentration of protein in solids phase, mg/mL

q_m maximum adsorption capacity, mg/mL

q_t theoretically achievable solids phase protein concentration at the outlet of ion exchanger particles assuming that all the proteins originally exist in the liquid phase are adsorbed to the ion exchangers, kg/m^3

Re_t particle Reynold number at free settling condition

R_{ld} overall protein adsorption rate in the downcomer, mg/mL·s

R_{sr} overall protein desorption rate in the solids phase in the riser, mg/g·s

t time, s

U_a auxiliary liquid velocity, m/s

U_t Superficial liquid velocity at $\varepsilon = 1$, as defined by Equation 6.5, m/s

U_l superficial liquid velocity, m/s

U_s superficial solid velocity, m/s

U_t particle terminal velocity, m/s

V_l liquid velocity (m/s or mm/s)

V_s solids velocity (m/s or mm/s)

X overall protein recovery in the LSCFB

X_d protein adsorption ratio in the downcomer

X_r protein desorption ratio in the riser

z distance from the bottom of a column, m

Greek Letters

α_{ld} equation constant, as defined by Equation 6.14

β_{ld} equation constant, as defined by Equation 6.15

γ_{ld} equation constant, as defined by Equation 6.16

δ_{ld} equation constant, as defined by Equation 6.17

ε bed voidage

ε_s solids holdup

ρ_l liquid density of liquid, kg/m^3

ρ_p density of particles, kg/m^3

ϕ_{ld} equation constants, as defined by Equation 6.20

Subscripts

d downcomer

e exit

l liquid phase

r riser

s solids phase

0 inlet

REFERENCES

Burns, M.A. and D.J. Graves, "Continuous Affinity Chromatography Using a Magnetically Stabilized Fluidized Bed." *Biotechnol. Prog.* **1**, 95 – 103 (1989).

Byers, C.H., W.G. sisson, T.S. Snyder, R.J. Beleski, U.P. Nayak and T.L. Francis, " Zirconium and Hafnium Separation in Sulfate Solutions Using Continuous Ion Exchange Chromatography." **US5618502** (1997).

Chase, H.A., "Prediction of the Performance of Preparative Affinity Chromatography." *J. Chromat.* **297**, 179-202 (1984).

Chase, H.A., "Purification of Proteins by Adsorption Chromatography in Expanded Beds." *TIBTECH* **12**, 296-303 (1994).

Cocker, T .M., C.J. Fee and A. Evans, "Preparation of Magnetically Susceptible Polyacrylamide/Magnetite Particles for Use in Magnetically Stabilized Fluidized Bed Chromatography." *Biotech. Bioeng.* **53**, 79-87 (1997).

Gordon, N.F., H. Tsujimura and C.L. Cooney, "Optimization and Simulation of Continuous Affinity Recycle Extraction." *Bioseparation* **1**, 9-12 (1990).

Habbaba, M.M., and K.O. Ulgen, "Analysis of Protein Adsorption to Ion Exchangers." *J. Chem. Technol. and Biotechnol.* **69**, 405-414 (1997).

Higgins, I.R., "Continuous Ion Exchange of Process Water." *Chem. Eng. Prog.*, **65**(6), 59-62 (1969).

Himsley, A., "Continuous Countercurrent Ion Exchange Process." **US4279755** (1981).

Karau, A., C. Benken, J. Thommes and M.R. Kula, "The Influence of Particle Size

Distribution and Operating Conditions on the Adsorption Performance in Fluidized Beds." *Biotech. Bioeng.* **55**, 55-64 (1996).

Kwauk, M., "Fluidization – Idealised and Bubbleless, with Applications." Ellis Horwood, N.Y. (1992).

Lan, Q., A.S. Bassi, J.-X. Zhu and A. Margaritis, "A Modified Langmuir Model for the Prediction of the Effects of Ionic Strength on the Equilibrium Characteristics of Protein Adsorption onto Ion Exchange/Affinity Adsorbents." *Chem. Eng. J.*, in press (2000a).

Lan, Q., A.S. Bassi, J.-X. Zhu and A. Margaritis, "Continuous Protein Recovery Using a Liquid-Solid Circulating Fluidized Bed (LSCFB) Ion Exchange System." *AICHE J.*, under revision (2000b).

Liang, W.-G., J.-X. Zhu, Y. Jin, Z.W. Wang, Z.Q. Yu and J. Zhou, "Radial Nonuniformity of Flow Structure in a Liquid-Solid Circulating Fluidized Bed." *Chem. Eng. Sci.***51**, 2001-2010 (1996).

Liang, W-G., S-L. Zhang, J-X. Zhu, Y. Jin, Z-Q. Yu and Z-W. Wang, "Flow Characteristics of the Liquid-Solid Circulating Fluidized Bed." *Powder Technol.* **90**, 95-102 (1997).

Liang, W-G. and J-X. Zhu, "A Core-Annulus Model for the Radial Flow Structure in a Liquid-Solid Circulating Fluidized Bed (LSCFB)." *Chem. Eng. J.* **68**, 51-62 (1997a).

Liang, W-G. and J-X. Zhu, "Effect of Radial Flowrate Nonuniformity on the Alkylation Reaction in a Liquid-Solid Circulating Fluidized Bed (LSCFB) Reactor." *Ind. Eng. Chem. Res.* **36**, 4651-4658 (1997b).

Mao, Q.M., R. Stockmann, I.G. Prince and M.T.W. Hearn, "Highly-erformance Liquid Chromatography of Amino Acids, Peptides and Proteins: CXXVI. Modelling of Protein Adsorption with Non-porous and Porous Particles." *J. Chromat.* **646**, 67-80 (1993).

Nixon, L., C.A. Ko*val.*, L. Xu, R.D. Noble and G.S. Slaff, "The Effects of Magnetic Stabilization on the Structure and Performance of Liquid Fluidized Beds." *Bioseparation* **2**, 217-230 (1991).

Porter, R.R., "Continuous Ion Exchange Process and Apparatus." **US3879287** (1975).

Pungor, E., N.B. Afeyan, N.F. Gordon and C.L. Cooney, "Continuous Affinity-Recycle Extraction: a Novel Protein Separation Technique." *Bio/Technol.* **5**, 604-608 (1987).

Richardson, J.F., "Incipient Fluidization and Particulates Systems." in "Fluidization", J.F. Davidson and D. Harrison, Eds., Academic Press, London (1971), pp 26 – 64.

Richardson, J.F. and W.N. Zaki, "Sedimentation and Fluidization." *Trans. Inst. Chem. Eng.* **32**, 35 – 53 (1954).

Rodrigues, M.I., C.A. Zaror, F. Maugeri and J.A. Asenjo, "Dynamic Modelling, Simulation and Control of Continuous Adsorption Recycle Extraction." *Chem. Eng. Sci.* **47**, 263-269 (1992).

Skidmore, G.L., Horstmann, B.J. and Chase, H.A., "Modelling Single-Component Protein Adsorption to the Cation Exchanger S Sepharose FF." *J. Chromat.* **498**, 113-128 (1990).

Slater, M.J. and P. Prud'homme, "Continuous Ion Exchange in Fluidized Beds." *Can. Mines Br., Tech. Bull.*, **158**, 1-67 (1972).

Thomas, H.C., "Heterogeneous Ion Exchange in a Flowing System." *JACS* **66**, 1664 – 1666 (1944).

Turner, J.C.R. and M.R. Church, "A Continuous Ion Exchange Column." *Trans. Instn. Chem. Engrs.* **41**, 283-288 (1963).

Yang, C. and G.T. Tsao, "Packed-Bed Adsorption Theories and Their Applications to Affinity Chromatography." *Advances in Biochemical Engineering* **25**, A. Fiechter, Ed., Springer – Verlag, New York, NY (1982), pp1-18.

Zheng, Y., J.-X. Zhu, J. Wen, S. Martin, A.S. Bassi, and A. Margaritis, "The Axial Hydrodynamic Behavior in a Liquid-Solid Circulating Fluidized Bed." *Can. J. Chem. Eng.* **77**, 284-290 (1999a).

Zheng, Y., J.-X. Zhu, J. Wen, S. Martin, A.S. Bassi, and A. Margaritis, "Hydrodynamic Behavior in a Liquid-Solid Circulating Fluidized Bed." In "*Circulating Fluidized Bed Technology* - III", J. Werther, Ed., Dechema, Fonkfurt (1999b), pp. 59-64.

Table 6.1 Properties of Diaion HPA25®

Matrix	Polystyrene (highly porous)
Functional Group	Quaternary Alkylamine
Ionic Form	Cl^{-1}
Average Diameter (d_p, mm)	0.32
Wet Density (ρ_s, g/mL)*	1.08
Total Exchange Capacity (Cl^-, meq/mL)	0.6
Exclusive Size (dalton)	>100,000
Terminal Velocity (U_t, m/s)	0.0045
Bed Expansion Index (n)	2.67

* Density of wet Diaion HPA25® particles equilibrated with 10 mM phosphate buffer

Table 6.2 Parameters of BSA adsorption/desorption onto/from Diaion HPA25® obtained in our laboratory

K_d (mg/mL)	k_1 (mL/mg·s)	q_m (mg/ml)	k (1/s)
0.00907	0.005	87.9	0.045

Figure 6.1 Schematic diagram of the Liquid Solid Circulating Fluidized Bed (LSCFB) ion exchange system

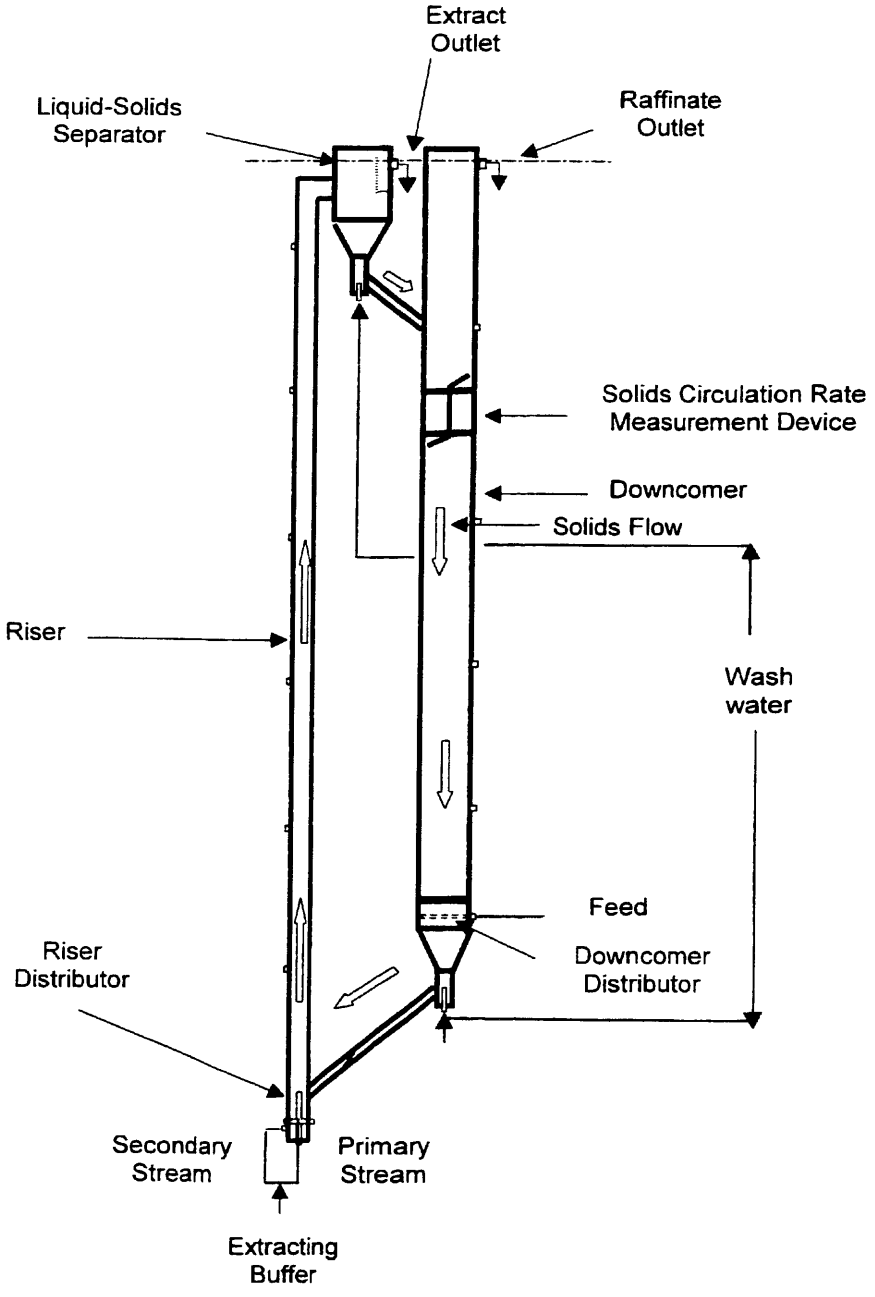

Extract
Outlet
Liquid-Solids
Separator
Raffinate
Outlet
Solids Circulation Rate
Measurement Device
Downcomer
Solids Flow
Riser
Wash
water
Feed
Riser
Distributor
Downcomer
Distributor
Secondary
Stream
Primary
Stream
Extracting
Buffer

Figure 6.2 Flow patterns in the downcomer and the riser: (a) counter-current contact of liquid and solids phases in the dense phase zone of the downcomer; (b) co-current contact of liquid and solids phases in the riser.

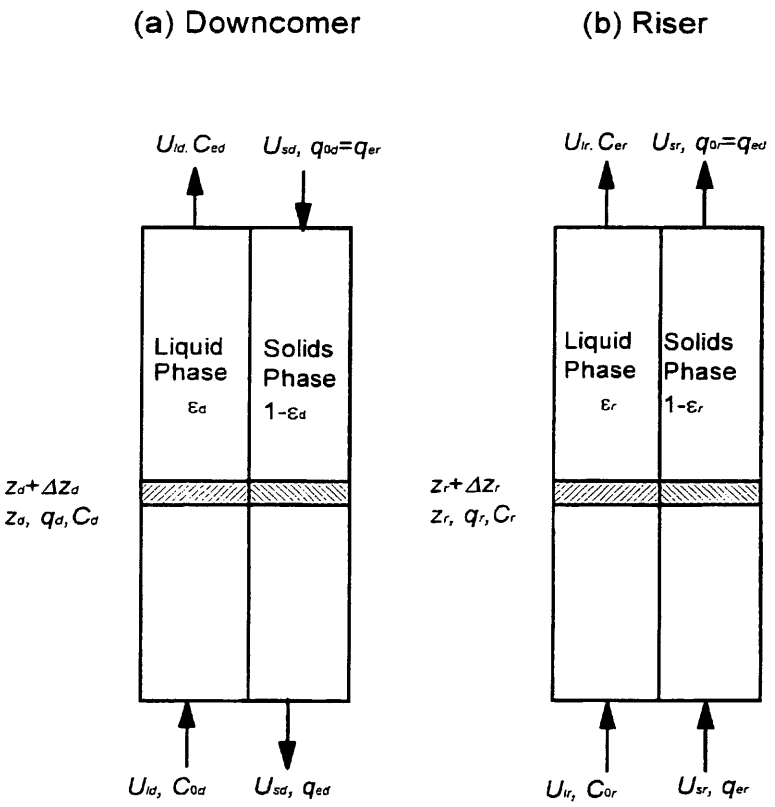


Figure 6.3 Dependency of solids holdup in the riser on the superficial liquid velocity in the riser (U_{lr}) (Beads: Diaion HPA25®; fluidization fluid: tap water; room temperature).

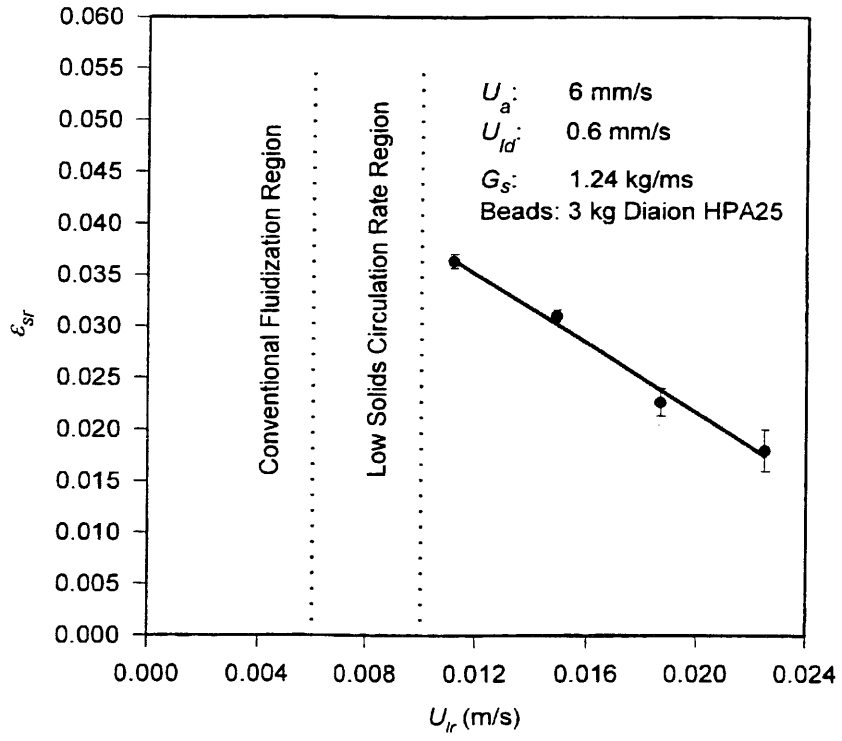


Figure 6.4 Typical experimental BSA adsorption profiles in the downcomer (U_{ld} = 0.0006 m/s, U_{lr} = 0.0113 m/s, G_s = 1.24 kg/m^2-s, H_d = 0.8 m, C_{0d} = 2 mg/mL, pH 7.0 and room temperature).

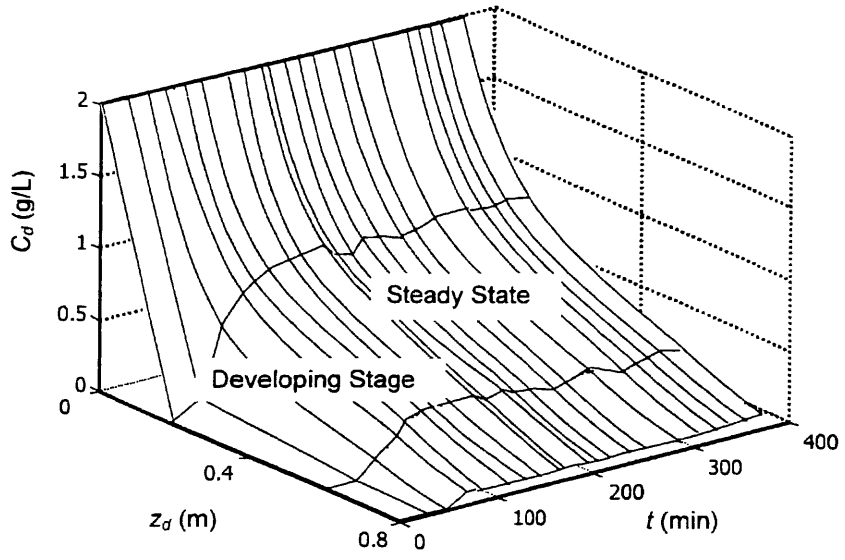


Figure 6.5 Typical experimental BSA desorption profiles in the riser (U_{fd} = 0.0006 m/s, U_{lr} = 0.0113 m/s, G_s = 1.24 kg/m^2·s, H_d = 0.8 m, C_{0d} = 2 mg/mL, pH 7.0 and room temperature)

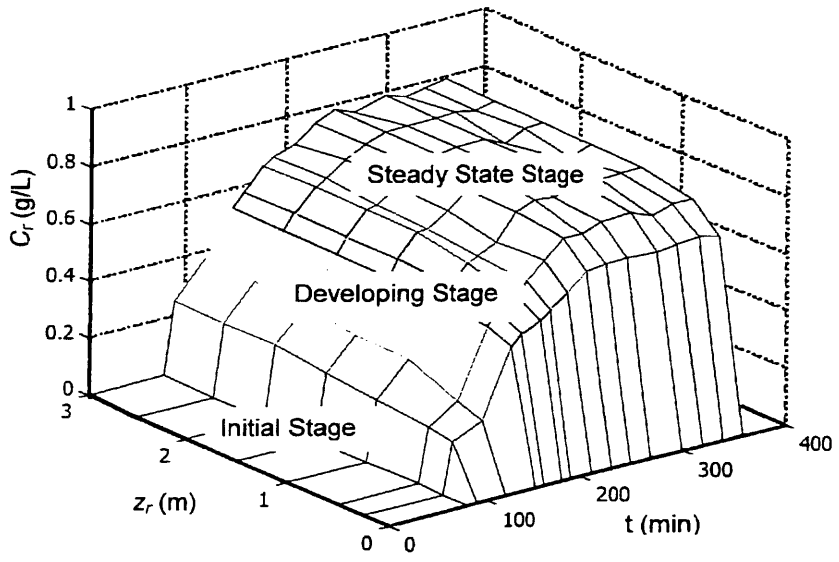


Figure 6.6 Comparison between the experimental and predicted steady state BSA desorption profiles in the riser at various superficial liquid velocity in the riser (U_{lr}) (U_{ld} = 0.0006 m/s, G_s = 1.24 kg/m^2-s, H_d = 0.8 m, C_{0d} = 2 mg/mL, pH 7.0 and room temperature).

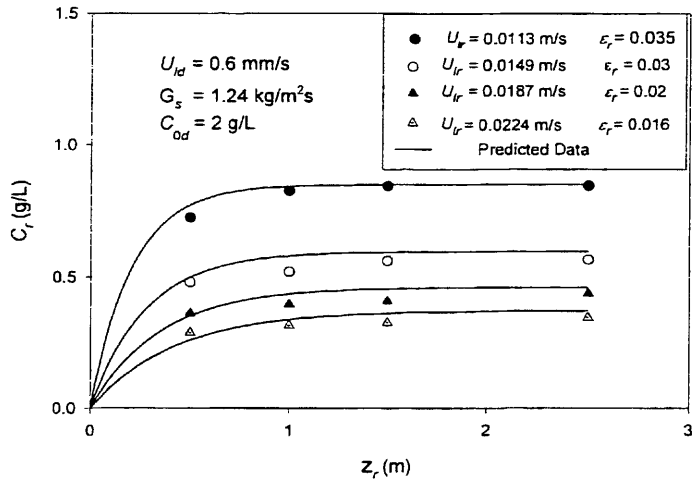


Figure 6.7 Comparison between the experimental and predicted steady state BSA adsorption profiles in the downcomer at various solids circulation rates (G_s) (U_{ld} = 0.0006 m/s, U_{lr} = 0.0113 m, C_{0d} = 2 mg/mL, pH 7.0 and room trature).

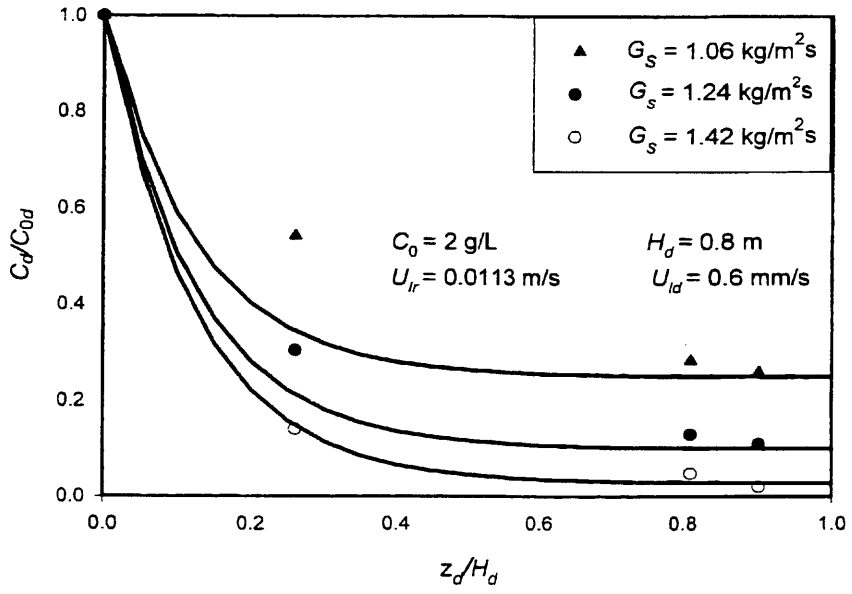


Figure 6.8 Simulation of the effects of superficial liquid velocity in the downcomer (U_{ld}) on the BSA adsorption onto and desorption from Diaion HPA25® in the LSCFB: (a) Adsorption in the downcomer; (b) Desorption in the riser. (U_{lr} = 0.0113 m/s, G_s = 1.24 kg/m^2·s, H_d = 0.8 m, C_{0d} = 2 mg/mL, pH 7.0 and room temperature)

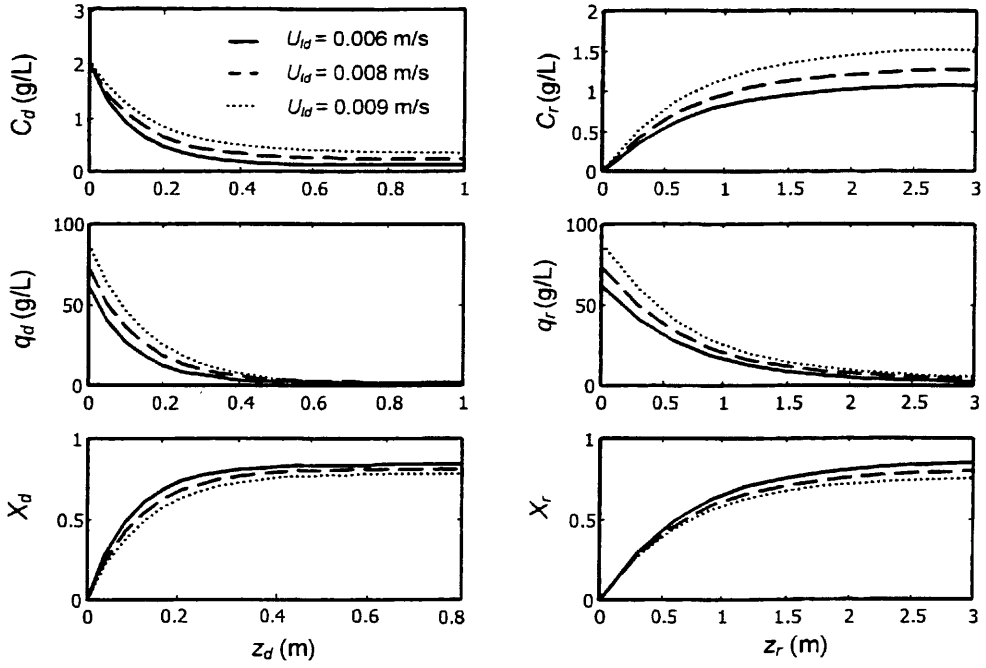


Figure 6.9 Simulation of the effects of solids circulating rate (G_s) on the BSA adsorption onto and desorption from Diaion HPA25® in the LSCFB system. (a) Adsorption in the downcomer; (b) Desorption in the riser. (U_{ld} = 0.0006 m/s, U_{lr} = 0.0113 m/s, H_d = 0.8 m, C_{0d} = 2 mg/mL, pH 7.0 and room temperature)

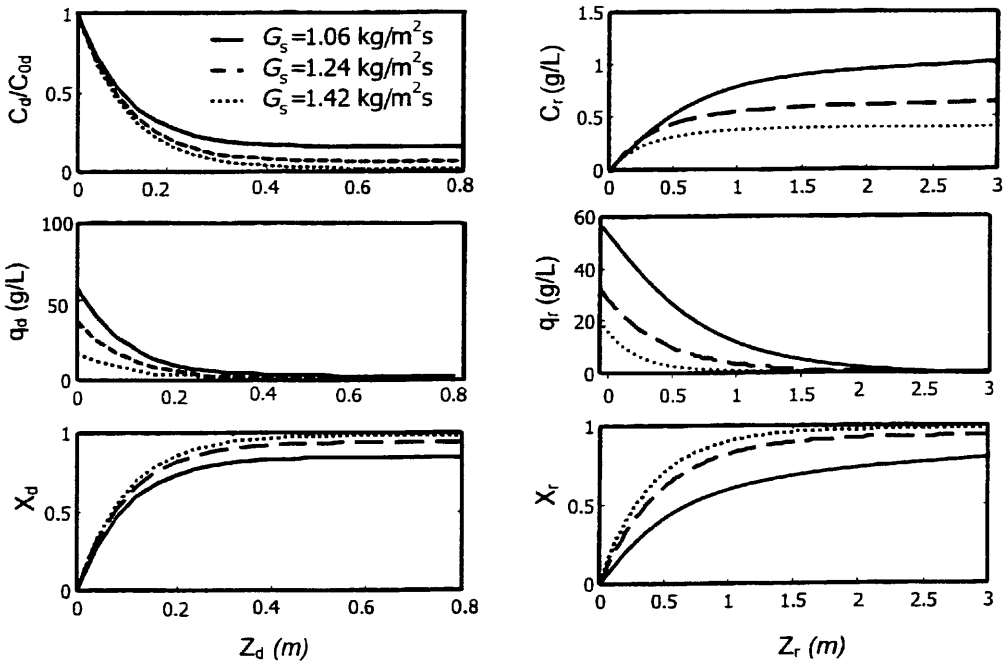
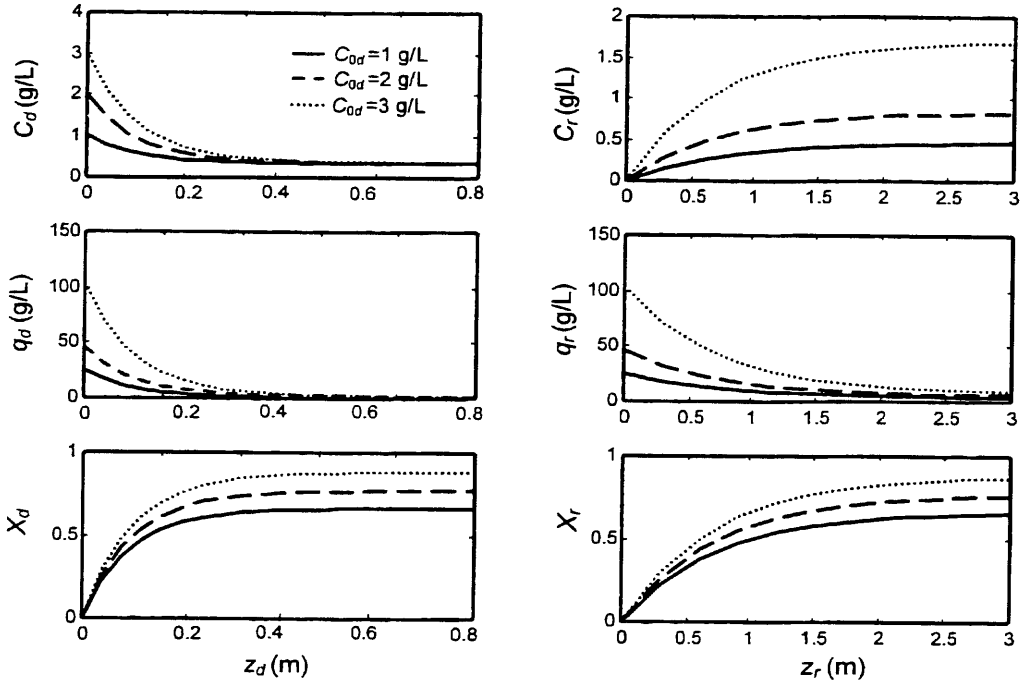


Figure 6.10 Simulation of the effects of BSA concentration in the feed on the BSA adsorption onto and desorption from Diaion HPA25® in the LSCFB. (a) Adsorption in the downcomer; (b) Desorption in the riser. (U_{ld} = 0.0006 m/s, U_{lr} = 0.0113 m/s, G_s = 1.24 kg/m^2·s, H_d = 0.8 m, pH 7.0 and room temperature).



Chapter 7. Investigation of the Continuous Recovery of BSA in an LSCFB Ion Exchange System

7.1 INTRODUCTION

The simplification of the downstream treatment is one of the key factors contributing to the cost reduction of a biological production process. This may be achieved in three ways: 1) integration of separate single steps into a new unit operation; 2) evolution of a batch process into a continuous process; and 3) the combination of steps 1 and 2. A typical biological broth usually contains a large amount of very small solids and relatively low concentration of desired product. The first task in developing a new isolation process for biological production hence usually focuses on the selection of an appropriate procedure for handling the solids present in the broth. This is typically achieved by using filtration or centrifugation. However, colloidal solids like cell debris and the viscous properties of biological broth frequently make those methods both costly and inefficient.

Whole broth extraction with a fluidized bed ion exchange system is a good strategy for down stream treatment as it eliminates the difficult solids separation step and recovers the desired

---

A version of this chapter has been submitted for publication.
Qingdao Lan, Amarjeet S. Bassi*, Jing-Xu (Jesse) Zhu, Argyrios Margaritis (2001) "Investigation of the Continuous Recovery of BSA in an LSCFB Ion Exchange System" *AIChE J.* (Submitted)

products directly from unclarified whole broth. The large bed voidage of a fluidized bed allows the particulates in the feed to pass through the bed while retaining the ion-exchange particles in the bed as the superficial liquid velocity was maintained in the range higher than the terminal velocity of the particulates in the feed and lower than the terminal velocity of the ion-exchange particles (Draeger and Chase, 1991; Chase, 1994). Continuous ion exchange using different fluidized bed systems has been a topic of extensive research (Turner and Church, 1963; Higgins, 1969; Slater and Prud'homme, 1972; Porter, 1975; Himsley, 1981; Pungor *et al.*, 1987; Burns and Graves, 1989; Gordon *et al.*, 1990; Rodrigues *et al.*, 1991; Byers *et al.*, 1997). Burns and Graves (1989) applied a two-column magnetically stabilized fluidized bed system for the continuous chromatography of biochemical products. Those authors, however, treated the system as comprised of two identical columns and no discussion was provided regarding the transportation of ion-exchange particles between those two columns. In addition, the operation of the magnetically stabilized fluidized bed system was complicated and costly. Gordon *et al.* (1990) reported the continuous affinity recycle extraction (CARE) of proteins using two well-stirred reactors. This system, although simple and easy to control, has the disadvantage of low ion exchange efficiency and the requirements of large processing volumes even for a moderate throughput requirement. Himsley (1993) patented a continuous counter-current ion exchange process from a feed liquor containing ions which when absorbed caused the density of the particles to increase. However, this device was designed only for the adsorption. The other operations of an ion exchange process, i.e., desorption, washing and regeneration were still carried out in a conventional packed bed process.

To overcome the above problems, an LSCFB system was proposed as an excellent candidate for the continuous recovery of protein from unclarified whole broth (Chapter 6). In the proposed LSCFB system, the adsorption and desorption (regeneration) is carried out in the two separated fluidized beds, the downcomer and the riser, in a continuous mode with the ion-exchange

particles circulating continuously between the two columns. The introduction of a liquid-solid circulating fluidized bed opens the possibility of developing an integrated unit operation that recovers products from the unclarified whole broth directly and continuously. The LSCFB has the advantages of a conventional fluidized bed, e.g., the applicability to unclarified whole broths and the low bed pressure drops. Most importantly, it is a continuous operation with simultaneous adsorption and desorption.

In Chapter 4, the concept of the LSCFB system was introduced and models were developed on the adsorption and desorption. The isothermal characteristics and the kinetics of BSA adsorption onto Diaion HPA25 have been reported in Chapter 5 and previous papers (Lan *et al.*, 2000b; Rowe *et al.*, 1999). The objective of the current work is to study the hydrodynamics of the system and to investigate the parameters affecting the protein recovery using a model protein, bovine serum albumin (BSA).

7.2 MATERIALS AND METHODS

7.2.1 Materials

Anion exchanger Diaion HPA25®, purchased from Sigma Chemical Co. (St Louis, MO), were used for all the hydrodynamic studies and BSA adsorption/desorption studies. The properties of Diaion HPA25® are listed in Table 1. Bovine serum albumin (BSA), purchased also from Sigma, was used as model protein in adsorption/desorption experiments. Phosphate buffer of pH 7.0 (10 mM) was used in all the adsorption/desorption studies. Hydrodynamic studies were conducted using tap water as the fluidization liquid.

7.2.2 Experimental Apparatus

As shown in Figure 7.1, the major components of the LSCFB system included a riser (1), a downcomer (8), a liquid-solid separator (2), a top solids return pipe (6), a bottom solids return pipe (11), a top wash section (5) and a bottom wash section (10). The riser was 3.0 m tall and 38 mm in diameter and the downcomer 2.5 m tall and 120 mm in diameter. Two separate liquid streams were used to fluidize the particles in the riser and the downcomer while the particles circulating between the two columns. The riser was operated in the high-velocity circulating fluidization regime and the downcomer in the low-velocity conventional fluidization regime. To secure the pressure balance between the riser and the downcomer, which is very important for the stable operation of an LSCFB system (Zheng and Zhu, 2000), the liquid outlets on the top of the downcomer and the separator were located at the same level. The distributor for the downcomer was a tubular ring, which was carefully designed in order to have a uniform liquid distribution while allowing the solids to flow through.

The distributor for the riser (14) was designed so as to divide the incoming stream into two sub-streams: the primary and the auxiliary streams. The primary stream entered through a tubing of 1.1 cm in I.D. extending 5.1 cm into the riser. The outlet of the primary stream was located above the solids entrance at the bottom of the riser. This design helped to increase the pressure drop across the bottom solids return pipe and made the system more stable. The purpose of the auxiliary stream was to mobilize the particles at the bottom, which were then entrained up the riser by the combination of the primary and the auxiliary streams.

The solids circulation rate in this apparatus was controlled by a butterfly valve located on the bottom solids return pipe. This mechanical valve was preferred over the hydraulic valve described by Zheng *et al.* (1999, 2000) due to the low density of the Diaion HPA25 anion exchange particles, which made the operation of a hydraulic valve difficult.

The solids circulation rate was measured by a device which consisted of a central vertical plate and two half butterfly valves. The central plate divided the column into two halves and the two butterfly valves were fixed at the top and the bottom of the two half-sections. By appropriately flipping over the two valves from one side to the other, particles circulated through the system could be accumulated in one side of the measuring section for a specific period of time to calculate the particle circulation rate. The pressure gradient in riser and the downcomer was measured using pressure manometers.

The dynamic seals between the riser and the downcomer were achieved by maintaining the two solids return pipes in the moving packed bed regime. The top wash section and the bottom wash section rinsed the particles before entering the solids return pipes and helped to dilute and prevent the inter-mixing of the liquids from the riser and the downcomer sections.

7.2.3 Continuous BSA Ion Exchange in the LSCFB System

Continuous bovine serum albumin (BSA) ion exchange in the LSCFB system was conducted with 2 g/L BSA solution as feed and 0.4 M NaCl solution as extracting buffer unless otherwise indicated in the text. Both BSA and NaCl solutions were prepared in 10 mM, pH 7.0 phosphate buffer. Other conditions were indicated in the text. In the continuous BSA ion exchange studies in the LSCFB, the feed protein solution was introduced from the tubular distributor into the bottom of the downcomer. The regenerated Diaion HPA25® ion exchange particles were introduced from the top solids return pipe into the top of the downcomer. The liquid velocity was controlled in such a way that the downcomer operated in the conventional fluidized regime

(liquid velocity in the downcomer was maintained lower than the terminal velocity of the ion exchange particles), where the ion exchange particles moved down counter-current to the rising feed liquid. As the particles and feed broth contacted counter-currently in the downcomer, the BSA in the broth was adsorbed onto the ion-exchange particles. The de-proteinized solution was discarded from the top of the downcomer. The loaded particles were then transferred to the bottom of the riser through the bottom solids return pipe after washing. The extracting buffer (0.4 M NaCl solution in 10 mM pH 7.0 phosphate buffer) was applied from the bottom of the riser. The superficial velocity in the riser (U_{lr}), which was the combination of the primary and the auxiliary streams, was kept higher than the terminal velocity of the Diaion HPA25® particles. The loaded particles were hence carried upward by this buffer stream while desorption proceeded. In the liquid-solid separator, the regenerated particles and the effluent were separated. Then, the regenerated particles were returned to the top of the downcomer through the top solids return pipe. During the process of continuous ion-exchange, samples were taken from different locations of the columns and the BSA concentration was determined by measuring the absorbance at 280 nm using a Cary Bio 50 UV-Visible spectrophotometer.

7.2.4 Measurement of Solids Holdup

The solids hold-up in the riser and the downcomer was calculated from the pressure gradients in the columns. The pressure gradient in the riser or downcomer column was measured by a manometer as shown in Figure 7.1 and was given as:

$$\frac{\Delta P}{\Delta z} = (1 + \frac{h}{\Delta z})\rho_l g \qquad 7.1$$

Given the fact that the liquid velocities in both the riser (U_{lr}) and the downcomer (U_{ld}) are very low (In the range of 10-30 mm/s for U_{lr} and less than 2.0 mm/s for U_{ld}), it is realistic to ignore the pressure drops due to the liquid flow. Therefore, the solids holdup, bed voidage and pressure gradient could be related as in equation 7.2:

$$\frac{\Delta P}{\Delta z} = (\varepsilon_s \rho_s + \varepsilon_l \rho_l) g \qquad 7.2$$

With $\varepsilon_s + \varepsilon_l = 1$, one then has the following relationship between the solids holdup and the pressure gradient:

$$\varepsilon_s = \frac{(\rho_s - \rho_l)}{\rho_s} \frac{h}{\Delta z} \qquad 7.3$$

7.2.5 Measurement of the Maximum Capacity of Diaion HPA25 Anion Exchange Particles

Measurement of the maximum capacity of Diaion HPA25® ion exchange particles was conducted by putting 10 ml swollen Diaion HPA anion exchange particles into a series of 125-ml flasks containing 25 ml of 10 mM phosphate buffer (pH 7.0) with various concentrations of BSA. The flasks were then sealed by parafilm "M" (American Can Company) and put on a shaker controlled at 25°C and 200 rpm. After adsorption for 36 hours (previous experiments had shown that equilibrium was reached under this condition), the supernatant was centrifuged at 10,000 rpm for 10 minutes. The protein concentration of the supernatant was analyzed by measuring the absorbance at 280 nm using a Cary Bio-50 UV-Visible spectrophotometer. The data was interpreted using the Sctarchard plot based on a modified Langmuir model (Lan *et al.*, 2000b, Chapter 5).

7.3 RESULTS AND DISCUSSION

1. The Superficial Liquid Velocity (U_{ld}) and the Fluidization in the Downcomer

The liquid velocity in the downcomer (U_{ld}) is a very important parameter for the LSCFB system because it has profound influences on the fluidization in the downcomer and the overall throughput of the system. When U_{ld} is maintained in a suitable range, the downcomer can be divided into three zones according to their different solids holdups: the dense phase zone, the dilute section and the freeboard zone (Figure 7.2). The dense section in the downcomer operates as a conventional fluidized moving bed (Kwauk, 1992) in which solids move down and liquid moves up. The axial solids holdup distribution in such a particulate moving fluidized bed is uniform and the bed expansion can be described by the generalized Richardson and Zaki equation (Richardson and Zaki, 1954; Kwauk, 1992), i.e.,

$$\frac{V_{ld}+V_{sd}}{U_i}=\varepsilon_d^{n-1} \qquad 7.4$$

where U_{ld} and U_{sd} are the liquid velocity and the solids velocity in the downcomer, respectively; ε_d is the bed voidage in the downcomer; and the bed expansion index, n, can be determined experimentally or from the following correlation:

$$n=\left(4.4+18\frac{d_p}{D}\right)\mathrm{Re}_t^{-0.1} \qquad 7.5$$

The dilute section is created when the particles are fed into downcomer through the solids entrance when the surface of the dense section is lower than the solids entrance. Ion exchange particles thus fall from the entrance to the dense section surface and this section of bed is the dilute section. The solids hold-up in this section is determined by the solids circulation rate.

When G_s is zero, the solids holdup in this section is zero. Since the stable operating G_s is small in the LSCFB system, the solids holdup in the dilute section is lower than that in the dense section. Similar to that of most liquid-solid conventional fluidized beds, the solids hold-up in the freeboard is nearly zero. There is a clear interface between the freeboard and the dilute section. Under most conditions, there is also a clear interface between the dilute section and the dense section. When G_s is very large and solids holdup of the dense section is low, however, the interface may disappear because the difference between the solids holdups of those two zones is not so evident.

The fractions of the dense section, the dilute section and the freeboard are determined mainly by the values of U_{ld} and G_s given a constant amount of particles in the system. As shown in Figure 7.3, the dense section height (H_d) increased significantly with the liquid velocity in the downcomer (U_{ld}) and decreased considerably with the increase of the solids circulation rate (G_s). When the height of the dense section was increased to the location of the solids entrance on the downcomer, the dilute section will be overlapped by the dense section, under which conditions the downcomer will have only two zones: the dense section and the freeboard. The freeboard, however, is an essential component of the downcomer for preventing the loss of ion-exchange particles. The values of U_{ld} and G_s should therefore be maintained in a range that guarantees a certain length of the freeboard.

In terms of protein adsorption in the downcomer, the dense section is the most important zone because most of the ion-exchange particles are in this zone and the protein remaining in the liquid phase in the dilute section and the freeboard should be very low under a non-breakthrough adsorption condition. Therefore, the bed height (H_d) and the solids holdup of the dense section (ε_{sd}) are important parameters for protein adsorption in the downcomer. Higher and denser dense section will increase protein adsorption, but a very high solids holdup may cause retention of the unwanted solids from the feed due to the reduced passage through the bed.

When the total amount of the ion-exchange particles circulating in the LSCFB is constant, the dense section height in the downcomer at steady state is dependent mainly on three factors: the liquid velocities in the riser (U_{lr}) and downcomer (U_{ld}), and the solids circulation rate (G_s). As discussed above, U_{ld} directly affects the bed expansion of the particles in the downcomer and hence the dense section height. On the other hand, U_{lr} and G_s influence the amount of ion-exchange particles available for the downcomer dense section when the total particles amount is constant. The higher the U_{lr} and the G_s, the less the particles available for the downcomer dense section as more particles are circulating in other parts of the LSCFB system.

7.3.1 The Superficial Liquid Velocity (U_{lr}) and the Solids Hold-up in the Riser

As discussed above, the riser of the LSCFB system operates in the circulating fluidization regime where particles are carried up by the liquid along the riser and compensated by the continuous feeding of particles into the base through the bottom solids return pipe. Figure 7.4 shows that the axial solids holdup distribution of Diaion HPA25 was uniform along the riser. This result was in agreement with that reported by Liang *et al.* (1997) and Zheng *et al.* (1999, 2000).

Figure 7.5 shows the significant effects of the superficial liquid velocity (U_{lr}) and the solids circulation rate (G_s) on the solids holdup in the riser (ε_{sr}). It is clear that at a given U_{lr}, ε_{sr} increased with the increase of G_s. On the other hand, for a particular G_s, ε_{sr} decreased with the increase of U_{lr}. Worth mentioning is that for a specific G_s value, the U_{lr} must be maintained above a critical value. In other words, if U_{lr} is lower than the critical value, the specified G_s is unachievable. This is shown in Figure 7.5 as the low solids circulation region. The conventional fluidization region shown in Figure 7.5 was the region where U_{lr} was so low that $G_s = 0$. That is,

no solids circulation was observed in this region and, by definition, the riser operated in the conventional fluidization regime.

7.3.2 Regeneration of Diaion HPA25® in the LSCFB System

The regeneration of the ion exchange particles in the LSCFB system was carried out in the riser. The extent of regeneration is a very important parameter for the stable operation of the system. Maximum capacity of regenerated ion exchange particles, as an indication of the extent of the regeneration, is one of the key factors that influence the dynamic adsorption capacity of the system. To measure the extent of regeneration, samples of regenerated ion exchange particles were taken from the liquid-solids separator and the maximum BSA adsorption capacities of those regenerated particle samples (q_m') were measured. Figure 7.6 shows the time profile of the maximum capacity of the regenerated ion exchange particles for the first run with fresh Diaion HPA25 anion exchange particles. In the initial stage, the normalized maximum capacity of the regenerated ion exchange particles (q_m'/q_m) was approximately 1.0. This was due to the fact that the particles carried up into the separator in the initial stage were only the fresh ion exchange particles initially packed in the bottom solids return pipe. Those particles did not contact with the feed before they were transported to the riser. In the developing stage, however, the regeneration rate decreased with time, indicating that a part of the adsorption capacity was lost due to fouling and the incomplete regeneration. However, the normalized maximum capacity was stabilized in the steady state stage at around 0.75.

It is interesting to find that, after 5 consecutive runs with a total treatment volume of about 900 L feed (representing a feed/particle ratio of 300 L/kg or 138.5 L/L), the q_m' of the regenerated ion exchange particles was still at approximately 62 mg/ml, representing a stabilized q_m'/q_m value of around 0.7. This result indicates that although the BSA adsorption capacity of the fresh Diaion HPA25 anion exchange particles was decreased by almost 30% in the first run, likely due to

fouling and incomplete regeneration, a steady state of regeneration was achieved so that the maximum protein adsorption capacity of the regenerated particles remained stable thereafter. This is very important for the stable operation of the system. It is still possible, however, when the system is applied for a long period of continuous operation, that the protein adsorption capacity may reduce further to a significant point that a thorough regeneration of the particles with stronger conditions becomes necessary.

7.3.3 Dynamic Adsorption Capacity of the System (*D*)

Protein loading rate is the amount of protein loaded onto the LSCFB system in a unit time. It can be calculated as follows:

$$L = Q_d C_0 = A_d U_{ld} C_0 \qquad 7.6$$

where Q_d is the flowrate of feed and A_d the cross-sectional area of the downcomer. For a particular LSCFB system A_d is a constant so that L is proportional to U_{ld} and C_0. Higher protein loading rate will increase the system throughput. However, protein loss through the raffinate will occur when the protein loading rate is higher than what the system can handle.

A dynamic adsorption capacity of the LSCFB system (D) is defined as the amount of proteins adsorbed onto the ion exchangers in the downcomer under the maximum allowable protein loading rate. The maximum allowable protein loading rate is defined here as the maximum protein loading rate for given operating conditions beyond which significant leakage of protein will happen. The dynamic adsorption capacity of an LSCFB system is determined by four major factors: the maximum BSA adsorption capacity of the regenerated ion exchange particles (q_m'), the solids circulation rate (G_s), the fluidization and backmixing in the downcomer, and the

adsorption equilibrium in the downcomer, particularly in the dense section. The dynamic adsorption capacity of the downcomer could thus be calculated as follows:

$$D = \frac{\kappa G_s A_r q_m'}{\rho_s \varepsilon_{mf}} = L_{\max} - (Q_d C_{ed})_{\max} = (L Q_d (C_0 - C_{ed}))_{\max} \quad 7.7$$

where A_r is the cross-sectional area of the riser and κ is a lumped correction factor determined by the fluidization, the backmixing and the adsorption equilibrium in the dense section particulate bed in the downcomer. κ equals unity if there is no backmixing (plug flow) for both liquid and solids in the dense section, and if the mass transfer is very fast so that the adsorption equilibrium is achieved instantly. Otherwise, κ is a constant less than 1. In addition, ρ_s, ε_{mf}, and A_r are all constant for a given LSCFB system. Therefore, the dynamic adsorption capacity of an LSCFB is proportional to G_s and q_m'. The subscript "max" indicating the conditions of maximum allowable loading rate.

The dynamic adsorption capacity of an LSCFB system represents the upper limit of the protein loading rate of a particular system. In other words, if the actual protein loading rate is larger than the dynamic adsorption capacity of the system, the ion exchange particulate bed in the downcomer will be "broken through" and significant amount of proteins will leak into the raffinate.

A unique feature of the LSCFB system is that it is suitable for the adsorption using ion exchange particles with relatively low adsorption capacity. Because loaded ion exchange particles are continuously regenerated in this system, the low capacity of ion exchange particles can be compensated to a certain extent. As discussed above, the dynamic adsorption capacity of the

system is determined by the q_m', G_s and the fluidization in the dense section. Therefore, with good fluidization and a relatively large G_s, a reasonably large magnitude of dynamic adsorption capacity of the LSCFB system can be achieved even for ion exchange particles with relatively low adsorption capacity.

7.3.4 Influence of Operating Conditions on BSA Adsorption Ratio in the Downcomer

The protein adsorption ratio in the downcomer, X_d, is determined by the following equation:

$$X_d = \frac{(C_{0d} - C_{ed})}{C_{0d}} \qquad 7.8$$

where C_{0d} and C_{ed} are the protein concentrations in the feed and the raffinate, respectively.

G_s is a very important parameter which influences the protein adsorption in the downcomer. The experimental results of BSA adsorption in the downcomer under conditions of C_{0d} = 2 g/L, U_{ld} = 0.6 mm/s, U_{lr} = 11.3 mm/s and various G_s are shown in Figure 7.7. It was clear that G_s had significant effects on the BSA adsorption. At a high G_s of 1.42 kg/m^{2}s, almost all BSA in the feed (98%) was removed. When G_s was reduced to 1.06 kg/m^{2}s, however, only about 70% of the BSA was removed, indicating significant loss of protein.

The remarkable influence of G_s on the protein adsorption in the downcomer can be illustrated by its effects on the dynamic adsorption capacity of the system. As discussed above, the dynamic adsorption capacity of an LSCFB system is proportional to G_s. The system thus has a remarkably higher dynamic capacity at G_s = 1.42 kg/m^{2}s than that at G_s = 1.06 kg/m^{2}s. In other words, the results indicate that the actual protein loading rate at the tested condition (U_{ld} = 0.6 mm/s and C_0

= 2 g/L) was higher than the dynamic adsorption capacity (the maximum allowable protein loading rate) of the system at the conditions of G_s = 1.06 kg/m^{2}s and U_{ld} = 0.6 mm/s so that a significant protein loss happened under those conditions.

The influence of the liquid velocity in the downcomer (U_{ld}) on the BSA adsorption is shown in Figures 8a and 8b. The experiments were carried out under conditions of C_{0d} = 2 g/L, U_{tr} = 11.3 mm/s, G_s = 1.42 kg/m^{2}s and various U_{ld}. The height of the dense section in the downcomer was carefully maintained at 0.8 m by controlling the amount of Diaion HPA25 particles in the system. When U_{ld} increased from 0.6 mm/s to 1.0 mm/s, the protein concentration in the raffinate increased remarkably from 0.04 g/L to 0.42 g/L (Figure 7.8a) and the adsorption ratio in the downcomer decreased accordingly from 98% to 79% (Figure 7.8b), indicating that a significant protein leakage happened at conditions U_{ld} = 10 mm/s. The influence of U_{ld} on the protein adsorption in the downcomer has two aspects: 1) It directly influences the protein loading rate. The protein loading rate increases proportionally with the increase of U_{ld}. 2) It affects the fluidization and backmixing of ion exchange particles in the dense section, which in turn influence the dynamic adsorption capacity of the system. The influence of U_{ld} on the dynamic adsorption capacity is somewhat a complicated issue. While the increase of U_{ld} increases the bed height of the dense section, which is beneficial for a higher dynamic adsorption capacity, it also increases backmixing, which tends to reduce the dynamic adsorption capacity.

7.3.5 Effects of Operating Conditions on BSA Desorption Ratio in the Riser and the Overall BSA Recovery

The protein desorption ratio in the riser is defined by the following equation:

$$X_r = \frac{(q_{0r} - q_{0r})}{q_{0r}} \qquad 7.9$$

where q_{0r} and q_{er} are protein concentrations in the solid phase at the solids entrance of the riser and in the separator, respectively. However, q_{0r} and q_{er} are usually difficult to measure. It is much more convenient to obtain the protein desorption ratio in the riser by the following equation:

$$X_r = \frac{X}{X_d} \qquad 7.10$$

where X is the overall protein recovery of the LSCFB system and X_d the protein adsorption ratio in the downcomer. The overall protein recovery is the ratio between the protein output flux in the extract and the input flux (the loading rate) in the feed. It can be calculated by the following equation:

$$X = \frac{Q_r C_{er}}{Q_d C_{0d}} \qquad 7.11$$

where Q_r and Q_d are the liquid flowrates in the riser and the downcomer, respectively. C_{er} is the protein concentration in the extract and C_{0d} the protein concentration in the feed.

The effects of U_{lr} on the adsorption in the riser were investigated under C_{0d} = 2 g/L, U_{ld} = 0.6 mm/s, G_s = 1.24 kg/m^{2}s and various U_{lr}. The results are shown in Figures 9a and 9b. When other conditions such as the solids circulation rate and protein concentration in the entering particles were constant, the protein concentration in the extract decreased significantly with the increase of the superficial liquid velocity in the riser (Figure 7.9a). This is because at higher U_{lr}, the same amount of protein recovered was diluted by more extract buffer. As shown in Figure 7.9b, however, the increase of U_{lr} resulted in an increase of the overall recovery rate.

7.3.6 The Stable Operation Window: Hydrodynamic Aspect

For a continuous system, one of the keys is how to achieve and maintain a stable and steady-state operation. There are two aspects of the stable operation of the LSCFB system: hydrodynamic stability and kinetic stability. The achievement and maintenance of hydrodynamic steady state is the prerequisite for the kinetic steady state. The hydrodynamic stable operating window for our particular system with respect to operating conditions U_{ld}, U_{lr} and G_s is shown in Figure 7.6. Although the hydrodynamic stable operating window is very system-dependent, some generalized principles exist and are be discussed as follows.

7.3.7 Superficial Liquid velocity in the downcomer (U_{ld})

Superficial Liquid velocity in the downcomer (U_{ld}) is one of the most important operation conditions affecting the stability of the system. The influence of U_{ld} includes the following two aspects: (1) the fluidization in the dense phase section; and (2) the passage of particulates in the feed through the ion exchange beads bed. Therefore, the liquid velocity in the downcomer should be large enough to fluidize the ion exchange bed to provide enough voidage for the pass of the particulates in the feed. If U_{ld} is lower than the above limit, particulates in the broth will be retained in the bed and the whole column will eventually be blocked.

On the other hand, the liquid velocity in the downcomer should not be larger than the terminal velocity of the ion exchanger particles to allow the particles to fall down in the downcomer. Furthermore, to prevent the lose of ion exchange particles, U_{ld} should be in such as magnitude that a section of freeboard is maintained in the downcomer. In this particular LSCFB system with

its downcomer dimension, ion exchange beads (Diaion HPA25 anion exchanger) and the bead amount (3.0 kg), the maximum U_{ld} was determined to be 0.9 mm/s, representing a maximum flowrate (feed plus bottom wash water) of 36.5 L/hr.

7.3.8 Superficial liquid velocity in the riser (U_{lr})

Superficial liquid velocity in the riser (U_{lr}) is another important operation condition with significant influence on the stability of the system. The U_{lr} must be higher than the terminal velocity of ion exchange beads to operate the riser in the circulating fluidization regime. The terminal velocity of Diaion HPA25 beads was determined as 4.5 mm/s or 18.5 L/hr in flowrate.

Too large a U_{lr}, however, will destabilize the system due to the accumulation of ion exchange particles in the liquid-solid separate. When the liquid velocity in the riser is close or higher than terminal velocity of the particles, the particles cannot be transferred into the downcomer. The maximum U_{lr} for this system was determined to be 29.3 mm/s or 119.4 L/hr.

7.3.9 Solids Circulating Rate (G_s)

Solids Circulating Rate (G_s) is, as discussed previously, an important parameter contributing to the dynamic adsorption capacity of the system, the higher the G_s, the larger the dynamic adsorption capacity of the system. G_s is also a very important parameter for the maintenance of the dynamic seal *between* the riser and the downcomer. As discussed previously, the dynamic seal between the riser and the downcomer is maintained by keeping the solids return pipes in the packed moving bed regime. At steady state, the amount of particles transferred into the solids return pipe from the downcomer, which is determined by the downward solids flux in the

downcomer, equals the particles transferred to the riser, which is determined by the upward solids flux in the riser. If, under given conditions, the upward solids flux represented by G_s in the riser is larger than the maximum possible downward solids flux in the downcomer, the solids holdup in the bottom solids return pipe will be reduced to make up the balance. If this condition continues, the solids holdup in the solids return pipe will eventually become so low that the dynamic seal cannot be maintained.

As shown in Figure 7.6, the maximum G_s is dependent on U_{ld} and U_{ld}. At the low U_{lr} range, the maximum upward solids flux in the riser is less than the maximum downward solids flux in the downcomer. Therefore, the maximum G_s is determined by the solids entraining capacity of the liquid. On the other hand, at high U_{lr} range, the maximum downward solids flux is less than the maximum solids flux in the riser, hence the maximum G_s is determined by the solids flux in the downcomer, which is dependent on the U_{ld}.

7.3.10 Removal of Contaminants from Product Streams

Results from this study as discussed above have shown that the LSCFB system is a good device for continuous protein recovery. In addition, because of the unique features associated with the LSCFB (high adsorption efficiency, applicability to unclarified streams, etc.), it is also suitable for the removal of contaminant ions from substrate, product or intermediate product streams. For instance, with the use of appropriate ion-exchange particles, the LSCFB system will be very efficient for the de-ionization of water and for the removal of colored bodies from fructose syrups. This system will be particularly beneficial for the selective removal of low concentration contaminants from raw substrate. For example, for the fermentation of citric acid using molasses

as sugar source, it is necessary to remove the ironic ions from molasses to channel the metabolism stream into the biosynthesis of citric acid. As molasses is a raw material containing particulates which are harmless to the fermentation process but hard to separate, it will be very advantageous to employ the LSCFB system under this situation.

7.4 CONCLUSIONS

An LSCFB system has for the first time been developed and demonstrated successfully for continuous protein extraction. Hydrodynamic studies show that the device was stable and suitable for continuous protein recovery. It is found that the downcomer could be divided into three zones according to the solids holdup: the dense section, the dilute section and the freeboard. The dense section is the most important zone for protein adsorption and the freeboard is an essential component for preventing the loss of ion exchange particles. Continuous BSA adsorption and desorption and regeneration of ion exchange particles in the system are studied with respects to the influence of different operating conditions. Important parameters such as protein loading rate, dynamic adsorption capacity, protein adsorption and desorption ratios, and overall protein recovery are defined and discussed. Results regarding the continuous BSA recovery using this system show a high protein removal efficiency of up to 98% and a moderate overall protein recovery of up to 84%. Results indicate that this system is promising for both protein recovery and the removal of contaminants from products or intermediate-products.

NOMENCLATURE

A	cross-sectional area of a column, m^2
C	concentration of BSA in the liquid phase, g/L or kg/m^3
d_p	particle mean diameter, m
D	dynamic adsorption capacity of the LSCFB system, g BSA/s or g BSA/h
G_s	solids circulation rate, kg/m^2s
H_r	riser height, m
H_d	dense section height in the downcomer, m
L	protein loading rate, g/s or kg/s
Q	flowrate of liquid in a column, m^3/s or L/min
q	concentration of protein in solids phase, g/L or kg/m^3
q_m	maximum BSA adsorption capacity of the ion exchange particles, g/L or kg/m^3
q_m'	maximum BSA adsorption capacity of the regenerated ion exchange particles, g/L or kg/m^3
R	Regeneration rate of ion exchange particles, dimensionless
t	time, s
U_l	superficial liquid velocity, mm/s
U_m	minimal fluidization velocity, mm/s
U_s	superficial solids velocity, mm/s
U_t	particle terminal velocity, mm/s
V_l	liquid velocity (mm/s)
V_s	solids velocity (mm/s)
X	overall protein recovery

X_d protein adsorption ratio in the downcomer

X_r protein desorption ratio in the riser

z distance from the bottom of a column, m

Greek Letters

ε_l bed voidage, dimensionless

ε_s solids holdup, dimensionless

ρ density, kg/m^3

κ equation constant, dimensionless

Subscripts

d downcomer

e exit

l liquid phase

r riser

s solids phase

max conditions under maximum loading rate

0 inlet (initial)

REFERENCES

Burns, M.A. and D.J. Graves, "Continuous Affinity Chromatography Using a Magnetically Stabilized Fluidized Bed," Biotechnol. Prog. 1, 95 – 103 (1995).

Byers, C.H., W.G. Sisson, T.S. Snyder, R.J. Beleski, U.P. Nayak and T.L. Francis, " Zirconium and Hafnium Separation in Sulfate Solutions Using Continuous Ion Exchange Chromatography." US5618502 (1997).

Chase, H.A., "Purification of Proteins by Adsorption Chromatography in Expanded Beds," *TIBTECH* **12**, 296-303 (1994).

Draeger, N.M. and Chase, H.A. 1991. "Liquid Fluidized Bed Adsorption of Protein in the Presence of Cells". *Bioseparation* **2**:67-80

Gordon, N.F., H. Tsujimura and C.L. Cooney, "Optimization and Simulation of Continuous Affinity Recycle Extraction." *Bioseparation* **1**, 9-12 (1990).

Higgins, I.R., "Continuous Ion Exchange of Process Water." *Chem. Eng. Prog.*, **65**(6), 59-62 (1969).

Himsley, A., "Continuous Countercurrent Ion Exchange Process." US4279755 (1981).

Lan, Q., J.-X Zhu, A.S. Bassi, A. Margaritis, Y. Zheng and G.E. Rowe, "Continuous Protein Recovery Using a Liquid-Solid Circulating Fluidized Bed Ion Exchange System: Modelling and Experimental Studies", *Can. J. Chem. Eng.* (2000b) (In press)

Lan, Q., A.S. Bassi, J.-X. Zhu and A. Margaritis, "A Modified Langmuir Model for the Prediction of the Effects of Ionic Strength on the Equilibrium Characteristics of Protein Adsorption onto Ion Exchange/Affinity Adsorbents", *Chem. Eng. J.* (2000b), (In press)

Liang, W-G, S.L. Zhang, J.-X. Zhu, J. Yong, Z.Q. Yu and Z.W. Wand, "Flow Characteristics of the Liquid-Solid Circulating Fluidized Bed", *Powder Technol.* **90**, 95-102 (1997)

Porter, R.R., "Continuous Ion Exchange Process and Apparatus." US3879287 (1975).

Pungor, E., N.B. Afeyan, N.F. Gordon and C.L. Cooney, "Continuous Affinity-Recycle Extraction: a Novel Protein Separation Technique." *Bio/Technology* **5**, 604-608 (1987).

Richardson, J.F. and W.N. Zaki, "Sedimentation and Fluidization," *Trans. Inst. Chem. Eng.* **32**, 35 – 53 (1954).

Rodrigues, M.I., C.A. Zaror, F. Maugeri and J.A. Asenjo, "Dynamic Modelling, Simulation and Control of Continuous Adsorption Recycle Extraction." *Chem. Eng. Sci.* **47**, 263-269 (1992).

Rowe, G. E., A. Margaritis, Q. Lan, A. S. Bassi and J.-X. Zhu, "A new kinetic model of protein adsorption on suspended anion-exchange particles", Biotech. Bioeng., 65(6) 613-621, 1999

Slater, M.J. and P. Prud'homme, "Continuous Ion Exchange in Fluidized Beds." *Can. Mines Br., Tech. Bull.*, **158**, 1-67 (1972).

Turner, J.C.R. and M.R. Church, "A Continuous Ion Exchange Column." *Trans. Instn. Chem. Engrs.* **41**, 283-288 (1963).

Zheng, Y., J.-X. Zhu, J. Wen, S. Martin, A.S. Bassi, and A. Margaritis, "Hydrodynamic Behavior in a Liquid-Solid Circulating Fluidized Bed", *Can. J. Chem. Eng.*, **77**, 284-290 (1999).

Zheng Y and Zhu J-X, "Overall Pressure Balance and System Stability in a Liquid-Solid Circulating Fluidized Bed", *Chem. Eng. J.*, in press

Zheng, Y., J.-X., Zhu, N. Marwaha and A.S. Bassi, "Radial Flow Structure in a Liquid-Solids Circulating Fluidized Bed," *Chem. Eng. J.* (2000), submitted.

Zhu J-X, Zheng Y, Karamanev DG, and Bassi AS, "(Gas-) Liquid-Solid Circulating Fluidized Beds and their Potential Applications to Bioreactor Engineering", *Can. J. Chem. Eng.*, **78**, 82-94.

Table 7.1 Properties of Diaion HPA25® Ion Exchange Particles

Matrix	Polystyrene (highly porous)
Functional Group	Quaternary Alkylamine
Ionic Form	Cl^{-1}
Average Diameter (d_p, mm)	0.32
Wet Density (ρ_s, g/mL)	1.08
Total Exchange Capacity (Cl^-, meq/mL)	0.6
Exclusive Size (dalton)	>100,000
Terminal Velocity (U_t, mm/s)	4.5
Bed Expansion Index (n)	2.67
BSA Adsorption Capacity (q_m, kg/m^3)	87.9

Table 7.2 Parameters for the Continuous BSA Recovery in the LSCFB System under Typical Operating Conditions

Flowrate of the Extracting Buffer (Q_r, L/min)	0.3
Flowrate of the Feed (Q_d, L/min)	0.64
Superficial Liquid Velocity in the Riser (U_{lr}, mm/s)	11.3
Superficial Liquid Velocity in the Downcomer (U_{ld}, mm/s)	0.6
Solids Circulation Rate (G_s, kg/m^{2}s)	1.42
BSA concentration in the Feed (C_0, g/L)	2
Height of the Riser Column (H_r, m)	3
Height of the Dense Section in the Downcomer (H_d, m)	0.8
Solids Holdup in the Riser (ε_r)	0.035
Solids Holdup in the Downcomer (ε_d)	0.34
Diaion HPA25 Regeneration Ratio (R, %)	0.734
BSA Desorption Ratio in the Riser (X_r)	0.86
BSA Adsorption Ratio in the Downcomer (X_d)	0.98
Overall BSA Recovery (X)	0.84
BSA Concentration at the Extract Outlet (C_{er}, g/L)	0.79
BSA Concentration at the Raffinate Outlet (C_{ed}, g/L)	0.04

Note: Results shown are the average of three parallel experiments.

Figure 7.1 Schematic diagram of the liquid-solid circulating fluidized bed (LSCFB) ion exchange system.
1. Riser, 2. Liquid-Solids separator, 3. Extract outlet, 4. Raffinate outlet, 5. Top washing section, 6. Top solids return pipe, 7. Solids circulating rate measuring device, 8. Downcomer, 9. Distributor of the downcomer, 10. Bottom washing section, 11. Bottom solids return pipe, 12. The primary stream in the riser distributor, 13. The auxiliary stream in the riser distributor, 14. Liquid distributor of the riser, 15. Butterfly valve, 16. Pressure manometer.

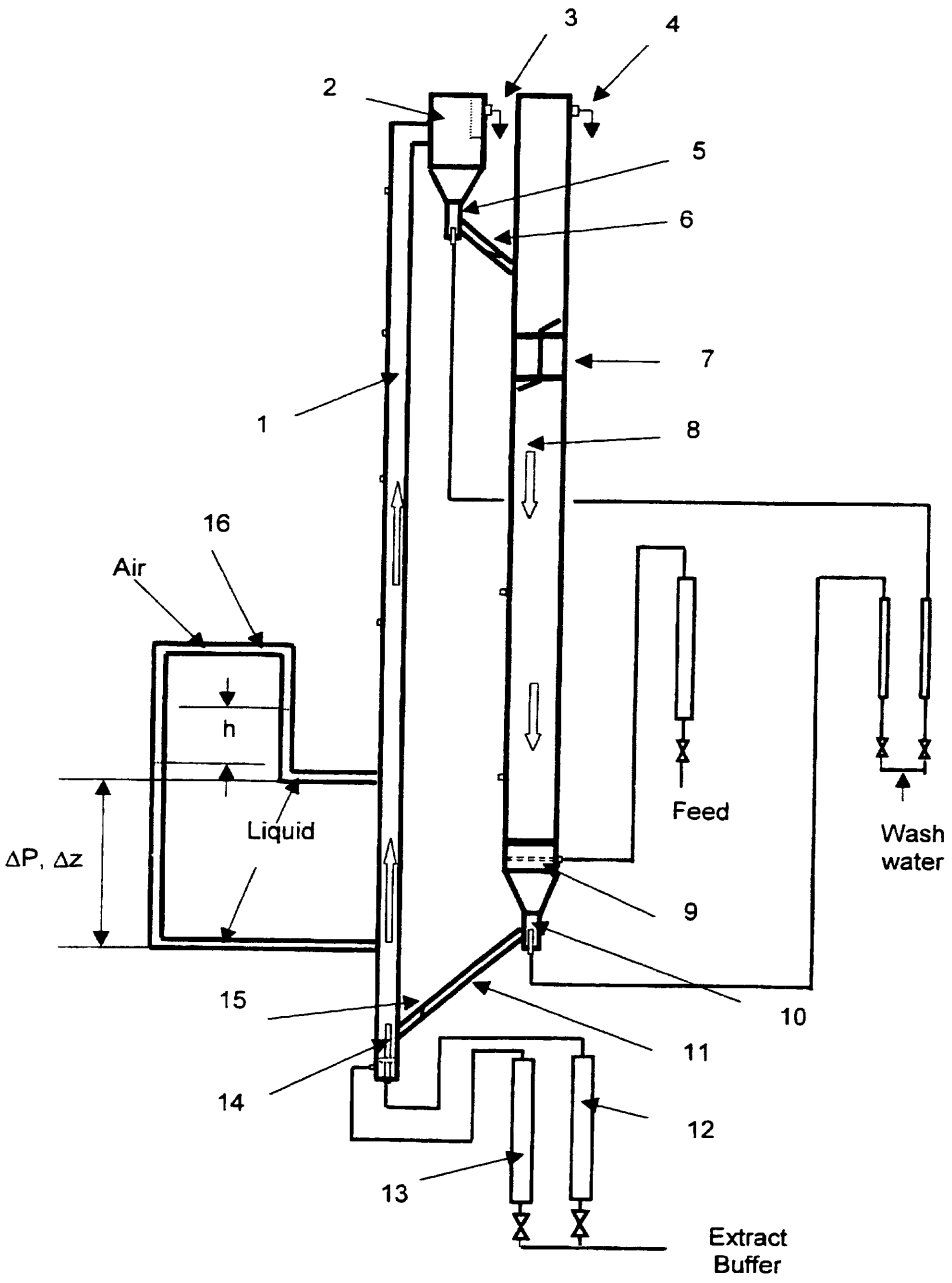

3
4
2
5
6
7
1
8
16
Air
h
Liquid
ΔP, Δz
Feed
Wash
water
9
10
15
11
14
12
13
Extract
Buffer

Figure 7.2.Schematic illustration of the three sections in the downcomer of an LSCFB system : (a) Freeboard Zone; (b) Dilute section; and (c) Dense Section.

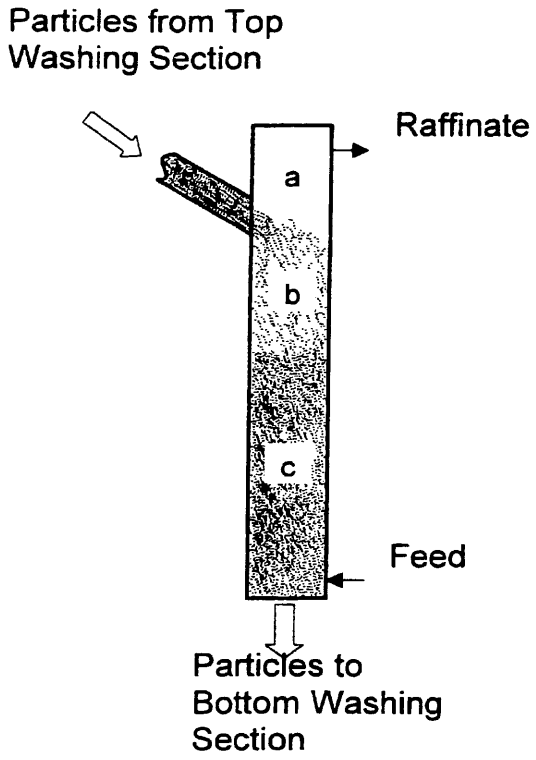


Figure 7.3. Dependency of the downcomer dense section height on the liquid velocity (U_{ld}) in the downcomer and the solids circulation rate (G_s), with a total of 3.0 kg Diaion HPA25 anion exchange particles.

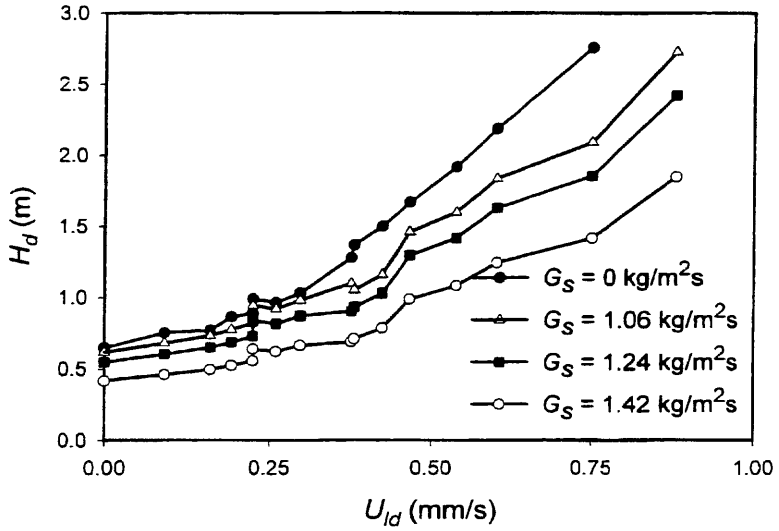


Figure 7.4 Axial distribution of the solids holdup in the riser (U_{ld} = 0.6 mm/s).

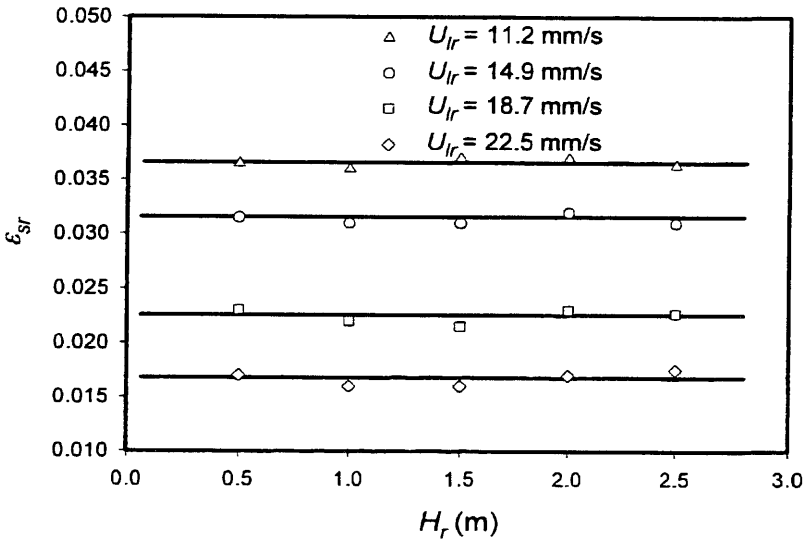


Figure 7.5 Influences of the superficial liquid velocity in the riser (U_{lr}) and the solids circulation rate (G_s) on the solids holdup in the riser (ε_{sr}) (U_{ld} = 0.6 mm/s).

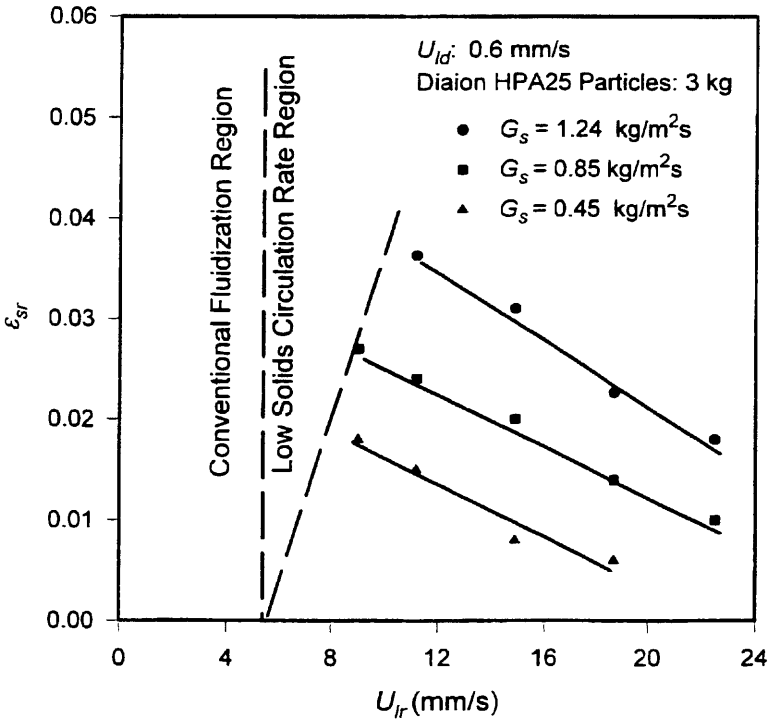


Figure 7.6 The characteristics of Diaion HPA25 regeneration in the riser (U_{ld} = 0.6 mm/s, U_{lr} = 11.3 mm/s, G_s = 1.24 kg/m^2·s, H_d = 0.8 m, C_{0d} = 2 g/L)

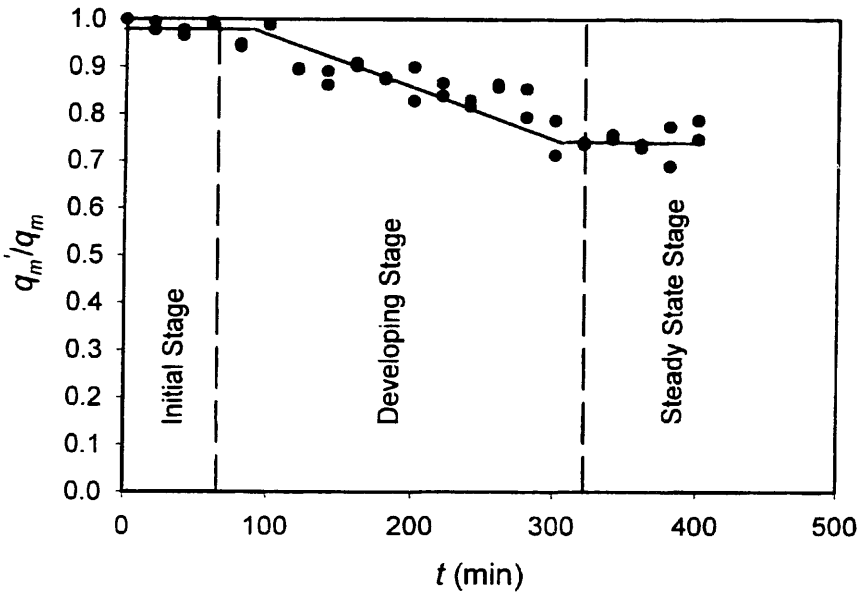


Figure 7.7 The effects of solids circulation rate on the characteristics of BSA adsorption in the downcomer (U_{ld} = 0.6 mm/s, U_{lr} = 11.3 mm/s, H_d = 0.8 m C_{0d} = 2 g/L).

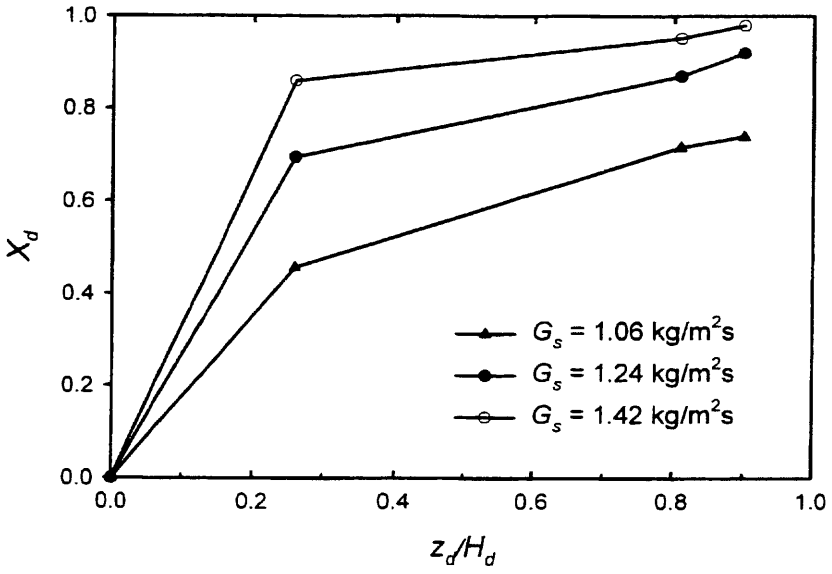


Figure 7.8 The effects of superficial liquid velocity (U_{ld}) on the characteristics of BSA adsorption onto Diaion HPA25 anion exchange particles in the downcomer (U_{lr} = 11.3 m/s, G_s = 1.24 kg/m^2·s, H_d = 0.8 m, C_{0d} = 2 g/L). (a) BSA concentration profiles. (b) BSA adsorption ratio profiles.

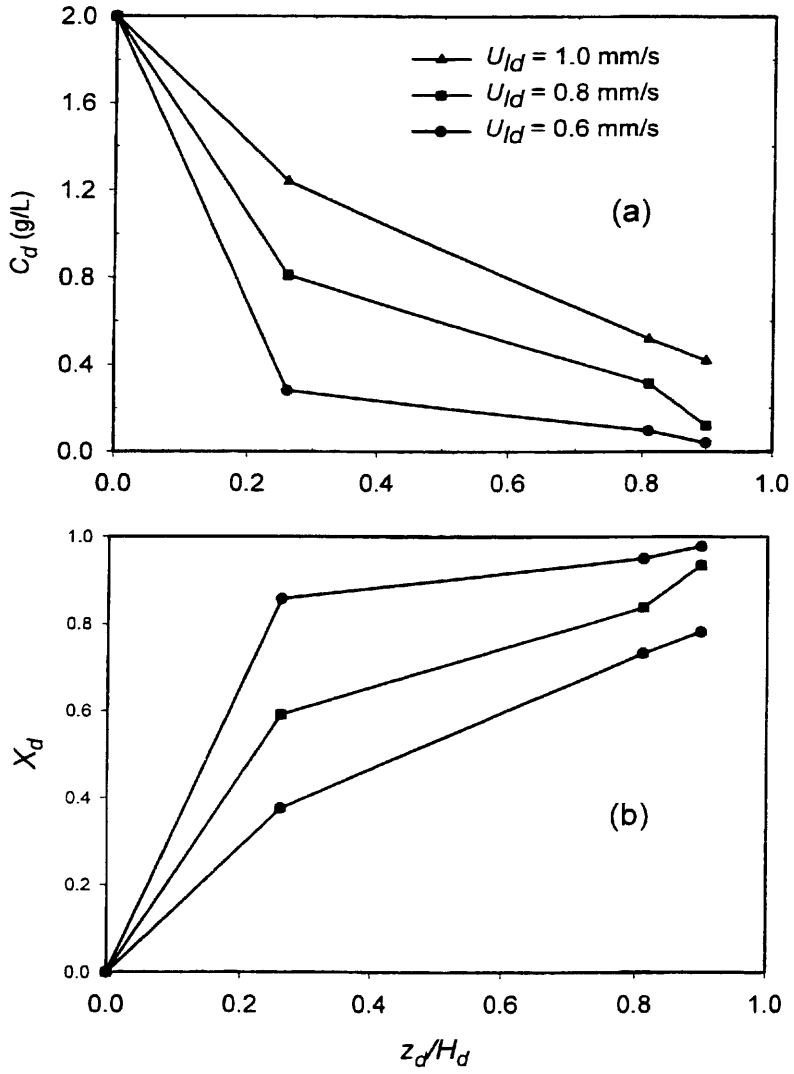

2.0
1.6
1.2
0.8
0.4
0.0
C_d (g/L)
U_{ld} = 1.0 mm/s
U_{ld} = 0.8 mm/s
U_{ld} = 0.6 mm/s
(a)
0.0
0.2
0.4
0.6
0.8
1.0
1.0
0.8
0.6
0.4
0.2
0.0
X_d
(b)
0.0
0.2
0.4
0.6
0.8
1.0
z_d/H_d

Figure 7.9 The effects of superficial liquid velocity (U_{lr}) on the characteristics of BSA desorption from Diaion HPA25 anion exchange particles in the riser (U_{ld} = 0.6 m/s, G_s = 1.24 kg/m^2·s, H_d = 0.8 m, C_{0d} = 2 g/L). (a) BSA concentration profiles; (b) BSA desorption ratio profiles.

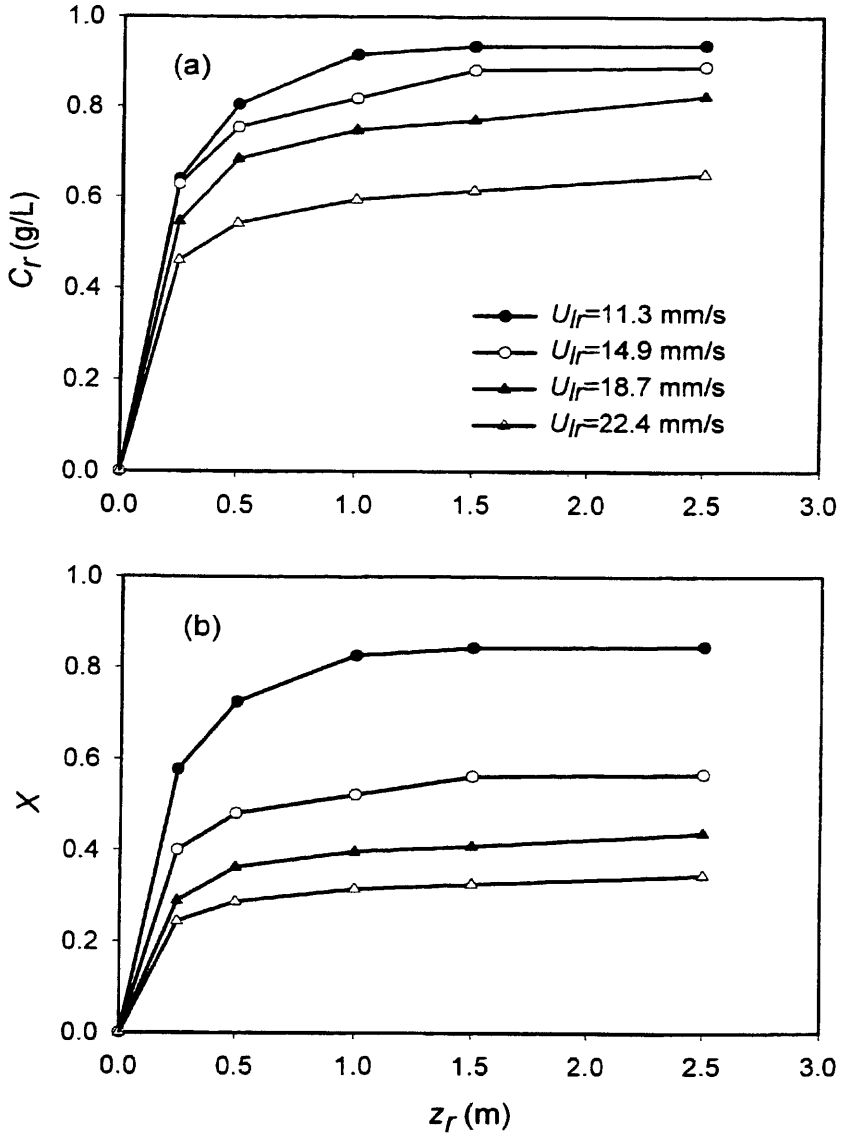
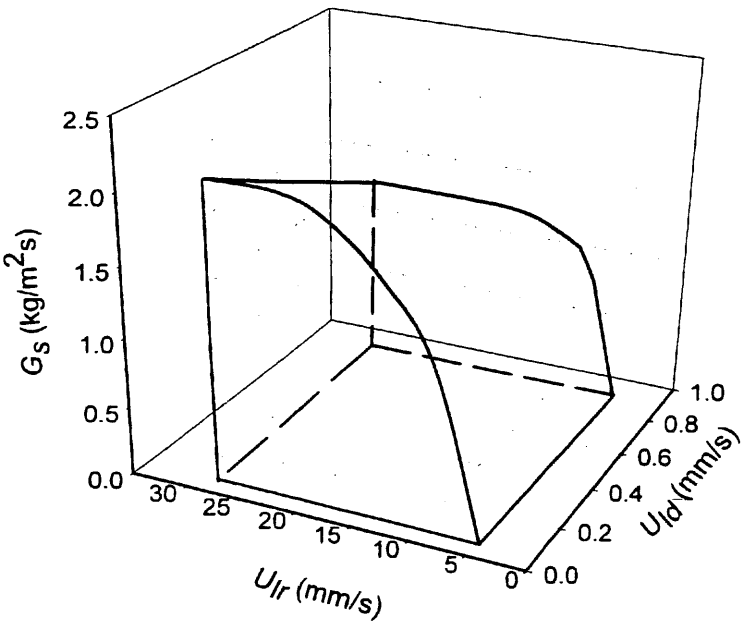

(a)
C_r (g/L)
U_{lr}=11.3 mm/s
U_{lr}=14.9 mm/s
U_{lr}=18.7 mm/s
U_{lr}=22.4 mm/s
(b)
X
z_r (m)

Figure 7.10 Hydrodynamic stable operation window of the LSCFB system with 3 kg Diaion HPA25 ion exchange particles. The fluidization liquid in the riser was 0.4 M NaCl buffer and in the downcomer tap water.



Chapter 8 Recovery of Proteins from Cheese Whey Using a Continuous Liquid-Solid Circulating Fluidized Bed Ion-exchange System

8.1 INTRODUCTION

Whey is the fluid portion of milk drained from the curd in cheese manufacturing. Typically, whey contains 7% solids. These solids consist of about 5-5.5% lactose, 0.04-0.2% milkfat, 0.7-0.9% protein and other nitrogenous matter, and 0.5% ash. Therefore, whey has a high biological oxygen demand (BOD) of 40,000-60,000 mg/L and 5 lb of whey would cause pollution equal to that of the waste from an average individual in one day. A cheese plant discarding 100,000 lb whey a day would require sewage disposal facilities the size of a town of 20,000 people (Johnson and Peterson, 1978). This is a significant environmental burden for the cheese manufacturing industry. On the other hand, the components of cheese whey can be exploited for beneficial uses as food additives, animal feed, healthy food and functional proteins (Etzel, 1995; Johnson and Peterson, 1978).

Ion-exchange has been used for the last two decades for the commercial production of whey protein isolate (WPI), which has exceptional functional properties and nutritional value (Burgess and Kelly, 1979; Huffman, 1996). However, since protein concentration in whey is fairly low, large volume of whey must be treated to recover proteins in an industrial scale. Therefore, the

---

A version of this chapter has been submitted for publication.
Qingdao Lan, Amarjeet Bassi*, Jing-Xu (Jesse) Zhu, Argyrios Margaritis (2001). "Recovery of Proteins from Cheese Whey Using a Continuous Liquid-Solid Circulating Fluidized Bed Ion-exchange System". *Biotech. Bioeng.* (submitted)

cost of the ion-exchange contributes significantly to the overall cost of the production of WPI, which at present can not compete with alternative proteins such as egg protein and soybean protein. Therefore, development of a highly efficient ion exchange process for whey protein purification is of genuine commercial interests.

In our previous studies (Chapters 6 and 7), a liquid-solid circulating fluidized bed continuous ion-exchange system (LSCFB) has been constructed and tested for the continuous recovery of bovine serum albumin (BSA) from synthetic protein solutions. An LSCFB system was basically a liquid-solid circulating fluidized bed equipped with ion-exchange beads. Its major components are a riser, a downcomer, a liquid-solid separator, two solids return pipes and two washing sections. The adsorption and desorption (regeneration) are carried out in the downcomer and the riser, simultaneously, in a continuous mode with the ion-exchange particles circulating continuously between the two columns. The feed is introduced into the downcomer and the extracting buffer into the riser. The riser operates in the circulating fluidization regime (Zheng *et al.*, 1999) and the downcomer operates as a fluidized moving bed (Kwauk, 1992).

The development of LSCFB system opens the possibility of developing a cost competitive ion-exchange process for the production of WPI. In this chapter, the application of LSCFB ion exchange extractor for continuous whey protein recovery is reported.

8.2 MATERIAL AND METHODS

8.2.1 Materials

Reconstituted cheese whey was prepared by dissolving whey powder (Sigma Co., St Louis, MO) into distilled water at appropriate concentration (1-7% w/v) before use. All the reconstituted whey solutions were brought to pH 6.0 by adjusting with 1 M HCl and NaCl solutions. Diaion HPA25 anion-exchange particles, purchased from Sigma Co. (St Louis, MO) were used as the adsorbents. The extracting buffer used for desorption of proteins in the riser was 0.4 M NaCl solution.

8.2.2 Analytical Methods

Total protein concentrations in liquid were measured by Bradford method using USA as standard protein (Dryer and Lata, 1989) and protein concentration in ion-exchangers were calculated by mass balance. The ionic strength in the reconstituted whey solution was analyzed by measuring the conductance of the solutions using a YSI Model 35 Conductance Meter (Yellow Spring Instrument Co., Inc., Ohio, USA). The ionic strength of a solution was expressed as the NaCl equivalent (mM) and obtained by checking a linear [NaCl]-conductance calibration curve. The optical density of a liquid stream was measured at appropriate wavelength using a Cary 50 UV-Visible Spectrophotometer (Varian Australia Pty Ltd., Mulgrave, Victoria 3170, Australia).

8.2.3 Continuous Protein Recovery from Whey Using the LSCFB System

The LSCFB system was as described in earlier studies (Lan *et al.*, 2000a, Chapters 5, 6, and 7). As shown in Figure 8.1, the major components of the LSCFB system included a riser (1), a downcomer (6), a liquid-solid separator (2), a top solids return pipe (4), a bottom solids return

pipe (9), a top washing section (3) and a bottom wash section (8). The riser was 3.0 m tall and 38 mm in diameter and the downcomer 2.5 m tall and 120 mm in diameter. Continuous whey protein recovery in the LSCFB system was conducted with the downcomer used for adsorption and the riser for desorption.

In the continuous protein recovery studies, the feed whey solution was introduced through the distributor into the bottom of the downcomer and the regenerated Diaion HPA25® ion-exchange particles through the top solids return pipe into the downcomer. The liquid velocity of the downcomer (U_{ld}), which was the combination of the feed and the bottom wash water, was controlled in such a way that the downcomer operated in the conventional fluidized regime, where the ion-exchange beads moved down countercurrent to the rising feed liquid. The de-proteinized solution was discarded from the raffinate exit at the top of the downcomer.

As discussed above, in the process of protein recovery, two liquid streams of different properties, i.e., whey solution of low ionic strength and high concentration of contaminants and the pure extracting buffer of high ionic strength, were involved in the downcomer and the riser separately. Therefore, a dynamic seal between the two columns aimed at prevent the mixing of the two liquid streams while allowing a stable circulation of ion-exchange solids was of crucial importance. This dynamic seal was achieved by maintaining the ion-exchange beads in the solids return pipes the packed bed regime. In such a situation, the operations in the riser and the downcomer are independent from each other except the circulation of solids in between those two columns through the liquid-solids separator and the solids returning pipes.

Since the whey contained contaminants such as milk fat drops, lactose, non-protein nitrogen, minerals and some particulates resulted from the denaturization and aggregation of proteins and other chemicals, a complete rinse of the loaded beads was definitely necessary for preventing those contaminants from polluting the effluent, which should be pure protein solution. Therefore,

the loaded beads were introduced into the bottom washing section before being transferred into the bottom of riser through the bottom solids return pipe.

The extracting buffer was applied from the bottom of the riser and were divided into two streams: the primary and the ancillary streams. The function of the ancillary stream was to stir up the ion-exchange beads at the bottom of the riser while most of the extracting buffer was injected into the riser as the primary stream at a point higher than the solids entrance at the bottom of the riser. This structure of the riser distributor maximized the pressure drop across the bottom solids return pipe and was beneficial for the stabilization of the system. The superficial liquid velocity in the riser (U_{lr}), which was the combination of the primary and the auxiliary streams, was kept higher than the terminal velocity of the Diaion HPA25® particles. The loaded particles were carried upward by this buffer stream while desorption proceeded. The ion-exchange beads were regenerated with the process of desorption and the regenerated beads were separated from the effluent in the liquid-solids separator.

8.3 RESULTS AND DISCUSSION

8.3.1 Washing Conditions

In the continuous protein recovery from cheese whey, complete washing is necessary before transferring the regenerated ion-exchange beads from the separator to the downcomer to get rid of the salt adsorbed onto the ion-exchangers. It is also crucial to clean the loaded ion exchange particles before they were transferred into the riser to prevent the pollution of the effluent by the contaminants in the feed. As discussed in Chapter 3, under the dynamic seal conditions, the regenerated and the loaded ion exchange particles were rinsed in the top and bottom washing sections, respectively.

The effectiveness of the bottom washing section at different wash water flowrate was studied under the following conditions: F_{feed} = 5.7 L/hr, F_{buffer} = 30 L/hr, F_{wt} = 1.8 L/hr and G_s = 1.42 kg/m^{2}s. The feed in the downcomer was the whole reconstituted whey (7% whey powder solution) and the extracting buffer 0.4 M NaCl at pH 7. The efficiency of the bottom washing section was measured as the OD_{600} values of effluents at different washing flowrates. As shown in Figure 8.2, F_{wb} had a strong influence on the efficiency of washing, especially at the low F_{wb} range. When the flowrate of wash water of the bottom washing section (F_{wb}) was zero, OD_{600} value was 1.81. However, when F_{wb} increased to 2.1 L/hr, OD_{600} decreased to 0.

It is worthwhile to note that since the I.D. of the washing section was very small, even a mediate F_{wb} may result in a large liquid velocity in this section. For example, at F_{wb} = 2.1 L/hr, the liquid velocity in the washing section (I.D. 36 mm) was 0.573 mm/s, higher than that in the downcomer. If the liquid velocity in the washing section is too large (close to the terminal velocity of the loaded ion-exchange beads), the passage of beads through the washing section will be slowed down and not enough beads can be transferred into the bottom solids return pipe and the riser. Obviously, stabilization cannot possibly be achieved under such a condition. In addition, increase of F_{wb} results in the increase of U_{ld}, which might influence the fluidization in the column and decrease the dynamic adsorption capacity of the system. Keep this in mind, F_{wb} should be maintained as the least possible value at which a thorough cleansing of the loaded beads is achieved. Therefore, F_{wb} was maintained as 2.1 L/hr in the following experiments.

The efficiency of the top washing section was determined by measuring the conductivity of the raffinate. Experiments were conducted under the following conditions: F_{feed} = 5.7 L/hr, F_{buffer} = 30 L/hr, F_{wb} = 2.1 L/hr and G_s = 1.42 kg/m^{2}s. The extracting buffer was 0.4 M NaCl. As shown in Figure 8.3, the conductance of raffinate at F_{wt} = 0 was 3.6×10^{-3} Ω. However, when F_{wt} was

increased to 1.8 L/hr, the conductance of raffinate decreased to 6.8×10^{-5} Ω. It was very close to the conductance of the control (6.1×10^{-5}). The control was the raffinate sample when the extracting buffer was replaced by water at F_{wt} = 0 L/hr and F_{wb} = 2.1 L/hr with all the other conditions same as above. This result indicates that the rinsing effects of the top washing section was sufficient. Similar to that of F_{wb}, there are some undesirable effects associated with a large F_{wt}, which include the destablization of the system and the dilution of the effluent. Therefore, F_{wt} was maintained as 1.8 L/hr in following experiments.

8.3.2 Typical Operation of Continuous Protein Recovery from Reconstituted Whey Solution

The results of a typical operation of whey protein recovery from the quarter-diluted reconstituted whey (1.75%) in the LSCFB system is shown in Figures 8.4 and 8.5. The operating conditions were as follows: F_{buffer} = 30 L/hr, F_{wt} = 1.8 L/hr, F_{wb} = 2.1 L/hr, F_{feed} = 11.4 L/hr, H_d = 0.96 m, C_0 = 1.38 g/L (C_0' = 1.25 g/L) and G_s = 1.42 kg/m^{2}s. The extracting buffer was 0.4 M NaCl and the total amount of Diaion HPA25 was 3 kg. Figure 8.4 shows the protein concentration profiles at different locations on the downcomer, that was, z_d = 0.25 m, z_d = 0.75 m and z_d = 2.5 m (the raffinate exit). According to their protein concentration profiles, protein adsorption at all the three locations could be divided into three stages: the initial stage, the developing stage and the steady state stage. In the initial stage, the protein concentration was zero, indicating that the ion-exchange beads in that layer was in the non-exchange zone and no protein adsorption occurred. The protein concentration in the developing stage increased with time. As time went on, the protein adsorption in a particular location reached steady state and the protein concentration at that location did not change with time anymore.

As shown in Figure 8.4, the protein concentration in liquid phase decreased with bed height in the downcomer. The protein concentration was 0.62 g/L at z_d = 0.25 and 0.41 g/L at z_d = 0.75, both much higher than zero but significantly lower than C_0'. This result indicates that the ion-exchange beads in both the locations were in the exchange zone. Therefore, the exchange zone was at least 0.5 m in height (the distance between those two sampling points) under those conditions. The protein concentration in the raffinate at steady state was 0.11 g/L. Considering the effects of backmixing, it is reasonable to consider that there was no significant breakthrough in such a set of conditions. As discussed above, the large height of the exchange zone can be explained by the backmixing and the slow kinetics of protein adsorption.

It is worthwhile to point out that the time duration of the initial and the developing stage of the protein adsorption in the downcomer were subject to the protein loading rate and the liquid velocity in the downcomer. With large protein loading rate and U_{ld}, the time duration of those stages were remarkably shorter than that with small ones.

Figure 8.5 shows the protein concentration profiles in the riser under the above conditions. Samples were taken from three locations: z_r = 0.25 m, z_r = 1.5 m, and z_r = 3 m (the effluent). Similarly, the desorption in the riser can also be divided into three stages: the initial stage in which the protein concentration in the liquid phase was zero, the developing stage in which the protein concentration in liquid phase increased with time, and the steady state stage in which the protein concentration in the liquid phase did not change with time. Nevertheless, the reasons for the existence of those three stages are totally different from that for the adsorption in the downcomer. In the initial stage, the ion-exchange beads transferred into the riser were those originally stored in the bottom solid return pipe and thus did not contact with the feed. Therefore, no protein was adsorbed onto those beads. In the developing stage, the ion-exchange beads transferred into the riser were those beads originally at the very bottom of the downcomer and

had only been exposed shortly to feed and the protein concentration in those beads was low. However, protein concentration in the beads transferred into the riser increased with time and so did the protein concentration in liquid phase since the beads coming later were exposed longer to the feed. Finally, the adsorption in the downcomer reached steady state and the protein concentration in the beads at its bottom remained constant. When those beads were transferred into the riser, the steady state in the riser was also established.

As shown in Figure 8.5, C_r increased with bed height. However, at H_r = 0.25 m, C_r at steady state was 0.41 g/L, only slightly lower than that in the effluent (0.47). Obviously, most of the protein was desorbed from the loaded ion-exchange beads in the bottom of riser. This was reasonable because the rate of desorption is fast. In addition, the large liquid velocity in the riser further increased the mass transfer and thus the desorption process. Although data show most of the protein was desorbed from the loaded beads in the section of riser of lower than 0.25 m, the remaining bed height was still essential for bead transfer and thorough regeneration.

8.3.3 Effects of Operating Conditions on Protein Recovery in the LSCFB System

Experiments of continuous whey protein recovery from reconstituted whey solutions were conducted at following conditions: F_{buffer} = 30 L/hr, F_{wt} = 1.8 L/hr, F_{wb} = 2.1 L/hr, F_{feed} = 11.4 L/hr, and G_s = 1.42 kg/m^{2}s. Two different F_{feed} and three different dilution ratios were investigated.

1. The influence of dilution ratio

The influence of dilution ratio has been tested for three different dilution ratios at two different F_{feed} values in the experiments (Table 8.1). Obviously, at the same feed flowrate, a high dilution ratio favored the adsorption in the downcomer. When F_{feed} was maintained at 5.7 L/hr, for

example, the overall protein recovery increased from 78.4% to 89.9% when the dilution ratio increased from 1 (the whole whey) to 4 (quarter-diluted whey). This effect was more dramatic when the feed flowrate was kept at 11.4 L/hr under which the overall recovery increased from 39.3% to 79.7% when the dilution ratio increased from 1 to 4. The protein concentration in the effluent, however, decreased with the increase of dilution ratio at both feed flowrates.

The influence of dilution ratio on the adsorption in the downcomer can be analyzed from two aspects: the protein loading rate and the dynamic adsorption capacity of the system. When the dilution ratio increased, the ionic strength decreased accordingly (Figure 7.6). As a result, the maximum adsorption capacity of regenerated ion-exchange beads (q_m) increased (Lan *et al.*, 2000b, Chapter 5). When other conditions such as G_s and U_{ld} remained the same, the dynamic adsorption capacity of the system increased as described by Equation 7.7. More significantly, the increase of dilution ratio resulted in the remarkable decrease of protein concentration in the feed and thus the protein loading rate when the feed rate was not changed. Therefore, the increase of dilution ratio had two different effects: increase of dynamic adsorption capacity of the system and decrease of the protein loading rate. Both of them were favorable for a complete adsorption in the downcomer.

While larger dilution ratio was beneficial for adsorption and increased the overall recovery, it also resulted in lower protein concentration in the effluent, increased the volume of raffinate, and reduced the throughput of the system. For this particular system at F_{feed} = 5.7 L/hr, the recovery of total protein from whole whey was 78.4%, lower than that from the quarter-diluted whey (89.9%). However, the throughput of the first condition was more than 3 times of that under the latter condition and the volume of raffinate generated was one quarter of the latter. In addition, the volume of effluent to be treated in the following operations for the recovery of the same amount of whey proteins would be 3 times more with the quarter-diluted whey than with the

whole whey. Considering the fact that the huge amount of whey needs to be treated nowadays, it is obvious that to treat the whole whey is more advantageous. In fact, the capacity of the LSCFB system to treat whole whey with relatively high recovery is one of the major unique features making it superior to other alternatives.

2. The influence of feed flowrate

The influence of feed flowrate (F_{feed}) is also shown in Table 8.1. Two different feed flowrates have been tested in the experiments with three different dilution ratios. The effects of F_f on the protein recovery were different at high dilution ratio from that at low dilution ratio. For the whole whey solution, the overall recovery decreased from 78.4% to 39.3% when F_{feed} increased from 5.7 L/hr to 11.4 L/hr, representing a decrease of 50%. When the dilution ratio was 4, the recovery at F_{feed} = 5.7 L/hr (89.9%) was still higher than that at F_{feed} = 11.4 L/hr (79.7%), but at much less extent (11.4%).

It is interesting to compare the recovery at different F_{feed} when the protein loading rate were the same. When the protein loading rate was 31.1 g protein/hr, for instance, the recovery at F_{feed} = 5.7 L/hr was 78.4%, but that for F_{feed} = 11.4 L/hr was only 57.6%. Similarly, when protein loading rate was 15.6 g protein/hr, the recovery at F_{feed} = 5.7 L/hr was 83.8%. However, this value decreased slightly to 79.7% at F_{feed} = 11.4 L/hr. Obviously, F_{feed} = 5.7 L/hr is more advantageous than F_{feed} = 11.4 L/hr under the conditions tested.

The effects of F_{feed} on the adsorption in the downcomer can be explained by its influence on the liquid velocity in the downcomer (U_{ld}) and its effect on the protein loading rate. Under the dynamically sealed conditions, U_{ld} was determined by the total of the flowrates of the bottom

wash water (F_{wb}) and the feed. When F_{wb} was constant, which was the case in these experiments, U_{ld} increased with F_{feed}. Because the downcomer operated as a fluidized moving bed, the fluidization in the downcomer, especially the fluidization parameters such the solids holdup, the bed height and the backmixing of the dense phase section, was significantly influenced by U_{ld}. In addition, increase of U_{ld} will also enhance the migration velocity of the exchange zone, which may result in breakthrough even at low protein loading rate. Therefore, the increase of U_{ld} will reduce the fluidization index (κ) of equation 7.7 and thus the dynamic adsorption capacity.

Although low F_{feed} is beneficial for the achievement of plug flow in the downcomer and advantageous for complete adsorption and high recovery, too small an F_{feed} will reduce the protein concentration in the effluent and reduce the throughput of the system. As a result, the system will be less competent because of the lowered efficiency. Therefore, the choice of F_{feed} is a balance between a higher protein recovery and a higher throughput. In the investigated, F_{feed} = 5.7 L/min is more beneficial.

3. Protein concentration in the effluent

Protein concentration in the effluent was relatively low under all the conditions tested. When the whole whey was treated at an F_{feed} of 5.7 L/hr, which was the optimal condition among the tested conditions, the protein concentration in the effluent was only 0.77 g/L, much less than the protein concentration in the feed (5.46 g/L). The problem of the low protein concentration in effluent was due to the inappropriate diameter ratio between riser and the downcomer. For the present apparatus, the downcomer/riser diameter ratio was 3.16, representing an area ratio of about 10-fold. However, the hydrodynamic characteristics of the LSCFB system required an U_{lr}/U_{ld} ratio of above 30 to operate the downcomer in the conventional fluidization regime and the riser in the

circulating fluidization regime with sufficient G_s. Due to those constraints of the apparatus, the flowrate of the extracting buffer must be 3 or more times as that of the feed ($F \propto U \times A$). Therefore, the effluent was diluted by the large volume of extracting buffer, together with the top wash water and the bottom wash water. This problem can be solved by increasing the diameter of the downcomer to a suitable dimension in the scale-up process, which will also increase the throughput of the system.

8.4 CONCLUSIONS

The LSCFB system was demonstrated to be a suitable method for the protein recovery from whole whey and the optimal conditions in the tested range were determined as F_{buffer} = 30 L/hr, F_{feed} = 5.7 L/hr F_{wt} = 1.8 L/hr, F_{wb} = 2.1 L/hr, G_s = 1.42 kg/m^{2}s, H_d = 0.73 m and C_0 = 5.64 g/L (C_0' = 3.99 g/L). Under those conditions, a throughput of 8.16 g protein/hr·(kg beads) was achieved with a recovery of 78.4%. The liquid velocity in the downcomer was found to be the most significant parameter affecting the dynamic adsorption capacity of the downcomer.

NOMENCLATURE

A Cross-sectional area of a column (m^2)

C Protein concentration in liquid phase (g/L)

C_0 protein concentration in feed (g/L)

C_0' protein concentration in feed corrected by the dilution factor due to the bottom wash water, $C_0' = \frac{F_f}{F_f + F_{wb}} C_0$, (g/L)

D Dynamic adsorption capacity of the sytem (g prtoein/hr)

F Flowrate of liquid (L/hr or m^3/s)

G_s Solids circulation rate (kg/m^2s)

I Ionic strength (mM or M NaCl equivalent)

K_d Dissociation coefficient at zero ionic strength (g/L)

q Protein concentration in the ion-exchange beads (mg/g beads)

q_m Maximum adsorption capacity at zero ionic strength (mg/g beads)

t Time (hr, min or s)

U Superfical velocity of liquid or solids in column (m/s)

V Velocity of liquid or solids in column (m/s)

V_{slip} Slip velocity (m/s)

x Distance from the base of a column (m)

Greek

ε_l Bed voidage

ε_s Solids holdup ($\varepsilon_l+\varepsilon_s = 1$)

η Equation constant describing the effects of ionic strength on apparent maximum adsorption capacity (M or g/L)

ρ Density (kg/m^3)

κ Fluidization index of dynamic adsorption capacity (equation 7.7)

Subscripts

b Bottom

buffer buffer

d Downcomer

e Exit

feed Feed

r Riser

t Top

w Wash water

0 Initial

REFERENCES

Burgess, KJ and Kelly, J. 1979. Selected functional properties of a whey isolate. *J. of Food Technology* 14: 325-329.

Chang YK and Chase HA.1994. "Expanded bed adsorption for the direct extraction of proteins. *Separations for Biotechnology* 3: 106-112.

Chase HA. 1994. Purification of Proteins by Adsorption Chromatography in Expanded Beds. *TIBTECH* 12: 296-303.

Draeger, NM and Chase HA. 1991. Liquid fluidized bed adsorption of protein in the presence of cells. *Bioseparation* 2: 67-68.

Dryer RL and Lata GF. 1989. *Experimental Biochemistry*. New York: Oxford University Press. p. 346.

Etzel MR. 1995. Whey protein isolation and fractionation using ion-exchangers. In: *Bioseparation processes in food*. R.K. Sight and S.H. Rizvi (eds.). New York : M. Dekker, pp. 390-415.

Gailliot FP, Gleason C, Wilson JJ, and Zwarick J. 1990. Fluidized bed adsorption for whole broth extraction. *Biotechnol. Prog.* 6: 370-375.

Huffman, LM. 1996. Processing whey protein for use as a food ingredient. *Food Techn.*, Feb. 1996: 49-54

Johnson, AH and Peterson MS. 1978. *Encyclopedia of Food Technology* 3: pp 870-875, Westport, Conn. : Avi Pub. Co.

Kwauk, M.1992. Fluidization – Idealised and Bubbleless, with Applications. Ellis Horwood, New York.

Lan Q, Zhu J-X, Bassi AS, Margaritis A., Zheng Y and Rowe GE. 2000a. Continuous Protein Recovery Using a Liquid-Solid Circulating Fluidized Bed Ion-exchange System: Modelling and Experimental Studies. *Can. J. Chem. Eng.* **78**: 858-866, 2000

Lan Q, Zhu J-X, Bassi AS, Margaritis A. 2000b. A Modified Langmuir Model for the Prediction of the Effects of Ionic Strength on the Equilibrium Characteristics of Protein Adsorption onto Ion-exchange/Affinity Adsorbents. *Chem. Eng. J.* 81(1-3): 179-186

Liang, W-G, Zhang S-L, Zhu J-X, Jin Y, Yu Z-Q and Wang Z-W. 1997. Flow Characteristics of the Liquid-Solid Circulating Fluidized Bed. Powder Technol. 90: 95-102.

Zheng, Y, Zhu J-X, Wen J, Martin S, Bassi AS and Margaritis A. 1999. The Axial Hydrodynamic Behavior in a Liquid-Solid Circulating Fluidized Bed. *Can. J. Chem. Eng.* 77: 284-290.

Table 8.1. Summary of parameters of whey protein recovery under different conditions

Feed Flow rate (L/hr)	Dilution Ratio	Protein Loading Rate (g/hr)	Protein Conc. in Effluent (g/L)	Adsorption Rate %	Overall Recovery (%)	Throughput (g/hr·kg)
5.7	1	31.2	0.77	79.9	78.4	8.2
	2	15.6	0.41	87.5	83.8	4.3
	4	7.8	0.23	90.1	89.9	2.4
11.4	1	62.2	0.77	40.4	39.3	8.2
	2	31.2	0.64	65.2	57.6	6.8
	4	15.6	0.39	82.8	79.7	4.1

Figure 8.1 Schematic diagram of the LSCFB system (1. Riser; 2. Liquid-Solids separator; 3. Top washing section; 4. Top solids return pipe; 5. Solids circulating rate measuring device; 6. Downcomer; 7. Distributor of the downcomer; 8. Bottom washing section; 9. Bottom solids return pipe; 10. Liquid distributor of the riser.)

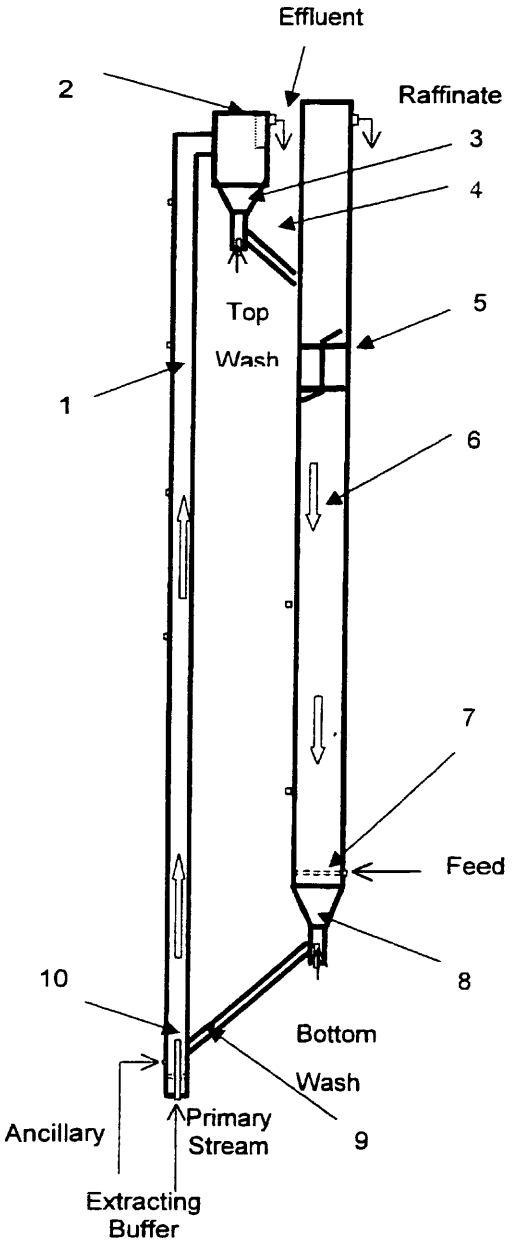

Effluent
2
Raffinate
3
4
Top
Wash
5
1
6
7
Feed
8
10
Bottom
Wash
Ancillary
Primary
Stream
9
Extracting
Buffer

Figure 8.2 OD_{600} of the effluent at different bottom wash water flowrate (F_{wb}) (F_{feed} = 5.7 L/hr, F_{buffer} = 30 L/hr, F_{wt} = 1.8 L/hr and G_s = 1.42 kg/m^{2}s. Feed: half diluted whey; Extracting buffer: 0.4 M NaCl).

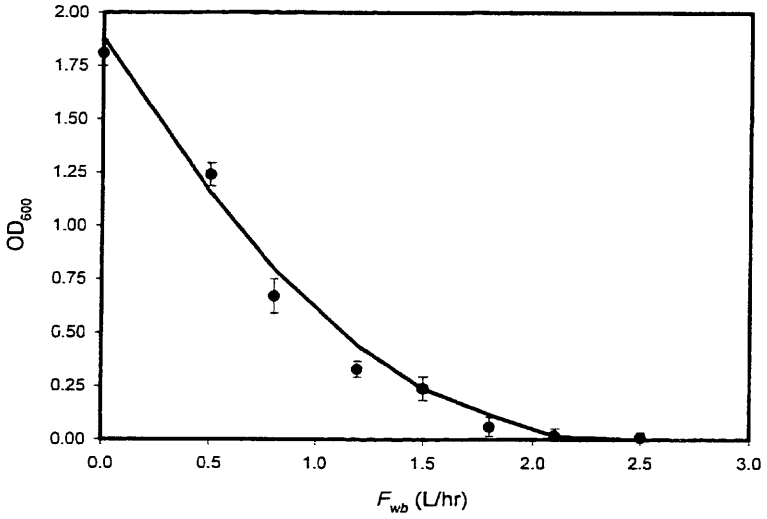


Figure 8.3 Conductance of the raffinate at different top wash water flowrates (F_{wt}) (F_{feed} = 5.7 L/hr, F_{buffer} = 30 L/hr, F_{wb} = 2.1 L/hr and G_s = 1.42 kg/m^{2}s. Feed: half-diluted whey (3.5%); Extracting buffer: 0.4 M NaCl).

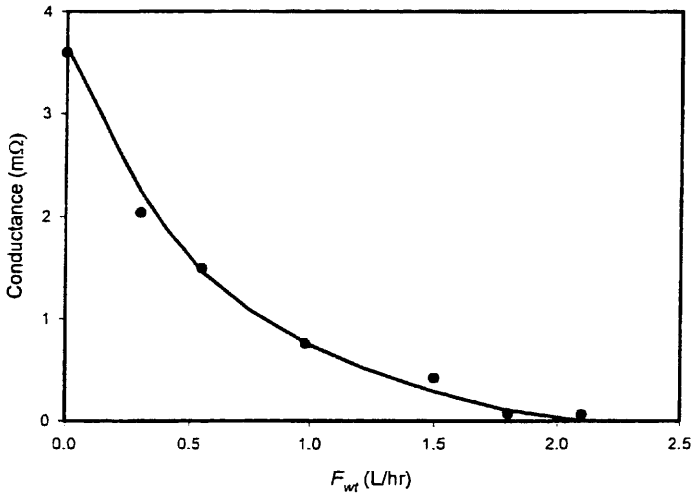


Figure 8.4 Protein concentration profiles at different locations of the downcomer in a typical continuous whey protein recovery in the LSCFB system. (Experimental conditions: F_{feed} = 5.7 L/hr, F_{buffer} = 30 L/hr, F_{wb} = 2.1 L/hr, F_{wt} = 1.8 L/hr, and G_s = 1.42 kg/m^{2}s; Extracting buffer: 0.4 M NaCl solution; Feed: quarter diluted whey (1.75% reconstituted whey).

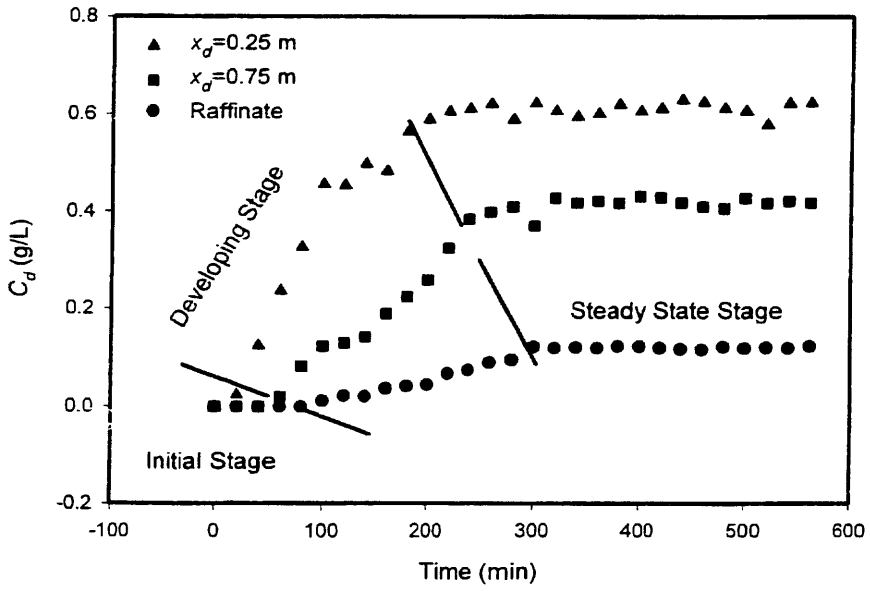


Figure 8.5 Protein concentration profiles at different locations of the riser in a typical continuous whey protein recovery in the LSCFB system. (Experimental conditions: F_{feed} = 5.7 L/hr, F_{buffer} = 30 L/hr, F_{wb} = 2.1 L/hr, F_{wt} = 1.8 L/hr, and G_s = 1.42 kg/m^{2}s.;Extracting buffer: 0.4 M NaCl solution; Feed: quarter diluted whey (1.75% reconstituted whey).

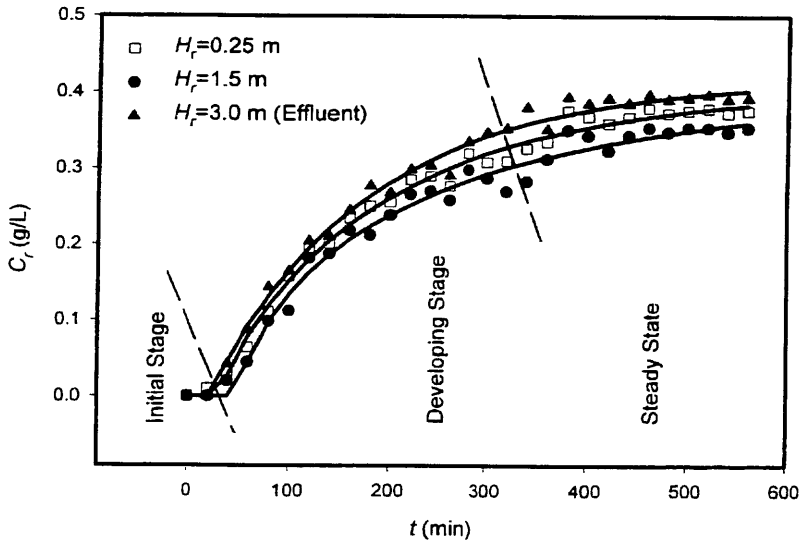
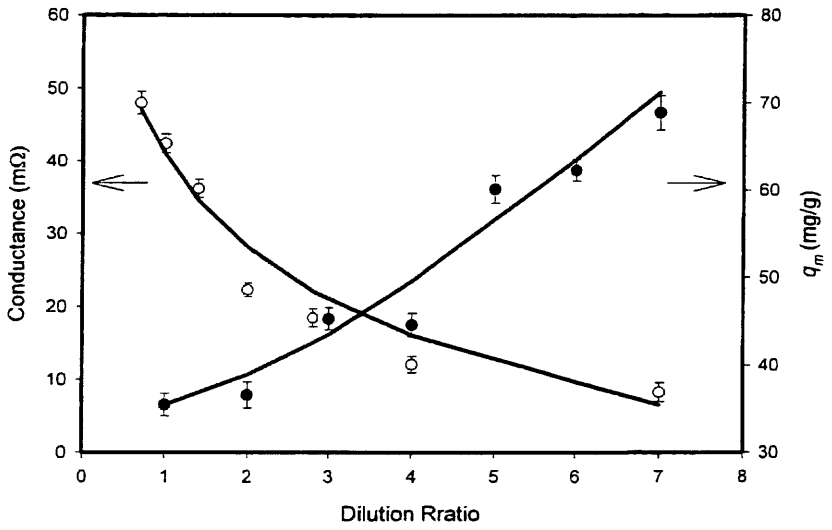


Figure 8.6 Effects of dilution ratio on the ionic strength of the whey solution and the maximum adsorption capacity of ion-exchange beads.



Chapter 9. Conclusions and Recommendations

9.1 CONCLUSIONS

9.1.1 Development of an LSCFB ion exchanger for protein recovery

An LSCFB continuous ion exchange system (LSCFB), which is basically an LSCFB system equipped with ion exchange particles with suitable hydrodynamic characteristics and protein adsorption capacity, has been developed for protein recovery from un-clarified whole broth. The system has been tested for protein recovery from BSA solution and from whey solution as well. It proved to be efficient at the present scale with a treating capacity of about 6 L whey/hr. The most significant advantages associated with the LSCFB system include the following:

- The large voidage of the ion exchange particles bed fluidized in the downcomer allows the passage of particulates. Therefore, an unclarified broth containing particulates can be treated directly by an LSCFB system without plugging the column. This is especially advantageous for the product recovery from biochemical broths since the separation of colloids such as cell debris from such broths is extremely difficult.
- The LSCFB is a device for continuous operation with adsorption and desorption occurs simultaneously in the two columns in a continuous mode.
- Since the ion exchange particles are continuously regenerated, even ion exchange particles with relatively low capacity and kinetics, which is common for ion exchange particles involved for protein recovery, can be used in such a system with high efficiency.

9.1.2 Hydrodynamic characteristics of the LSCFB system

As an integrated system with both a fast column and a slow column, hydrodynamic behavior of the LSCFB system is very complicated because each type of column carries with it some hydrodynamic implications and to couple them together, limitations come hand in hand with the merits of a comprehensive system.

1. Dynamic Seal between the riser and the downcomer

The LSCFB system is basically a system having two coupled columns with liquid streams of different properties and with solids circulating between the two columns. In such a system, the dynamic seal between the two columns is of essential importance. The dynamic seal has been achieved by maintaining a "particle plug" in the solids return pipes with novel designs balancing the oval pressure drop, the solids circulation and the solids washing. The following parameters have been identified as affecting the dynamic seal and more comprehensive studies are necessary for understanding the underlying principles:

- Liquid velocity in the downer (downcomer)
- Solids circulation rate between the riser and the downcomer
- Flowing properties of the solids
- Structure of the distributor and the bottom section of the downcomer
- Structure of the washing sections
- Structure of the liquid-solids separator

2. Hydrodynamic characteristic of the riser

The hydrodynamic behaviors of the riser were very similar to those reported by previous workers (Liang *et al.*, 1997; Zheng *et al.*, 1999) when the dynamic seal was maintained properly.

3. Hydrodynamic characteristics of the downcomer

The hydrodynamic behavior of the downcomer of an LSCFB system in the way that the whole downcomer can be divided into three sections: namely the dense section, the dilute section and the freeboard. In the section the formation and the functions of the three sections were discussed.

9.1.2 Continuous protein recovery using the LSCFB system

The overall protein recovery was 84.0% for BSA at a throughput of 21.5 g/hr·(kg beads) and that for whey proteins was 78.4% at a lower throughput of 8.2 g/hr·(kg beads). The efficiency for protein recovery from BSA solution was much higher than that from the whole whey. This is because the high ionic strength and the fouling effects of the milk-fats in whey solution reduced the dynamic capacity of the system.

A dynamic adsorption capacity of the LSCFB system has been defined as the indication of the maximum allowable protein loading rate to the system. The dynamic capacity is determined by the maximum capacity of the adsorbents, the mass transfer efficiency, the fluidization and backmixing in the downcomer and the solids circulating rate between the riser and the downcomer. A large solids circulating rate can make up to a certain extent the problem caused by the low capacity and mass transfer efficiency associated with large ion exchange particles.

9.1.3 Modelling of continuous protein adsorption/desorption in the LSCFB system

The protein adsorption in the downcomer and the desorption in the riser were modeled based on some simplification assumptions such as plug flows in both the riser and the downcomer and the second order and first order reaction kinetics for the adsorption and desorption, respectively. The design equations derived were found practical guidelines for the design of an LSCFB system.

9.1.4 Protein ion exchange

9.1.4.1 Equilibrium Studies

- The isotherms of BSA adsorption onto Diaion HPA25 was found to be well integrated by Langmuir equation.
- The adsorption capacity and the affinity of the adsorption were proved to been high pH-dependency and ionic strength dependency as well. It was demonstrated that if pH is less than pH 4 or if the ionic strength is larger than 0.2 M NaCl equivalent, the adsorption is zero.
- The above results suggested that a buffer of either a pH less than pH 4.0 or a salt concentration larger than 0.2 M NaCl can be used as the extracting buffer.
- A simple empirical model based on Langmuir isotherm has been developed to account for the influence of ionic strength on the protein adsorption onto ion exchange/affinity adsorbents. The model was validated using both experimental and literature data.

9.1.4.2 Kinetics studies

Kinetic studies concerning the BSA adsorption/desorption have been conducted using a CSTR system. Results show that the adsorption is rather slow, possibly due to the large particle size of Diaion HPA25 anion exchangers. On the other hand, the desorption of the BSA from loaded

particles was very fast, especially in the early stage. About 80% of the total loaded proteins were desorbed instantly. However the stripping lagged off in the later stage, again, due to the large particle size of the particles.

9.2 RECOMMENDATIONS

Experiments with the present apparatus has indicated that the LSCFB system is an outstanding candidate for the protein recovery. However, there are still some remarkable problems associated with it that must be solved before the successful commercialization. Those problems include the dramatically reduced dynamic capacity of the system due to the strong backmixing in the downer, the greatly limited stable operating range because of the poor design (well, due to the lack of data and experience in the early stage) and the low protein concentration in the extract as a result of the poor riser/downer diameter ratio. Some thoughts and recommendations regarding further studies in this area are presented as follows.

9.2.1 Improvement of the Design of the LSCFB system with the following new features

- A new solids distributor for the downer to achieve a uniform radial solids distribution
- An improved liquid distributor for the downer to minimize the backmixing
- Improved liquid-solid separator and washing sections to enlarge the stable operating range
- An optimized riser/downer diameter ratio for elevating the protein concentration in the extract
- Development of affinity adsorbents with high selectivity and better hydrodynamic properties

9.2.2 Studies on the hydrodynamics in the downer

Hydrodynamic behaviors in the downer of a riser-downer LSCFB system is a new subject and very few works have been done in this area. We have reported that the downcomer of a riser-downer LSCFB system can be divided into three zones according to their different solids holdups and the dense section is the most important zone. The dense section is virtually a moving conventional fluidized bed in which the particles fall down and liquid goes up (Kwauk, 1992). Further elucidation of such a moving conventional fluidized bed relies on more comprehensive studies with carefully designed downer fluidized beds. Studies on the effects of operating conditions such as superficial liquid velocity, solids circulation rate, solids entry and the design of distributor on parameters such solids holdup, axial solids holdup distribution and the backmixing in the dense section and the height of the dense section will help to elucidate the hydrodynamic behaviors in the downer and provide practical guide lines for the design and scale up of an LSCFB system.

9.2.3 Studies on the hydrodynamics in the riser

As discussed above, the hydrodynamics of the riser is a relative well studied topic as a few authors have studied systematically the hydrodynamics in the riser of an LSCFB system. However, data reported so far are still limited and system-dependent. Data regarding the riser hydrodynamic of particles of small diameters (50 – 300 μ) and light densities (less than 1200 kg/m^3), which are commonly used in biochemical engineering processes, are extremely limited. Therefore, further studies on the hydrodynamic behaviors of an LSCFB riser are still necessary.

9.2.4 Study the application of the LSCFB system in recovery of proteins from different broths.

Different biological broths may be different in properties such as pH, viscosity, density, ionic strength, and particulates. Besides, different proteins may required different adsorbents. Therefore, the application of the LSCFB system to biological streams instead of whey solution requires comprehensive studies with regard the particular broth.

9.2.5 Other potential applications for the LSCFB ion exchange system

The LSCFB ion exchange system has the potential of being worldwide accepted as a high efficient substitute for the batch packed bed ion exchange systems, which are essential units in water treatment, food industry, pharmaceutical industry, wastewater treatment process, metal recovery and related areas. More specifically, with the selection of appropriate ion exchangers and application researches, it could be employed in the following processes:

- Protein recovery and peptide recovery
- Amino acid recovery
- Nucleic acid recovery
- Organic acid recovery
- Metal ion recovery
- Recovery of other products from food and pharmaceutical industries
- Removal of contaminants

REFERENCE

Liang, W.G., Z.Q. Yu, Y. Jin, Z.W. Wang, Y. Wang, "Synthesis of Linear Alkylbenzene in a Liuid-Solid Circulating Fluidized Bed Reactor." *J. Chem. Technol. Biotechnol.* **62**: 98 (1995)

Liang, W-G., S-L. Zhang, J-X. Zhu, Y. Jin, Z-Q. Yu and Z-W. Wang, "Flow Characteristics of the Liquid-Solid Circulating Fluidized Bed." *Powder Technol.* **90**, 95-102 (1997).

Zheng, Y., J.-X. Zhu, J. Wen, S. Martin, A.S. Bassi, and A. Margaritis, "The Axial Hydrodynamic Behavior in a Liquid-Solid Circulating Fluidized Bed." *Can. J. Chem. Eng.* **77**, 284-290 (1999)

APPENDIX A. COPYRIGHT RELEASE FROM THE JOURNAL "CANADIAN JOURNAL OF CHEMICAL ENGINEERING

Qingdao Lan
A2-939 Western Rd
London Ontario N6G 1G3
Tel/Fax: (519) 438-5951
E-mail: qlan@uwo.ca

Dinah Laprairie, Assistant Publishing Editor
The Canadian Journal of Chemical Engineering
130 Slater Street, Suite 550
Ottawa, ON, K1P 6E2, Canada
Tel: 613-232-6252
Fax: 613-232-5862
E-mail: dlaprairie@cheminst.ca

Dear Ms. Dinah Laprairie:

Urgent: Request of a Letter of Reprint Permission

I am submitting you a request for a letter of permission allowing me to include an article published on the CJChE in my Ph.D. dissertation. I have submitted a similar email to the publishing office a few weeks ago and have gotten no answer yet. The due date for the final submission of my thesis is April 30th, 2001 and, as you can see, I am in a real emergent situation. Your response to my request will be highly appreciated.

Title: Continuous Protein Recovery Using a Liquid–Solid Circulating Fluidized Bed Ion Exchange System: Modelling and Experimental Studies
Authors: Qingdao Lan, Jing-Xu (Jesse) Zhu, Amarjeet S. Bassi, Argyrios Margaritis, Ying Zheng and Gerald E. Rowe
Canadian Journal of Chemical Engineering Volume 78 (5) 858, 2000

I am looking forward to hearing from you shortly in this regard.

Sincerely

Qingdao Lan

Permission Granted.
Good luck!
Dinah Laprairie
20 April 01

APPENDIX B. COPYRIGHT RELEASE POLICY OF ELSEVIER SCIENCE: REGARDING THE INCLUSION OF MATERIALS IN CHAPTER 5 IN THIS THESIS FROM "CHEMICAL ENGINEERING JOURNAL"

What rights do I retain as author?

As an author, you retain rights for large number of author uses, including use by your employing institute or company. These rights are retained and permitted without the need to obtain specific permission from Elsevier Science. These include:

- Patent and trademark rights or rights to any process or procedure described in the article
- The right to photocopy or make single electronic copies of the article for their own personal use, including for their own classroom use, or for the personal use of colleagues, provided those copies are not offered for sale and are not distributed in a systematic way outside of the employing institution
- The right to post the article on a secure network (not accessible to the public) within the employer's institution
- The right to retain a preprint version of the article on a public electronic server such as the World Wide Web. Elsevier Science does not require that authors remove from publicly accessible servers versions of their paper that differ from the version as published by Elsevier Science. See also our information on electronic preprints for a more detailed discussion on these points.
- Posting of the article as published on a public server can only be done with Elsevier Science's specific written permission

- The right, subsequent to publication, to use this article or any part thereof free of charge in a printed compilation of works of their own, such as collected writings or lecture notes
- If the article is a "work for hire" made within the scope of the author's employment, the employer may use all or part of the information in this article for intra-company use
- **The right to include the article in a thesis or dissertation provided that this is not to be published commercially**
- The right to present the paper at a meeting or conference and to hand copies of the paper to the delegates attending the meeting
- The right to publish a different or extended version of the paper so long as it is sufficiently new to be considered a new work
- The right to expand the article into book-length form for publication
- The right to re-use parts of the paper in other works, provided that the new work is not to be published commercially.

http://www.elsevier.com/homepage/authors/?main=/homepage/about/ita/copyright.shtml#permission

CURRICULUM VITAE

NAME: Qingdao (Chris) Lan

PLACE OF BIRTH: Hubei, China

POST-SECONDARY EDUCATION:

The University of Western Ontario
London, Ontario, Canada
May 1997- April 2001 Ph.D.

Wuxi University of Light Industry
Wuxi, China
1988-1991 M.E.Sc.

SCHOLARSHIPS AND AWARDS

Ontario Graduate Scholarship in Science and Technology (OGSST)
2000 – 2001

Special University Scholarship (SUS)
1997 – 2000

International Graduate Student Scholarship (IGSS)
1997-1999

SELECTED PUBLICATIONS

Lan, Q., A. Bassi, J.-X. Zhu and A. Margaritis, "A Modified Langmuir Model for the Prediction of the Effects of Ionic Strength on the Equilibrium Characteristics of Protein Adsorption onto Ion Exchange/Affinity Adsorbents". *Chem. Eng. J.* 179-186 (2001)

Lan, Q., J.-X. Zhu, A. Bassi, A. Margaritis, Y. Zheng and G. Rowe, "Continuous Protein Recovery Using a Liquid-Solid Circulation Fluidized Bed Ion Exchange System: Modelling and Experimental Studies." *Can. J. Chem. Eng.* 78: 858-866 (2000)

G. E. Rowe, A. Margaritis, Q. Lan, A. S. Bassi and J.-X. Zhu, "A new kinetic model of protein adsorption on suspended anion-exchange resin particles", *Biotech. Bioeng.*, 65(6) 613-621, 1999

Jin, Q., Q. Lan and B. Zhu, "The breeding of thermotolerant citric acid overproducing strains from Aspergillus niger". *Acta Microbiologica Sinica* (Chinese with English Abstract) 33(3): 204-209 (1993)

CONFERENCE PRESENTATIONS

Lan Q., A.S. Bassi, J.-X. Zhu and A. Margaritis, "An Investigation on the Protein Adsorption in an LSCFB Ion Exchange System", Presentation at 49th Canadian Chemical Engineering Conference. 1999.10, Saskatchewan, Ontario, Canada

Lan, Q. and F. Chen, "Effects of Nitrogen Sources on the Cell Growth and Phycocyanin Biosynthesis of Spirulina platensis". Presentation at the 48th Canadian Chemical Engineering Conference. London, Ontario, Canada, 1998.10.

Lan, Q., A. Bassi and A. Margaritis, J.-X. Zhu, and G. Rowe, "Whey Protein Recovery in Liquid Solid Circulating Fluidized Beds". Presentation at 48th Canadian Chemical Engineering Conference. 1998.10, London, Ontario, Canada


جامعة اليرموك
المكتبة
LIBRARY
University of Yarmouk